Electron flow and energy conservation in hydrogenotrophic methanogenesis

Kyle C. Costa

A dissertation
submitted in partial fulfillment of the
requirements for the degree of

Doctor of Philosophy

University of Washington
2013

Reading Committee:
John A. Leigh, Chair
David A. Stahl
John A. Baross

Program Authorized to Offer the Degree:
Microbiology

University of Washington

Abstract

Electron flow and energy conservation in hydrogenotrophic methanogenesis

Kyle C. Costa

Chair of the Supervisory Committee:
Professor John A. Leigh
Microbiology

Methanogenesis is a globally important process responsible for the generation of >90% of the CH_4 present on Earth. Despite this importance, key biochemical details concerning methanogenesis have eluded characterization. Presented here is a global analysis of the bioenergetics and substrate utilization in hydrogenotrophic methanogenesis: the reduction of CO_2 to CH_4. It was long thought that hydrogenotrophic methanogenesis proceeded linearly; however, this model fails to take into account how energy conservation occurs. The first step of the pathway is endergonic, but the source of energy to power this reaction was unknown. Results presented here show that the first and last steps are physically and energetically coupled. Hence the methanogenesis pathway is cyclic rather than linear. This presents another problem in that all metabolic cycles must replenish intermediates to guard against decaying flux. This replenishing reaction is facilitated by a membrane-bound hydrogenase activity. Finally, methanogens are thought to require hydrogen for growth. By generating a model for methanogenesis, I show this is not the case: hydrogenotrophic methanogens are capable H_2-independent growth in the presence of alternative substrates such as formate. Taken together, these data provide for a model for the biological generation of CH_4 through the hydrogenotrophic pathway. Although these data generate a molecular a model for methanogenesis, key details

about how the process is regulated remain a mystery. Later chapters of this work describe the early stages of an experimental system to identify elements essential for the regulation and expression of methanogenesis genes.

TABLE OF CONTENTS

LIST OF FIGURES

LIST OF TABLES

ACKNOWLEDGEMENTS

This dissertation would not have been possible without the help of many people. First and foremost, I thank my advisor John Leigh for being supportive and providing clear guidance while simultaneously allowing me the freedom to follow my interests and find my own way. I must also thank members of my graduate committee (John Baross, Caroline Harwood, Colin Manoil, and David Stahl) for years of advise, guidance, and support. Specifically, I thank Dave Stahl and John Baross for taking the time to read and review this manuscript. I also thank all the members of the Leigh lab, past and present, especially Tom Lie who taught me the basic molecular biology and reverse genetics tools that made all this work possible. Much of the work in this manuscript would not have been possible without collaborations with members of numerous research groups, so I thank Murray Hackett, Nitin Baliga, Barny Whitman, David Stahl, and Samuel Miller, as well as the members of their labs, for reagents, the use of equipment, and training when needed.

DEDICATION

I dedicate this dissertation to my parents, James and Debra Costa, who have always been incredibly supportive, regardless of what I chose to pursue. Whenever I have the need, they are always at my side. I also dedicate this dissertation to my older siblings, Amy and Keith. I could not have asked for two better or more caring role models.

CHAPTER 1

Introduction

This dissertation outlines details of the pathway of hydrogenotrophic methanogenesis that lead to net energy conservation and the utilization of multiple electron donors for CO_2 reduction. In this introduction, I will describe all the known methanogenic pathways. Although methylotrophic and aceticlastic methanogenesis are distinct from hydrogenotrophic methanogenesis, several of the novel electron flow pathways of hydrogenotrophic methanogenesis described in later chapters have similarities and differences to methylotrophic and aceticlastic methanogenesis. Therefore, it is important to understand how all three pathways function. Finally, I will discuss what is known about how the individual steps of methanogenesis are regulated. Later chapters will describe new approaches to understanding and characterizing regulatory systems.

Pathways of methanogenesis

Methanogenic archaea produce methane from a variety of substrates. There are three basic types of methanogenesis. In the first type, hydrogenotrophic methanogenesis (Fig. 1.1), CO_2 is reduced to CH_4 with four molecules of H_2 providing the necessary eight electrons. Some hydrogenotrophs can also utilize formate, which substitutes for H_2. When formate acts as the electron donor, it is oxidized to CO_2 to generate two moles of electrons per mole of formate. Finally, a restricted number of hydrogenotrophs can use secondary alcohols for methanogenesis. Alcohols are oxidized to ketones via an F_{420}-dependent alcohol dehydrogenase to generate reduced electron carriers for CO_2 reduction to CH_4 (155). The second type, methylotrophic methanogenesis (Fig. 1.2), uses methylated compounds such as methanol, methylamines and methylsulfides as electron acceptors to make CH_4. Finally, aceticlastic methanogenesis generates CH_4 and CO_2 from acetate (Fig. 1.2). Although this dissertation will focus on pathways of hydrogenotrophic methanogenesis, it is worthwhile to cover the details of methylotrophic and aceticlastic methanogenesis to place these studies in context.

Hydrogenotrophic methanogenesis occurs in seven steps: four two-electron reductions, two C1 transfers, and a dehydration. The first step of methanogenesis involves the reduction of CO_2 to a formyl group covalently attached to the carrier molecule methanofuran via formylmethanofuran dehydrogenase (Fwd). This reduction represents an endergonic reaction

and is coupled to the exergonic reaction of heterodisulfide reduction in the last step of methanogenesis (25, 70, 136). The formyl group of formyl-methanofuran is subsequently transferred to the N5 of tetrahydromethanopterin (H_4MPT) and a dehydration results in cyclization to generate methenyl-H_4MPT. The methenyl group undergoes a reduction to generate a methylene group, then another reduction to generate a methyl group that is then transferred to the third carrier: the sulfhydryl-containing coenzyme M (CoM). The methyl is fully reduced to CH_4 by another sulfhydryl-containing coenzyme, coenzyme B (CoB) generating a mixed disulfide of CoM and CoB. The mixed disulfide (heterodisulfide) is reduced to regenerate CoM and CoB in an exergonic reaction that is energetically coupled to the reduction of CO_2 to formylmethanofuran to start another cycle of methanogenesis (25, 55, 70, 135).

Methanogenesis with methylated compounds (methanol, methylamines, methylsulfides) is mostly restricted to the *Methanosarcinales* and normally involves both reduction and oxidation of the methyl group to generate methane. Methyl groups enter the methanogenic pathway as methyl-CoM and are subsequently reduced to methane. The reduction of the methyl group to CH_4 requires two electrons; a second methyl group being oxidized to CO_2 by running the first six steps of methanogenesis in reverse generates these electrons. As methyl oxidation to CO_2 generates six electrons, three moles of methane can be produced for each mole of CO_2 evolved. The oxidative branch of the pathway is inhibited when exogenous H_2 is provided demonstrating that H_2 utilization is preferred to the energetically costly oxidation of methyl-CoM to CO_2. In fact, some methanogens, such as *Methanosphaera stadtmanae*, specialize in methyl group reduction using H_2 and are incapable of oxidation of methyl groups.

Methanogenesis from acetate generates both CH_4 and CO_2 in the aceticlastic reaction, so named because the methyl carbon of acetate is cleaved off and reduced to methane by the oxidation of the carboxyl carbon. Therefore, the stoichiometry of CH_4 and CO_2 production is 1:1. In this reaction the methyl group enters the methanogenic pathway at the level of methyl-H_4MPT. Aceticlastic methanogenesis is restricted to the genera *Methanosarcina* and *Methanosaeta*.

Reactions of hydrogenotrophic methanogens

***Generation of reduced electron carriers (ferredoxin, F_{420})* by hydrogenases and formate dehydrogenases.** Methanogens use two main electron carriers in CO_2 reduction to CH_4: F_{420}

and ferredoxin. There are three known pathways of F_{420} reduction in hydrogenotrophic methanogenesis. Methanogens growing on H_2 generate reduced F_{420} via a cytoplasmic F_{420} reducing hydrogenase (Frh (or Fru/Frc *Methanococcus maripaludis*)). Methanogens that use formate have a cytoplasmic F_{420} reducing formate dehydrogenase (Fdh). This is a two-subunit enzyme where the α subunit contains the formate oxidizing site, and the β subunit contains the F_{420} reducing site. It is noteworthy that H_2 can be generated from formate via formate:F_{420} oxidoreductase activity and reduced F_{420}:H_2 oxidoreductase activity by Fdh and Frh respectively (88). The H_2 produced is proposed to function as the electron donor for ferredoxin generation that is required for anabolic CO_2 fixation (90, 110). Additionally, the H_2-dependent methylenetetrahydromethanopterin dehydrogenase (Hmd) and the F_{420}-dependent methylenetetrahydromethanopterin dehydrogenase (Mtd), both catalyzing the fourth step of methanogenesis (see below), are reversible and can be used to generate reduced F_{420} from H_2 or H_2 from reduced F_{420} in the Hmd:Mtd cycle (59).

Reduced ferredoxin is essential for biosynthetic reactions of methanogens (90, 110), and is required for the first step of CO_2 reduction. Reduced ferredoxin is generated by a membrane bound [NiFe] hydrogenase, termed the energy converting hydrogenase (Ech, Eha, Ehb), which utilizes H_2 as the electron donor and consumes membrane potential. In some methanogens, reduced F_{420} and reduced ferredoxin may be interchangeable. *Methanosarcina mazei* F_{420} dehydrogenase ζ subunit (FpoF) catalyzed ferredoxin:F_{420} oxidoreductase activity when expressed in *Escherichia coli* (152). Additionally, deletion of *fpoF* in *M. mazei* resulted in the loss of this activity of cytoplasmic fractions (152). These data suggest that F_{420} and ferredoxin are interconvertable in some methanogens.

Reduction of CO_2 to formylmethanofuran. Formylmethanofuran dehydrogenase (Fmd) catalyzes the endergonic reduction of CO_2 and methanofuran (MFR) to formyl-MFR. This reaction is highly endergonic ($\Delta G' = +45$ kJ mol^{-1}) under low H_2 partial pressures where most methanogens are naturally found. The energy for the Fmd reaction can be driven by reverse electron flow as determined in cell suspension experiments in *Methanosarcina* (68). Fmd is a molybdenum-containing enzyme consisting of six subunits in *Methanosarcina* species (142). In other species, a tungsten containing form (Fwd) can also be found. *In vitro* studies show that all subunits of the enzyme are not essential for activity when artificial electron donors are assayed (147).

The physiological electron donor for Fmd is reduced ferredoxin. Enzyme assays either rely on reduction of viologen dyes with formyl-MFR running the reverse reaction or $TiCl_2$ and MFR running the forward reaction (12, 15). Because of the dependence of Fmd on reduced ferredoxin, it was thought that a membrane bound energy converting hydrogenase could generate the ferredoxin utilized by Fmd; in *Methanosarcinales* this hydrogenase is Ech and in hydrogenotrophs, as will be discussed in chapter 3, it appears to be Eha (79). Ech and Eha are highly similar to the NADH:quinone oxidoreductase complex of bacteria and catalyze the reversible reduction of ferredoxin from H_2 and reverse electron flow. This hypothesis was supported by studies in *M. barkeri* that demonstrated an inability of a Δ*ech* mutant to grow by reducing CO_2 and form formyl-MFR as a methanogenic intermediate (97). These data suggest a model where Ech and Eha have H_2:ferredoxin oxidoreductase activity that is dependent on the consumption of membrane potential. The ferredoxin produced then carries electrons to Fmd where CO_2 reduction takes place. CO_2 reduction in organisms that obligately reduce CoM-S-S-CoB via the cytoplasmic heterodisulfide reductase HdrABC, such as *Methanococcus* spp. and *Methanothermobacter* spp., also occurs concomitantly with heterodisulfide reduction by flavin-based electron bifurcation (see below).

Reduction of C1 groups on tetrahydromethanopterin. Tetrahydromethanopterin (H_4MPT) is a structural analog of tetrahydrofolate (H_4F) and acts as the second C1 carrier in methanogenesis. In *Methanosarcina* spp. H_4MPT is substituted by the chemically similar tetrahydrosarcinopterin (H_4SPT). C1 units bound to H_4MPT undergo a dehydration and two reductions. Enzymes using H_4MPT as a substrate are formyl-MFR:H_4MPT formyltransferase (Ftr), methenyl-H_4MPT cyclohydrolase (Mch), F_{420} dependent or H_2 dependent methylene-H_4MPT dehydrogenase (Mtd or Hmd), and methylene-H_4MPT reductase (Mer). Hmd and Mtd catalyze reversible reactions that can be used to generate reduced electron carriers for other steps in methanogenesis (see above) (59). The methyl-H_4MPT:CoM methyltransferase will be discussed in more detail in the next section.

Ftr and Mch catalyze reactions involving the C1 group at the oxidation level of formate. Ftr catalyzes the formation of 5-formyl-H_4MPT from formyl-MFR (35). Under physiological pH, the formation of 5-formyl-H_4MPT from formyl-MFR was thermodynamically favorable. The formation of 5-formyl-H_4MPT differs from H_4F chemistry where 10-formyl-H_4F is the intermediate formed. Mch catalyzes a dehydration reaction that forms 5,10-methenyl-H_4MPT; Mch was shown to favor 5-formyl-H_4MPT as a substrate over H_4F derivatives or 10-formyl-H_4MPT (30).

Mtd and Hmd are each capable of generating a C1 intermediate at the oxidation level of formaldehyde in the form of methylene-H_4MPT. All methanogenic archaea contain Mtd, whereas Hmd is only present in some methanogens. The methylene group generated in this reduction is bound to both the N5 and N10 nitrogens of H_4MPT. Mtd differs from the H_4F dependent enzymes in that it does not contain a flavin or FeS clusters (132). Mtd is a single subunit enzyme that thermodynamically favors the formation of 5,10-methylene-H_4MPT over methenyl-H_4MPT 26 fold; although the reaction is reversible (132).

The final reductive step involving H_4MPT is the formation of methyl-H_4MPT catalyzed by the F_{420} dependent enzyme Mer. In contrast to H_4F dependent enzymes, Mer does not contain a flavin (89). The crystal structure of Mer demonstrates that it likely exists in a dimeric state, although tetrameric Mer was observed in *Methanopyrus kandleri* (126).

Methyl transfer and generation of membrane potential: the energy-conserving step of methanogenesis. Methyl-H_4MPT:CoM methyltransferase (Mtr) is a corrinoid containing protein that catalyzes the exergonic formation of methyl-CoM concomitant with the generation of chemiosmotic membrane potential (positive outside) by the translocation of sodium ions (47). Mtr is the only membrane-associated enzyme involved in the core methanogenic pathway in all species of methanogens. The enzyme complex is composed of eight subunits, and is dependent on the presence of Na^+ (149). When purified from *M. mazei* Gö1, the native enzyme, embedded in membrane vesicles, translocated 1.7 moles Na^+ per mole methyl-CoM formed (84). For a detailed review about Mtr, see (47).

The MtrA subunit is a largely hydrophilic protein with a hydrophobic C-terminal tail that anchors the enzyme to the cytoplasmic side of the membrane (50). This subunit also binds the cobamide prosthetic group. MtrA bound cob(I)amide and methyl-cob(III)amide are known catalytic intermediates in the methyl transfer reaction. Purified MtrH exhibits methyl-H_4MPT:cob(I)amide methyltransferase activity (61) so it is thought to catalyze the formation of the methylated corrinoid. Upon methylation to methyl-cob(III)amide, MtrA undergoes a structural change. Upon demethylation, the original structure is restored and Na^+ translocation occurs (149). Methyl-cob(III)amide:CoM methyltransferase activity is thought to be catalyzed by MtrE (47) which is one of the most hydrophobic subunits of the enzyme complex. Additionally, MtrE has a large cytoplasmic component with a zinc binding domain suggesting its involvement

in the methylation of a thiol group as all enzymes known to methylate a thiol group contain zinc (91). The presence of zinc in MtrE, its hydrophobicity, and the structural changes associates with methyl-transfer suggest a methyltransferase reaction catalyzed by MtrE that is coupled to Na^+ translocation (47, 149).

Reduction of CH_3-CoM to CH_4. Methyl-coenzyme M reductase (Mcr) catalyzes the methane forming step in all methanogens and as such is often used as a marker gene for identifying methanogenic organisms in the environment. Mcr uses coenzyme B (7-mercaptoheptanoylthreonine phosphate) to reduce methyl-CoM (2-(methylthio)ethanesulfonate) to methane and a heterodisulfide (CoM-S-S-CoB). In order for Mcr to be active, a highly reduced Ni(I) is required in the active site. A crystal structure has been solved for Mcr and shows that it exists in a $\alpha_2\beta_2\gamma_2$ configuration and contains two active sites buried deeply in the enzyme with a channel that allows substrate entry (40). The reaction is dependent on a reduced nickel-tetrapyrrole cofactor (F_{430}) that is buried deep in the active site cleft. Methyl-CoM binds first to F_{430} before CoB enters and leads to methane formation via a debated mechanism.

There are three proposed catalytic mechanisms for Mcr. Proposal I involves binding of methyl-CoM followed by release of a radical form of CoM and generation of a methyl-Ni(III) intermediate (40). Proposal II involves generation of a methyl radical and CoM-S-Ni(II) (107). Proposal III involves reductive cleavage of the methyl thioether resulting in formation of methyl-Ni(III) and simultaneous release of CoM-S-S-CoB (36). The final electron for reduction of the methyl group to methane is derived from CoB, which is recruited to the enzyme after binding of methyl-CoM (40). Recent data derived from crystallographic studies of Mcr bound to various CoB derivatives suggests that CoB does not induce a conformational change in the enzyme (22). This suggests a role for methyl-CoM in altering the structure of the enzyme upon binding that leads to the recruitment of CoB and the successful cleavage of the methyl thioether.

Reduction of the mixed disulfide of CoM and CoB. The reaction catalyzed by Mcr releases methane as a metabolic waste product along with the heterodisulfide of coenzyme M and coenzyme B (CoM-S-S-CoB). The thiol-containing forms of these cofactors must be regenerated in order for subsequent rounds of methanogenesis to occur. Additionally, reduction of the heterodisulfide is an exergonic process and is considered an energy-conserving step of methanogenesis catalyzed by heterodisulfide reductase (Hdr). Members from all methanogenic

orders sequenced to date contain a cytoplasmic HdrABC enzyme complex that reduces the heterodisulfide (70, 136).

Electron donors for heterodisulfide reduction include a number of substrates. Hdr is associated with a hydrogenase in all methanogens studied. H_2:heterodisulfide oxidoreductase activity has been demonstrated in vitro using enzyme purified from *Methanothermobacter* spp. (125). It was thought that the Hdr-associated hydrogenase was essential (108); however, experiments in subsequent chapters of this dissertation show that during methanogenesis with formate as the electron donor in *Methanococcus maripaludis*, this enzyme is dispensable suggesting an electron flow pathway from formate to Hdr via an associated formate dehydrogenase.

HdrABC has been studied in great detail in *Methanothermobacter* spp. HdrABC purified from this organism exists as in a complex with an associated hydrogenase (Mvh) (54, 125). HdrA contains non-covalently bound FAD in a 1:1 stoichiometric ratio. Additionally, HdrA and HdrC both contain multiple 4Fe:4S clusters. Finally, The HdrB subunit was shown to contain a novel 4Fe:4S binding site with a $CX_{31-39}CCX_{35-36}CXXC$ motif that represents the active site of heterodisulfide reduction (49). The Mvh hydrogenase binds to the α subunit of HdrABC in order to transfer electrons from H_2 to the active site of heterodisulfide reduction. Based on these data, the path of electron flow through Hdr is thought to be from Mvh to HdrA through HdrC and finally to the active site in HdrB.

Hdr catalyzes an exergonic reaction in methanogenesis that should be involved in energy conservation; however, there is no experimental evidence to indicate a membrane association of HdrABC for the generation of chemiosmotic membrane potential (136). Therefore, the question has long been: what is the mechanism of energy conservation in methanogens utilizing HdrABC? The solution to this problem was recently proposed and verified experimentally by Rudolf Thauer and colleagues (70, 136). The FAD molecule of HdrA acts as a site of flavin-based electron bifurcation (see below) where the exergonic reduction of the heterodisulfide is coupled to the endergonic reduction of ferredoxin in a 1:1 stoichiometric ratio (70). The ferredoxin reduced is proposed to act as the electron donor for the first reductive step of hydrogenotrophic methanogenesis (see above). In a subsequent chapter, I will discuss how the protein that catalyzes this step of methanogenesis is physically associated with Hdr in *M. maripaludis* (25).

Electron bifurcation as a form of energy conservation

Flavin-based electron bifurcation is a mechanism utilized by anaerobic organisms to generate low potential electrons in an ATP-independent manner. The reaction mechanism is similar to ubiquinone-based electron bifurcation in the cytochrome *bc1* complex of the aerobic respiratory chain (65). In flavin-based electron bifurcation, low potential electron carriers are reduced by substrates with higher mid-point redox potential; the energy for this reduction comes from the concomitant reduction of electron carriers with higher mid-point redox potential than the donor substrate. For example, the first flavin-based electron bifurcating enzyme complex to be studied was from butyric acid-forming *Clostridium kluyveri*. This complex reduces both crotonyl-CoA (E_0' = -10 mV) and ferredoxin (E_0' = -400 mV) simultaneously with electrons derived from NADH (E_0' = -320 mV) (78). Thermodynamically, the reduction of ferredoxin by NADH seems impossible, but the exergonic reduction of crotonyl-CoA drives the reaction forward.

Since the discovery of flavin-based electron bifurcation in 2008, several bifurcating enzyme complexes from anaerobic organisms have been described (11, 25, 64, 70, 78, 143-146). Proteins catalyzing these reactions utilize a variety of substrates as electron donors, including H_2, formate and NADH. Additionally, organisms capable of this activity are found in both the Archaea and the Bacteria. However, there are several thematic similarities between all the flavin-based reactions: (i) all enzymes contain either a FAD or FMN cofactor, (ii) all enzymes are cytoplasmic, (iii) all enzymes operate in a negative redox potential range (-300 $\pm$ 200 mV), and (iv) all organisms described to date that carry out these reactions are anaerobic (143). For the most part, the enzymes that catalyze flavin-based electron bifurcation reactions were shown to operate only in the forward direction *in vitro*; however, there are exceptions to this (143, 145). For example, a [FeFe]-hydrogenase from *Morella thermoacetica* catalyzes both the forward, electron bifurcating reduction of ferredoxin and NAD with H_2 and the reverse, electron confurcating generation of H_2 from reduced ferredoxin and NADH (145). Despite the great diversity in the activities of these electron bifurcating enzymes, it is clear that the ability of anaerobic organisms to generate low-potential electrons without consuming ATP represents a third form of energy conservation in addition to substrate level phosphorylation and the generation of chemiosmotic membrane potential.

Reactions of methylotrophic methanogens

A second type of Hdr used by methylotrophs. In addition to the cytoplasmic HdrABC described above, the *Methanosarcinales* contain a membrane bound, cytochrome containing, two-subunit heterodisulfide reductase (HdrDE) enzyme that generates chemiosmotic membrane potential concomitant with heterodisulfide reduction. The electron transport chain involving HdrDE accepts electrons from methanophenazine (a lipophilic, redox active cofactor). Reduced methanophenazine is generated via a membrane associated hydrogenase or a F_{420} dehydrogenase (1). HdrDE has been studied in *Methanosarcina.* Hdr purified from membranes of *Methanosarcina barkeri* is a two-subunit, cytochrome-*b*-containing enzyme (55). HdrE contains the heme and HdrD contains the active site of CoM-S-S-CoB reduction, which is a 4Fe-4S cluster with a novel $CX_{31-39}CCX_{35-36}CXXC$ motif (49, 55, 128). HdrDE can also be purified with a hydrogenase and catalyzed the reduction of CoM-S-S-CoB with H_2 concomitant with the translocation of protons across the membrane to generate a chemiosmotic membrane potential (56).

Reactions of methylotrophic methanogenesis. Methyl groups attached to methanol, methylamines, and methylthiols enter the core methanogenic pathway at the level of methyl-CoM. Three enzymes are required for the activation of methanol for methanogenesis: two methyltransferases (MT1 and MT2) and corrinoid-containing protein involved in methyl transfer to CoM (20). There are specific enzyme systems for each of the methyl-containing substrates, even within a single genome (16). The corrinoid protein is the methyl transfer center. MT1 catalyzes the methylation of the corrinoid and MT2 catalyzes the transfer of the methyl group to form methyl-CoM. Like all proteins that catalyze the methylation of a thiol, MT2 proteins contain zinc (91). As methyl groups enter at the level of methyl-CoM, there is no opportunity for energy conservation by the Na^+-translocating methyltransferase Mtr. Instead, energy conservation occurs via generation of membrane potential by electron transport to the heterodisulfide involving HdrDE. Therefore, methanogens that lack this form of Hdr do not normally utilize methanol as a substrate. As described above, methanogenesis from methanol has both a reductive and an oxidative branch with the oxidative branch generating the reduced electron carriers needed in the reductive branch.

Deletion of *mtr* and *mer* abolishes growth on methanol, but methanogenesis is still possible (150, 151) demonstrating the presence of a Mtr/Mer bypass pathway in the oxidative branch of

methanogenesis from methanol in *M. barkeri*. Thus, there is a second pathway to generate methylene-H_4MPT from methanol, but the enzymes involved in this oxidation remain unknown.

HdrABC is present in all sequenced members of the *Methanosarcinales* that are capable of growth on methanol. Although these organisms contain the membrane bound, cytochrome containing HdrDE enzyme, HdrABC appears to be important during growth on methanol (7). HdrABC is down regulated in *Methanosarcina acetivorans* during growth on acetate but not methanol. Additionally, when a Δ*hdrABC* mutant was constructed, this organism had a growth defect when grown with methylotrophic substrates. These data suggest a mechanism where ferredoxin produced at the final step of the oxidative branch of methanogenesis from methanol is used to reduce CoM-S-S-CoB via the HdrABC complex rather than through use of the membrane bound HdrDE (7). However, more data is needed to fully characterize the importance of the HdrABC complex during growth on methanol.

The aceticlastic pathway of methanogenesis. Members of the genera *Methanosarcina* and *Methanosaeta* are capable of utilizing acetate to generate CH_4 and CO_2. This is known as the aceticlastic reaction as the molecule of acetate is cleaved to generate both a methyl group (further reduced to methane) and CO (further oxidized to CO_2). Acetate is activated for entry into the aceticlastic reaction by acetate kinase and phosphotransacetylase (Ptr). It appears that ~475 million years ago, these genes were horizontally transferred from *Clostridia* to the ancestor of *Methanosarcina*, suggesting a late evolution of aceticlastic methanogenesis (43). Acetate kinase generates acetyl-phosphate using ATP as the phosphate donor. Ptr then transfers the acetyl group to HS-CoA to generate acetyl-CoA. These enzymes run in the reverse direction in fermentative bacteria to generate acetate as a metabolic byproduct. Acetyl-CoA synthase/carbon monoxide dehydrogenase (Acs/Cdh) is the enzyme that catalyzes the aceticlastic reaction generating CO_2 and methyl-H_4SPT, which enters the main methanogenic pathway and is further reduced to CH_4.

Ptr is proposed to bind acetyl-phosphate with phosphate positioned near the catalytic pocket and the methyl group of acetate protected in a hydrophobic pocket (73). HS-CoA binds and an aspartate residue in the active site pocket removes the proton from the sulfhydryl group allowing $^{-}$S-CoA to react with the carbonyl carbon of acetate. Donating the proton to the remaining phosphate ion regenerates the aspartate and the substrates are released to allow for another

round of catalysis. Acetyl-CoA can enter central metabolism either for energy metabolism or as a substrate for anabolic reactions.

The Acs/Cdh enzyme complex is a five-subunit enzyme that catalyzes a bidirectional reaction. The structure of this complex for *M. barkeri* was recently elucidated (46). During aceticlastic methanogenesis, acetyl-CoA is converted to methyl-H_4SPT as a substrate for methanogenesis; whereas during hydrogenotrophic methanogenesis, methyl-H_4SPT or methyl-H_4MPT are converted to acetyl-CoA as the last step in the acetyl-CoA pathway of CO_2 fixation that is common to all methanogenic archaea (8). Acs/Cdh contains a corrinoid cofactor that facilitates the methyl transfer from acetate to H_4SPT (46). The C-C cleavage reaction takes place in the β subunit via a Ni-Ni-[4Fe-4S] cofactor. CO is transferred to the α subunit, which contains a Ni-Fe active site that catalyzes the oxidation of CO to CO_2 coupled to the reduction of ferredoxin. The produced CO_2 diffuses out of the cell and is converted to HCO_3^- by a carbonic anhydrase positioned outside of the cell, possibly to remove a reaction product from the cytoplasm and keep overall metabolism more energetically favorable (4).

Reduced ferredoxin produced by Acs/Cdh is used to generate both H_2 and membrane potential. The membrane bound Ech hydrogenase that is involved in generation of reduced ferredoxin in the hydrogenotrophic pathway of CO_2 reduction can run in the reverse reaction and generate H_2 by oxidation of ferredoxin (96, 97). It was recently shown that the Ech reaction is fully reversible and also generates a proton motive force during ferredoxin oxidation (153). The stoichiometry of the reverse reaction is one proton translocated per ferredoxin oxidized. The H_2 generated can be used for CoM-S-S-CoB reduction, and the proton motive force used for ATP synthesis.

Regulation of genes involved in substrate utilization

The majority of methanogens are dependent on the reduction of CO_2 with H_2 as the electron donor. Hydrogenotrophic methanogens grow under H_2 pressures ranging from 10 Pa in some natural systems to 220,000 Pa during ideal laboratory conditions (136). Much work has been done to show that the rate of methanogenesis is dependent upon the availability of H_2: methanogens will utilize H_2 even when it is unnecessary for survival. In other words, when H_2 concentrations in excess of what is needed to sustain growth are present in the environment, methanogens will partially uncouple methanogenesis from biosynthesis (for examples see (26, 28)). This phenomenon has been termed overflow metabolism, energy spilling, or growth

uncoupling (118).This phenotypic response to high concentrations of H_2 gas reveals that methanogens are capable of responding to H_2 in the environment. Recent studies have revealed some of the changes that occur in response to H_2 and various other nutrients, and are described below, but regulatory proteins that cause these changes are still uncharacterized. There are many reports that growth in syntrophic culture results in transcriptional changes for methanogenesis genes, hydrogenases, and formate dehydrogenases (127, 157). Despite the lack of candidate regulators, experiments described below show that methanogens are also capable of sensing and responding to H_2 without a dependence on a bacterial partner to propagate signals.

F_{420}-dependent reactions are regulated in response to H_2. Methanogens from phylogenetically distinct lineages show similar regulation of genes encoding F_{420}-dependent products (57, 99, 100). Thus, genes encoding Mtd, Fdh, Mer and the F_{420}-reducing hydrogenases show higher mRNA levels in cells grown with limiting concentrations of H_2. Hmd catalyzes the same reaction as Mtd, but uses H_2 as a direct electron donor rather than F_{420}. Generally, *hmd* expression is inversely correlated with *mtd* expression. Studies looking at protein abundance with *M. maripaludis* show that the differences in mRNA abundance carry over to differences in protein abundance (159). These data are interesting because the ratio of $F_{420}H_2$ to F_{420} in cells is directly correlated with the concentrations of H_2 available for growth (29). Therefore, while cells could be directly sensing H_2 in the environment, the possibility also exists that the intracellular ratio of reduced to oxidized F_{420} is primarily responsible for sensing the H_2 state of the environment. It has been proposed that when oxidized F_{420} builds up, cells increase Mtd, Fdh, Mer, and F_{420}-reducing hydrogenase expression in order to maintain a constant availability of $F_{420}H_2$ for methanogenesis (57). To date, no studies have identified candidate proteins that function as H_2, F_{420}, or $F_{420}H_2$ sensors in methanogens.

Hydrogenase and formate dehydrogenase regulation. As stated above, several hydrogenases and formate dehydrogenases are regulated in response to H_2 or syntrophy; however, there are many additional factors that impact the expression of genes encoding these enzymes. An analysis of *Methanothermobacter thermoautotrophicus* grown with numerous environmental stimuli agreed with previous findings that F_{420}-dependent steps of methanogenesis showed an apparent increase in mRNA abundance during H_2 depletion (71). This study additionally found that stress, such as 500 mM NH_4Cl addition or growth at high temperature, resulted in decreased mRNA abundance for the membrane-bound, energy-

converting hydrogenases Eha and Ehb. These hydrogenases showed a similar expression profile as genes involved in anabolism (CO dehydrogenase/acetyl-CoA synthase, pyruvate oxidoreductase, and 2-oxoglutarate reductase) suggesting their importance for CO_2 assimilation and that cells suppress anabolism during stress (71).

All hydrogenases and formate dehydrogenases encoded in methanogen genomes are metalloenzymes (58, 69). The hydrogenase active sites are of the [Fe], [NiFe], or [NiFeSe] varieties while formate dehydrogenase active sites are [Mo] or [MoSe] containing. When nickel becomes limiting, genes for [Fe] hydrogenase are upregulated while genes for [NiFe] and [NiFeSe] hydrogenases are downregulated (2, 3). Proteins that contain selenium in the form of selenocysteine are generally present in both selenium and cysteine containing forms. The expression of genes encoding the cysteine forms are repressed in the presence of high selenium concentrations (103). Finally, formate dehydrogenase expression is decreased in *Methanobacterium formicicum* when cells are starved for molybdenum (92). All of these data highlight the inherent challenges in studying hydrogenase and formate dehydrogenase regulation. An enzyme such as the F_{420}-reducing [NiFe] hydrogenase of *M. maripaludis* may be regulated in response to at least four different signals: syntrophic growth, H_2 availability, Ni concentration, and Se concentration.

Figures

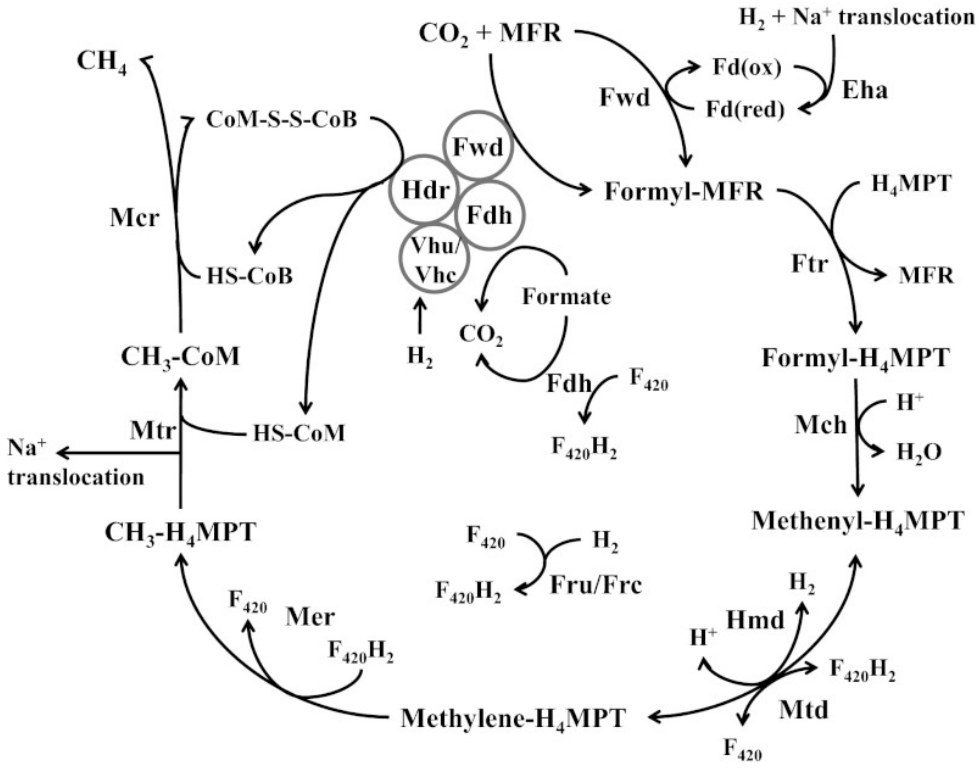

Figure 1.1. The methanogenic pathway in *Methanococcus maripaludis*. Eha, energy-converting hydrogenase A; Fdh, formate dehydrogenase; Fru and Frc, F_{420}-reducing hydrogenases; Ftr, formyl-MFR:H_4MPT formyltransferase; Fwd, formyl-MFR dehydrogenase; Hdr, heterodisulfide reductase; Hmd, H_2-dependent methylene-H_4MPT dehydrogenase; Mch, methenyl-H_4MPT cyclohydrolase; Mcr, methyl-CoM reductase; Mer, methylene-H_4MPT reductase; Mtd, F_{420}-dependent methylene-H_4MPT dehydrogenase; Mtr, methyl-H_4MPT-CoM methyltransferase; Vhu and Vhc, F_{420}-nonreducing (Hdr-associated) hydrogenases. Figure from (79).

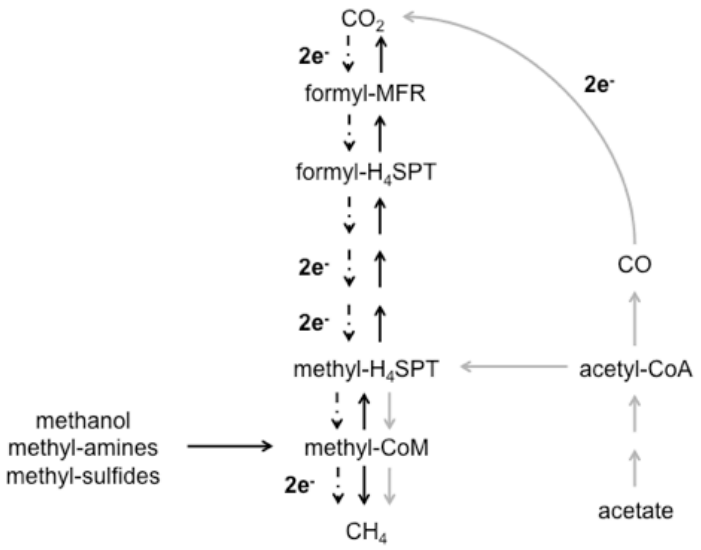

Figure 1.2. Reactions of hydrogenotrophic (dashed arrows) methylotrophic (black arrows) and aceticlastic (grey arrows) methanogenesis in *Methanosarcinales*. All pathways share the reduction of methyl-CoM as the uniting feature. Stoichiometrically, four methylated compounds enter at the level of methyl-CoM and one is oxidized to generate the electrons for the reduction of the other three. In the aceticlastic reaction, the methyl carbon of acetate is reduced to methane using electrons from the carbonyl carbon. The number of electrons transferred in each redox reaction is listed next to the appropriate arrows. MFR, methanofuran; H_4SPT, tetrahydrosarcinopterin; CoM, coenzyme M. Figure modeled from (44).

CHAPTER 2

A protein complex involved in formate utilization and energy conservation

Originally published as an article in *Proceedings of the National Academy of Sciences*:

Costa, Kyle C., Phoebe M. Wong, Tiansong Wang, Thomas J. Lie, Jeremy A. Dodsworth, Ingrid Swanson, June A. Burn, Murray Hackett, John A. Leigh (2010) Protein complexing in a methanogen suggests electron bifurcation and electron delivery from formate to heterodisulfide reductase. *Proc Natl Acad Sci USA*. 107: 11050-11055.

Summary

In methanogenic archaea, the final step of methanogenesis generates methane and a heterodisulfide of coenzyme M and coenzyme B (CoM-S-S-CoB). Reduction of this heterodisulfide by heterodisulfide reductase (Hdr) to regenerate HS-CoM and HS-CoB is an exergonic process. Thauer *et al*. suggested that in hydrogenotrophic methanogens the energy of heterodisulfide reduction powers the most endergonic reaction in the pathway, catalyzed by the formylmethanofuran dehydrogenase, via flavin-based electron bifurcation. Here we present evidence that these two steps in methanogenesis are physically linked. We identify a protein complex from the hydrogenotrophic methanogen, *Methanococcus maripaludis*, that contains Hdr, formylmethanofuran dehydrogenase, F_{420}-nonreducing hydrogenase, and formate dehydrogenase (Fdh). In addition to establishing a physical basis for the electron bifurcation model of energy conservation, the composition of the complex also suggests that either H_2 or formate (two alternative electron donors for methanogenesis) can donate electrons to the heterodisulfide—H_2 via F_{420}-nonreducing hydrogenase or formate via Fdh. Electron flow from formate to the heterodisulfide rather than the use of H_2 as an intermediate represents a previously unknown path of electron flow in methanogenesis. We further tested whether this path occurs by constructing a mutant lacking F_{420}-nonreducing hydrogenase. The mutant displayed growth equal to wild-type with formate but markedly slower growth with hydrogen. The results support the model of electron bifurcation and suggest that formate, like H_2, is closely integrated into the methanogenic pathway.

Introduction

The biochemical steps in methanogenesis from CO_2 are well known, but the interactions that lead to net energy conservation are not well understood. The steps in the pathway are diagrammed in Fig. 1.1 (136). The first step involves the reduction of CO_2 and covalent attachment to a unique cofactor, methanofuran (MFR), via the action of formylmethanofuran dehydrogenase (Fwd) to generate formyl-MFR. This represents an energy-consuming step in the pathway, and is dependent on reduced ferredoxin, thought to be produced at the expense of a chemiosmotic membrane potential via the energy-conserving hydrogenase Eha. Next, the formyl group is transferred to another carrier, tetrahydromethanopterin (H_4MPT), and is then reduced to generate methyl-H_4MPT. The methyl group is then transferred to yet another carrier, coenzyme M (HS-CoM), by methyl-H_4MPT-CoM methyltransferase (Mtr) to generate methyl-S-CoM. At this point, Na^+ ions are translocated across the cell membrane. The final step involves reduction of the methyl group to CH_4 and capture of HS-CoM by coenzyme B (HS-CoB) to form a CoM-S-S-CoB heterodisulfide. In order to regenerate HS-CoM and HS-CoB, another enzyme is used, heterodisulfide reductase (Hdr).

Most methanogens can use H_2 as the electron donor, and many can also use formate. Reduced coenzyme F_{420} ($F_{420}H_2$) is a required intermediate, and can be generated from H_2 by F_{420}-reducing hydrogenase (Fru) or by a cycle involving the enzymes H_2-dependent methylene-H_4MPT dehydrogenase (Hmd) and F_{420}-dependent methylene-H_4MPT dehydrogenase (Mtd) (88). When formate is the electron donor, it is oxidized to CO_2 by a formate dehydrogenase (Fdh) that yields $F_{420}H_2$.

How net energy is conserved in most methanogens is not well understood, since the membrane potential generated during the methyl transfer from H_4MPT to HS-CoM would appear to be depleted by Eha to fuel the reduction of CO_2 to formyl-MFR. The solution to this dilemma apparently resides in the exergonic heterodisulfide reduction step. Methanogens from the order *Methanosarcinales*, known as the methylotrophic methanogens, have a membrane-bound electron transport chain involving the quinone-like methanophenazine and a cytochrome-containing Hdr complex that translocates protons across the cell membrane concomitant with CoM-S-S-CoB reduction, resulting in net energy conservation (136) . However, all other methanogens (the hydrogenotrophic methanogens) lack methanophenazine and cytochromes, have a cytoplasmic Hdr, and are not known to generate a membrane potential at this step (136). Nevertheless, these organisms grow rapidly and are found in numerous anaerobic

environments. It was recently proposed that methanogens without cytochromes use flavin-based electron bifurcation from Hdr to simultaneously reduce CoM-S-S-CoB and reduce ferredoxin for formylmethanofuran dehydrogenase to generate formyl-MFR (136). If this were to occur, then ferredoxin reduction by Eha would not be required and net energy conservation would result.

It was our intention to find protein-protein interactions involving Hdr that may indicate if there are potential pathways for energy conservation that have eluded prior characterization in methanogens without cytochromes. To this end, we performed experiments with the hydrogenotrophic methanogen, *Methanococcus maripaludis*. *M. maripaludis* is ideal for such an undertaking due to its rapid growth under laboratory conditions, a well-developed set of genetic tools (98, 139), the ability to grow in continuous culture under conditions of defined nutrient limitation (52), and the availability of an exhaustive dataset from quantitative measurements of the proteome (158, 159).

Methods

Strain construction. Strains, PCR primers, and plasmids used in this study are described in Table 2.1. MM901 was used as the background strain for all genetic manipulations. To construct MM901, which contains a deletion of the uracil phosphoribosyltransferase gene (Δ*upt*), pBLPrt (98) was digested with MluI-XhoI followed by extension with Klenow (New England Biolabs) and blunt-end ligation to generate pBLPrtsmhpt. This vector was transformed into *M. maripaludis* S2 as described (98) and selected in McCas medium (98) containing 1 mg/mL neomycin followed by selection for a mutant containing the in-frame deletion of *upt* on medium containing 250 μg mL^{-1} 6-azauracil to resolve the merodiploid. MM901 was transformed with constructs derived from the suicide vector pCRUptNeo to make other markerless gene replacements. pCRUptNeo was constructed exactly as described for the suicide vector pCRPrtNeo (98) except the *upt* gene was amplified with Easy-A polymerase (Stratagene) and ligated into the appropriate vectors. To create genomic copies of HdrB1 or HdrB2 with a C-terminal 6x-His tag, the 3' region of the gene for HdrB1 or HdrB2 was PCR amplified using Phusion DNA polymerase (Finnzymes) with primers encoding a 10 amino acid extension and blunt-end ligated to a PCR fragment derived from the downstream genomic region of the gene to place the primer-encoded His-tag at the 3' end of the open reading frame. The fragment was ligated to XbaI-NotI digested PCRUptNeo. The resulting vector was

transformed into strain MM901 as described (98), with selection of the mutant on McCas plates containing the 250 μg mL^{-1} 6-azauracil in place of 8-azahypoxanthine, to make strains MM1263 and MM1264. A genomic copy of FdhA1 was created with a 13 amino acid extension containing a 6xHis-tag in a deletion strain of the *fdh2* locus. First, *fdhA2B2* was deleted to generate MM1262 by PCR amplifying genomic regions flanking the genes with Herculase DNA polymerase (Stratagene), digesting the products with AscI and ligating them together. This construct was transferred to XbaI-NotI digested pCRUptNeo and transformed into MM901 as described above. The FdhA1 gene was PCR amplified and ligated into SpeI-AscI digested pLCW40neo (32) upstream of a 6x-His tag to make pLCW40*fdhA1*. The region downstream of *fdhA1* in S2 genomic DNA was PCR amplified and blunt-end ligated to the 3' end of the gene encoding the His-tag (PCR amplified from pLCW40*fdhA1*) and the construct was transferred into XbaI-NotI digested pCRUptNeo. The resulting plasmid construct was then transformed as above into strain MM1262 to generate MM1265. The region encoding the *vhuA* and *vhuU* genes was deleted following the same procedure as the deletion of *fdh2* except mutants with reduced growth on H_2 were enriched once as described (72) in McCas medium (98) with 2.5 μg mL^{-1} puromycin and a headspace of H_2:CO_2 and colonies screened for the mutation were grown under a N_2:CO_2 atmosphere on formate medium containing 7.5 g L^{-1} noble agar and 250 μg mL^{-1} 6-azauracil. Deletion of *vhcA* in this background was done as described for deletion of *fdh2* except cells were transformed on formate medium and merodiploids were selected with 5 mg mL^{-1} neomycin. The *vhu vhc* double mutant was designated MM1272. Deletion and His-tag constructs were verified by DNA sequencing and mutations were verified by PCR screens and Southern blot.

Growth of strains with hydrogen excess, hydrogen limitation, or formate. Cultures for each strain were grown in a chemostat under conditions of H_2 limitation/phosphate excess or H_2 excess/phosphate limitation as described in (52, 57) and modified in (159). Cultures were grown until steady state was reached and OD_{660} remained stable at ~0.6 for >48 hours. Cultures were then collected as described below. For growth with formate as the sole electron donor cultures were grown in 400-mL batch culture at 37ºC with agitation at 200 rpm with described medium (88) with 20 mM NH_4Cl in place of casamino acids (formate medium). Cultures were grown for ~24 hours to a final OD_{660} of ~0.4 to 0.5 and collected as described below.

***Affinity purification of tagged proteins*.** 400 mL from each chemostat culture was collected

anaerobically as described (32), brought into an anaerobic chamber (Coy Laboratory Products, Grass Lakes, MI) and transferred into a 0.5 L centrifuge bottle. Formate grown cultures were brought directly into an anaerobic chamber and transferred to a 0.5 L centrifuge bottle. Samples were then centrifuged anaerobically at 4ºC at 12,800xg for 25 minutes. The resulting cell pellet was suspended in 1-2 mL residual growth medium and placed in 5-mL glass tubes with an atmosphere of N_2:H_2 (95:5) and stored at -80ºC for up to 2 months. All purifications were done under anaerobic conditions in an atmosphere of N_2:H_2 (95:5) in an anaerobic chamber. Cells were thawed and sonicated on ice using a Microson ultrasonic cell disrupter at setting 8. Cell lysate was centrifuged at 16,000xg for 10 minutes. The crude protein extract was collected and combined with 25 mM HEPES pH 7.5, 10 mM sodium dithionite, 100 mM NaCl, and 10 mM imidazole as binding buffer. Finally, 0.5 mL of Ni^{2+} resin (Novagen Inc.) was added and the mixture was incubated anaerobically at 37ºC while shaking for one hour. After incubation, sample was placed in a Poly-Prep chromatography column (Bio-Rad) under the same atmosphere and the supernatant was allowed to run through the column. The resin was washed 3 times with 5 mL binding buffer, then eluted with the same buffer containing 100 mM (for HdrB1 and HdrB2) or 200 mM (for FdhA1) imidazole. After elution, samples were stored in elution buffer at -80ºC until ready for mass spectrometric analysis. SDS/PAGE of the purified proteins was done with 4-20% gradient gels (Pierce) and is shown in Fig. 2.1.

Mass spectrometry of purified protein samples. After thawing, 100 µL of the sample was diluted with 100 µL of 10% acetonitrile in Millipore water containing sufficient trypsin (Promega sequencing grade) to make the final trypsin-protein ratio approximately 1:3 to 1:10. A larger than normal quantity of trypsin was used due to the presence of dithionite in the elution buffer. After digestion at 37ºC for 12 hours, samples were placed in a Speed-Vac (Jouan RTC60) to bring final volumes to 50 µL. Capillary HPLC/tandem mass spectrometry was performed in a data-dependent manner using a single dimension separation with a Michrom Magic 2002 HPLC modified in-house (158) for capillary operation and interfaced to a Thermo LTQ linear ion trap mass spectrometer. The samples were loaded on a 10 cm × 75 µm i.d. Aqua C18 reversed phase capillary column fabricated in-house, flushed 15 min with Millipore water for desalting, then eluted with a binary gradient as reported previously for the reversed phase portion of a two dimensional separation (158, 159). The raw data files were searched against the *M. maripaludis* inferred protein database (58, 158, 159) using Sequest (39) and peptide level results were organized at the protein level using DTASelect (131) such that all redundant identifications were saved, thus allowing a summation of the spectral counts associated with each protein-encoding

ORF in the database. All Sequest and DTASelect adjustable parameters were set as described (158, 159).

Analysis of mass spectral data. SCs (numbers of peptide detections for a given protein, i.e. spectral counts (45, 85, 167)) has been established as an accurate method for measuring relative protein abundance in *M. maripaludis* (159). For each protein sample analyzed, SCs were tabulated for all proteins that had an SC of at least 10 in at least one sample. Three proteins that were detected in all samples and that did not appear enriched in the experimental strains relative to the control strains were chosen as a basis for normalization (reference proteins). For each protein detected, ratios of SCs in each experimental sample (MM1263, MM1264, or MM1265) to SCs in the control sample (MM901 or MM1262) grown under the same condition were then calculated using each reference protein as follows: normalized ratio = ($SCprotein_{exp}$ $SCprotein_{cont}$) / ($SCref_{exp}$ $SCref_{cont}$).

Analysis of the vhuAU vhcA mutant during growth on H_2/CO_2 or formate. MM901 or MM1272 was grown to OD_{660} ~0.6 in formate medium. Cultures were washed once with 5 mL N-free medium (82) and ~0.5 mL was transferred to tubes containing 5 mL either McCas with a headspace of H_2:CO_2 (80:20) at 40 psi or formate medium with 0.2% casamino acids and a headspace of N_2:CO_2 (80:20) at 30 psi and grown at 37ºC at 200 rpm agitation. Cell density (OD_{660}) was monitored.

Results

***Heterodisulfide reductase complexes with F_{420}-nonreducing hydrogenase, formate dehydrogenase, and formylmethanofuran dehydrogenase*.** To characterize the protein interactions that take place between Hdr and associated proteins, the β subunits of Hdr were C-terminally tagged with a 10 amino acid extension containing a 6x-His tag. The β subunits were used for purification as this subunit has been demonstrated to contain the active site for heterodisulfide reduction (49). The *M. maripaludis* genome encodes two Hdrs (58), and either HdrB1 (strain MM1263) or HdrB2 (strain MM1264) was tagged to determine if there were differences between the protein interactions of each. In addition, we had preliminary evidence (based on early purification experiments) that one of two Fdhs encoded in the *M. maripaludis* genome might be included in protein complexes with Hdr. Therefore, we also constructed a strain (MM1265) in which FdhA1 was C-terminally tagged with a 13 amino acid extension

containing a 6x-His tag. To avoid any confounding influence of the second formate dehydrogenase, Fdh2, the FdhA1 His-tag was constructed in a background strain that contained an in-frame deletion of the *fdh2* gene cluster. In each case, the His-tagged version of the protein replaced the wild type gene in the genome. Growth experiments showed that each His-tagged protein was functional (Fig. 2.2). Thus, a strain containing His-tagged HdrB1 and a null mutation in *hdrB2* grew normally, as did a strain containing His-tagged HdrB2 and a null mutation in *hdrB1*. Since Hdr is essential, each His-tagged protein must be functional. Similarly, MM1265 containing His-tagged FdhA1 and a deletion of *fdh2* grew normally on formate. Since Fdh is required for growth on formate, His-tagged FdhA1 must be functional.

For protein preparations, three experimental strains were grown: MM1263 containing His-tagged HdrB1, MM1264 containing His-tagged HdrB2, and MM1265 containing His-tagged FdhA1. Two control strains were also grown: the parental strain MM901 containing no His-tagged proteins, and strain MM1262 containing the deleted *fdh2* and no His-tagged proteins. All five strains were grown under three conditions: hydrogen excess or limitation in a chemostat and batch culture with formate as the sole electron donor. This is because several genes are regulated in response to hydrogen availability in *M. maripaludis* (57), and there could be differences in the composition of the Hdr complex in response to different growth conditions. Cell extracts were made from all 15 cultures and protein purifications were done anaerobically using Ni-affinity columns. Purified samples were analyzed by mass spectrometry. Spectral counts (SC) were tabulated for any protein that returned ≥10 SC in any of the three growth conditions with the three experimental strains (all SC data can be found at http://www.pnas.org/content/suppl/2010/05/21/1003653107.DCSupplemental/st01.docx).

For each protein, SCs were compared. From an initial inspection of the data it appeared that there were two groups of proteins—those that consistently had similar SCs in all five strains (background proteins), and those that had markedly greater SCs in MM1263 and MM1264 (the experimental strains) compared to MM901 (the control strain) or in MM1265 (experimental) to MM1262 (control). To distinguish clearly between those groups of proteins, three proteins among the background proteins (reference proteins) were used as the basis for the calculation of normalized SC ratios (see Methods). The results are presented in Table 2.3. A protein was considered enriched by co-purification with the His-tagged protein if the normalized SC ratio was greater by at least three standard deviations than the average ratio for the 13 background proteins, or if more than 5 SCs were detected in the experimental sample while none was seen

in the control (NC). The results are summarized in Table 2.4. Subunits from five different proteins copurified with both of the His-tagged HdrBs and with His-tagged FdhA1: These proteins were Hdr1, Hdr2, Fdh1, the selenocysteine-containing F_{420}-nonreducing hydrogenase (Vhu), and the tungsten-containing formylmethanofuran dehydrogenase (Fwd). The findings supported these conclusions regardless of which of the three reference proteins was used for the normalization calculation. None of these proteins was observed to bind nonspecifically to His-tagged constructs in *M. maripaludis* (32). In general, multiple subunits of a given protein were enriched in the experimental samples, although a few subunits were not detected. Generally, the relative abundances of subunits from each protein were in agreement with those found in proteomic studies of whole cell extracts from *M. maripaludis* (158, 159), and those subunits that were not detected here were detected at low levels in the whole proteome. The five proteins were enriched in samples from all three growth conditions, except for Fdh1 under H_2 excess and all proteins under H_2 excess with His-tagged FdhA1. The absence of Fdh in these samples is not surprising because *fdh* expression is markedly down-regulated when cells are grown under H_2 excess (57).

Each of the four enzymes represented in the complex is encoded in the genome in two different forms, but only in the case of the HdrB and HdrC subunits were both purified in the complexes. Thus, both HdrB1 and HdrB2, and both HdrC1 and HdrC2, were generally present in the complex; however, both are not required to make a functional Hdr (Fig. 2.2). Hdr is a tetramer of trimers in the $\alpha_4\beta_4\gamma_4$ configuration in methanogens (54), and evidently the B1 and B2 subunits are interchangeable, as are the C1 and C2 subunits. In the case of the F_{420}-nonreducing hydrogenase and HdrA, the two forms of the enzyme contain selenocysteine (Vhu and $HdrA_u$) or cysteine (Vhc and $HdrA_c$). Only the selenocysteine forms were detected here, consistent with previous studies of regulation by selenium predicting that only the former should be expressed in our selenium-containing medium (9). Indeed, in two studies of the whole proteome of *M. maripaludis* the selenocysteine proteins were detected at least 100-fold more frequently than the cysteine proteins (158, 159). Two formylmethanofuran dehydrogenases are represented in the genome, tungsten-containing (Fwd) and molybdenum-containing (Fmd). Only Fwd was detected here, and in the whole proteome the Fwd subunits were detected at least 10-fold more frequently. Of the two Fdhs, Fdh1 found in the complex with Hdr was also detected at least 10-fold more frequently in the proteome than Fdh2. In contrast, the HdrB and C subunits were detected in more similar amounts in the proteome, with HdrB2 and C2 detected only two to four-fold more frequently than HdrB1 and C1. Hence, the enzyme forms detected in the complexes

with Hdr and Fdh1 were consistently those that were more frequently detected in the proteome.

F_{420}-nonreducing hydrogenase is not essential for growth on formate. The presence of Fdh in a complex with Hdr suggested the possibility of direct electron flow between these two enzymes. If this is the case, then F_{420}-nonreducing hydrogenase might not be needed for growth on formate because H_2 generated from formate (via $F_{420}H_2$) (88) would not be necessary for heterodisulfide reduction. To test this hypothesis, we constructed in-frame deletions that eliminated the genes encoding the putative active subunits for hydrogen oxidation in both copies of the F_{420}-nonreducing hydrogenase, *vhuAU* and *vhcA*. *M. maripaludis* was transformed with these constructs and a Δ*vhuAU* Δ*vhcA* mutant (MM1272) was successfully obtained after growth on formate. The mutant grew on formate similarly to the wild type strain, but grew poorly on H_2 (Fig. 2.3). The slight growth on H_2 might be explained via a poorly understood $F_{420}H_2$:heterodisulfide oxidoreductase activity that has been demonstrated for the closely related *Methanococcus voltae* (19). In any case, F_{420}-nonreducing hydrogenase clearly plays the major role in heterodisulfide reduction with H_2 but is unnecessary for heterodisulfide reduction with formate.

Discussion

We have reported here evidence for a protein complex that comprises four separate enzymes: heterodisulfide reductase, F_{420}-nonreducing hydrogenase, formate dehydrogenase, and formylmethanofuran dehydrogenase. The co-elution of these proteins with three separate protein subunits under three different growth conditions strongly suggests that the observed complex exists *in vivo* and may be involved in energy conservation. The interaction of Hdr with F_{420}-nonreducing hydrogenase was suggested previously in studies of these enzymes in *Methanothermobacter marburgensis* (125, 130). Indeed, in some methanogens the α subunit of Hdr is fused to the δ subunit of the F_{420}-nonreducing hydrogenase (130). However, the presence of Fdh and Fwd in the complex with Hdr is novel. The results provide new insight into electron flow during methanogenesis with formate, and supports the electron bifurcation mechanism for energy conservation during methanogenesis. A model for the role of the protein complex is presented in Fig. 2.4.

The Fdh-Hdr interaction. Previously only the F_{420}-nonreducing hydrogenase was thought to deliver electrons to Hdr. Hdr purified from *M. marburgensis* was observed to associate with an

F_{420}-nonreducing hydrogenase, but not with Fdh (125, 130). However, this organism is not known to grow with formate as the sole electron donor (148). The association of Fdh with Hdr suggests a pathway of electron flow to Hdr that does not involve H_2. Electrons may flow from formate to Hdr via Fdh. In support of this hypothesis, we were able to eliminate Vhu and Vhc and retain rapid growth on formate, while growth was markedly decreased on H_2 (Fig. 2.3). This finding contrasts with an unsuccessful attempt to delete *vhuU* in *M. voltae* (108), even under conditions of selenium starvation where this organism would theoretically generate a truncated VhuU peptide. However, in that study only H_2, not formate, was used as the electron donor. To our knowledge our Δ*vhuAU* Δ*vhcA* mutant is the only mutant thus far among hydrogenotrophic methanogens that has a growth defect specifically on H_2. Its phenotype supports a recent suggestion that H_2 may not be a required intermediate for methanogenesis from formate in *M. maripaludis* (88), although it may still be needed for biosynthesis. Interestingly, most members of the *Methanomicrobiales* lack genes encoding the F_{420}-nonreducing hydrogenases yet still grow well on H_2; this suggests that there may still be other proteins that interact with Hdr and mediate electron transfer from H_2 to Hdr for reduction of CoM-S-S-CoB in these organisms (perhaps the F_{420}-reducing hydrogenase) (135).

It should be noted that in addition to providing electrons for Hdr during growth on formate, Fdh must also provide $F_{420}H_2$, which is required for at least one step in methanogenesis (methylene-H_4MPT reductase (Mer)), and which is also used by F_{420}-dependent methylene-H_4MPT dehydrogenase (Mtd). It has been suggested that $F_{420}H_2$ could also donate electrons to Hdr, based on work in *M. voltae* that observed an interaction between Hdr and F_{420}-reducing hydrogenase in purified membrane fractions (19). However, deletion of F_{420}-reducing hydrogenase in *M. maripaludis* had no effect when cells were grown on formate, suggesting that $F_{420}H_2$:heterodisulfide oxidoreductase activity is not important under these conditions (88).

The Hdr-Fwd interaction. Observations made over 30 years ago demonstrated that CH_3-S-CoM addition to cell extracts stimulated CO_2 reduction to methane (48). This phenomenon, termed the RPG effect, is only observed in methanogens that lack cytochromes. The Hdr-Fwd interaction found here can explain the RPG effect by invoking electron transfer to Fwd through the action of Hdr. In fact, an interaction between Hdr and Fwd was first proposed in 1988 (116) and was later implicated in potential flavin-based electron bifurcation by Hdr to drive the first step in methanogenesis (136). Because previous Hdr purifications did not show any interaction between Hdr and Fwd (125, 130), it is likely that the physical interaction between these two

proteins is weak, and our method of purification, which involved minimal manipulation, was able to retain Fwd bound to Hdr. HdrA is known to contain one mole of FAD per mole of HdrA (125), and it is likely that, through flavin-based electron bifurcation, HdrA can reduce ferredoxin that is then used by Fwd. The FwdF subunit of formylmethanofuran dehydrogenase is purified as part of the complex and is a predicted polyferredoxin (63); this may be the ferredoxin that mediates electron transfer to Fwd after bifurcation.

Conventional models of methanogenesis hold that reduced ferredoxin used to power the endergonic reduction of CO_2 to formyl-MFR is generated via the action of Eha. Studies of formylmethanofuran dehydrogenase activity in *M. marburgensis* demonstrated that it copurified with a hydrogenase activity, but the identity of the hydrogenase, and any other interacting peptides, was not determined (147). However, Eha consumes membrane potential to generate reduced ferredoxin, leaving little or no net energy for ATP synthesis. CO_2 reduction to formyl-MFR using electrons bifurcated by Hdr would retain membrane potential for ATP synthesis (136). The *in vivo* action of Eha may, therefore, be to generate reduced ferredoxin for anabolism as is the case for the paralogous Ehb (110). However, it is tempting to speculate that under certain conditions Eha can still play a role in CO_2 reduction to formyl-MFR. There is a well characterized phenomenon in methanogens without cytochromes where growth is decoupled from methanogenesis under certain conditions (28). This may be ecologically beneficial in that rapid utilization of nutrients such as H_2 can result in methanogens without cytochromes outcompeting other organisms in the environment. Electron flow from the Eha hydrogenase would result in a futile cycle where methane production and hydrogen consumption rates would increase. Reduction of ferredoxin by Eha may dominate at high partial pressures of H_2 while reduction of ferredoxin by Hdr may dominate at low partial pressures.

Tables and figures

Table 2.1: Strains, Primers, and plasmids used in this study

Strain	Notes
S2	Wild type *M. maripaludis* (154)
MM901	S2 with an in frame deletion of the uracil phosphoribosyltransferase gene (Mmp0680)
MM1262	MM901 with an in frame deletion of *fdhA2B2* (Mmp 0138 and 0139)
MM1263	MM901 with a 6x C-terminal Histidine tag on HdrB1 (Mmp1155)
MM1264	MM901 with a 6x C-terminal Histidine tag on HdrB2 (Mmp1053)
MM1265	MM1262 with a 6x C-terminal Histidine tag on FdhA1 (Mmp1298)
MM1272	MM901 with an in frame deletion of *vhuAU* and *vhcA* (Mmp 1694, 1693, and 0823)

Primer	Sequence (5'-3')	notes
HdrB1-Cterm-F	GGCCGCGGCCGCGGTACTGAAAAAATTGCTGAAAGAG	NotI
HdrB1-ds-R	CTAGTCTAGATTCCATTGGATGTTCTACTCCTGC	XbaI
HdrB1-Cterm-R/His	TTAGTGATGGTGATGGTGATGACGACCTTCGATTTCCATATTTATTCCAAGC	5' phosphate
HdrB1-ds-F	AATATTTAATCCTTAGACGGAGGGG	5' phosphate
HdrB2-ds-R	GGCCGCGGCCGCATATACGTTTCAAAAAACATCGAATCCG	NotI
HdrB2-ds-F	TTCCTTTTTTCTTTTTTTAATAAAAATTTAAAATTTAAAAATAATATTTATTCGATTG	5' phosphate
HdrB2-cterm-his-R	TTAGTGATGGTGATGGTGATGACGACCTTCGATGTATCCTAATTTTTGAAGTAATGG	5' phosphate
HdrB2-cterm-F	CTAGTCTAGAGAGAAAATGTTGTAAAACCATTGGCTG	XbaI
VhuU-ds-F	AAAAGGCGCGCCTAAAACTTCTCTAACCGAACCC	AscI
VhuA-us-R	AAAAGGCGCGCCACATAGAGTCACCATCC	AscI
Fwd_ds_R	AAAATCTAGACGAGTTATTTTCTTCAGTCGTAGGATACCG	XbaI
VhuA-us-F	AAAAGCGGCCGCTCTGATGTAGTTAAAGCAG	NotI
VhcA-us-F	AAAAGCGGCCGCTGGATTATATTCTTCCAGG	NotI
VhcA-us-R	AAAAGGCGCGCCACATTATATCACCGTATTTAG	AscI
VhcA-ds-F	AAAAGGCGCGCCTAGGGGATATCATGATCAAG	AscI
VhcA-ds-R	AAAATCTAGAACAAGAATCTTTGTCAACTACTGC	XbaI
Mmp0138UrevAscI	AAGGCGCGCCCGGTCATTATTCCACCTTTTAATTTTATAC	AscI
Mmp0139DforAscI	AAGGCGCGCCTTAATGATAGTTACAGGTATGCCTAATTTC	AscI
Mmp0139DrevNotI	AAGCGGCCGCTTGTTTCTCTTTGTTTTGAAAGAACATACG	NotI
Mmp0138UforXbaI	AATCTAGAATGAATGTCACTTTCTAAGATGTGCAAC	XbaI
wlgstartsrev	GCATTTCACCTATTAGTTATCTATAAAATTATAATATC	
wlgTAATGTCC	TAATGTCCTTAACAATATCTATTATCTC	
Mmp1298for	ATGGAATTAGACTTCATTCATACGATTTGC	
Mmp1298revAscC	GTGGCGCGCCTATTTTTTCCACCTTTGCAGCAC	AscI
Mmp1298forCXbaI	AATCTAGAGTGAAGACCCTGGAACTCCAATTCTCC	XbaI
Mmp1298DrevNotI	AAGCGGCCGCCTTGTCGATTTCTTCTTTTACAACGTCTTTGGG	NotI
Mmp1298Dfor	TTTTCCCAAAATCGGGATTTTAAACGAGGG	
Mmp1298revC	TTAGTGATGGTGATGGTGATGGACGACCTTCGATGGCGCGCCTATTTTTTCCACC	
HdrB2_100-400_F	AAAAGCGGCCGCTAGATATGCCTGGTGCATCC	NotI
HdrB2_100-400_R	AAAAGGATCCTGTCTACACCGATTTCTTTGTAG	BamHI
HdrB2_400-700_F	AAAAATCGATAAATCAGAGAAAATGTTGTAAAACCATTGGC	ClaI
HdrB2_400-700_R	AAAACTCGAGAAGAATGGACATACGTTAACTGTAGC	XhoI
HdrB1_100-400_F	AAAAGCGGCCGCTTGGAATACAATTGCACCC	NotI
HdrB1_100-400_R	AAAAGGATCCCAAAATAAAGTACTTCCGTTAAGTG	BamHI
HdrB1_400-700_F	AAAAATCGATATTATGGTACTGAAAAAATTGCTGAAAGAG	ClaI
HdrB1_400-700_R	AAAACTCGAGCATACTTCCGTTACACAATCGC	XhoI
UptBgl2	GGAAGATCTTTATTCTAAATTGTGCATTTGTG	BglII
UptNsi1	CCAATGCATGATAAAAGATGAAAGATGGG	NsiI

Plasmids	Description	Reference
pCRuptneo	Similar to pCRprtneo from (98). *prt* gene replaced with *upt* gene.	this study
pBLPrt	plasmid containing *neo*^{R}, *hpt,* and Δ*upt*.	(98)
pBLPrtsmhpt	pBLPrt with a deletion of most of the *hpt* gene	this study
pLCW40neo	Expression vector for *M. maripaludis* S2 His-tag linker and *neo*^{R}	(32)
pCRuptΔ*fdhA2B2*	In-frame deletion of *fdhA2B2* in pCRuptneo	this study
pCRuptΔ*vhuAU*	In-frame deletion of *vhuAU* in pCRuptneo	this study
pCRuptΔ*vhcA*	In-frame deletion of *vhcA* in pCRuptneo	this study
pCRupt*hdrB1*-his	C-termial His-tag encoded *hdrB1* in pCRuptneo	this study
pCRupt*hdrB2*-his	C-termial His-tag encoded *hdrB2* in pCRuptneo	this study
pCRupt*fdhA1*-his	C-termial His-tag encoded *fdhA1* in pCRuptneo	this study
pLCW40*fdhA1*	*fdhA1* upstream of His-tag linker in pLCW40neo	this study
pJK3	pJK3 suicide vector containing puromycin N-acetyl-transferase (*pac*)	(95)
pJK3*hdrB1::pac*	pJK3 with the middle of *hdrB1* disrupted with the *pac* gene	this study
pJK3*hdrB2::pac*	pJK3 with the middle of *hdrB2* disrupted with the *pac* gene	this study

Table 2.2: Normalized SC ratios. Non-shaded squares indicate enrichment in purified his-tagged protein complex. Values are normalized ratios of SCs for experimental strain specified to control strain MM901 or MM1262. See Methods for calculation of normalized ratios.

		hydrogen excess								
protein		MM1263			MM1264			MM1265		
		E_{Slp}	E_{PycA}	E_{GapN}	E_{Slp}	E_{PycA}	E_{GapN}	E_{Slp}	E_{PycA}	E_{GapN}
MMP1697	HdrA	27.6	33.8	26.8	13.1	17.6	49.4	0.4	0.9	0.6
MMP1155	HdrB1	NC(155)	NC(155)	NC(155)	NC(12)	NC(12)	NC(12)	ND	ND	ND
MMP1053	HdrB2	6	7.4	5.9	14.8	20	56.1	ND	ND	ND
MMP1154	HdrC1	NC(45)	NC(45)	NC(45)	NC(11)	NC(11)	NC(11)	ND	ND	ND
MMP1054	HdrC2	10.4	12.7	10.1	11.3	15.1	42.7	ND	ND	ND
MMP1298	FdhA	1.4	1.8	1.4	0.8	1.1	3.2	ND	ND	ND
MMP1297	FdhB	ND	ND	ND	ND	ND	ND	ND	ND	ND
MMP1694	VhuA	72.6	89.1	70.6	41.1	55.1	155.3	ND	ND	ND
MMP1696	VhuD	15.3	18.8	14.9	8.9	12	33.8	ND	ND	ND
MMP1695	VhuG	NC(53)	NC(53)	NC(53)	NC(12)	NC(12)	NC(12)	ND	ND	ND
MMP1693	VhuU	NC(45)	NC(45)	NC(45)	ND	ND	ND	ND	ND	ND
MMP1248	FwdA	15.1	18.5	14.7	8.3	11.1	31.3	0.6	1.3	0.8
MMP1691	FwdB	25.8	31.6	25.1	19.8	26.5	74.7	1	1.9	1.2
MMP1249	FwdC	36.4	44.7	35	20.7	27.8	78.2	ND	ND	ND
MMP1247	FwdD	NC(18)	NC(18)	NC(18)	NC(7)	NC(7)	NC(7)	ND	ND	ND
MMP1245	FwdF	NC(24)	NC(24)	NC(24)	NC(21)	NC(21)	NC(21)	ND	ND	ND
MMP1520	unknown	1	1.3	1	0.5	0.6	1.7	0.6	1.2	0.8
MMP1370		1	1.2	1	0.5	0.7	1.9	0.7	1.4	0.9
MMP0658	unknown	2	2.4	1.9	1.5	2	5.7	0.4	0.9	0.5
MMP0164	CbiX	0.7	0.9	0.7	0.3	0.4	1	0.8	1.5	1
MMP0383	Slp	1	1.2	0.9	1	1.3	3.8	0.5	1	0.6
MMP0269	unknown	0.6	0.7	0.5	ND	ND	ND	0.9	1.8	1.2
MMP1515	hsp60	0.9	1.1	0.9	1.4	1.9	5.3	0.8	1.5	0.9
MMP0477	unknown	ND	ND	ND	1.4	1.9	5.3	1	1.9	1.2
MMP0133	guaB	ND	ND	ND	ND	ND	ND	1.3	2.5	1.6
MMP0258	rpl12p	ND	ND	ND	ND	ND	ND	ND	ND	ND
MMP0548	hisB	1.2	1.5	1.2	ND	ND	ND	0.6	1.1	0.7
MMP0341	pycA	0.8	1	0.8	0.7	1	2.8	1	2	1.3
MMP1487	gapN	1	1.3	1	0.3	0.4	1	0.8	1.6	1
Average of rows MMP1520 – MMP1487		1.0	1.3	1.0	0.8	1.1	3.2	0.8	1.5	1.0
Average + 3 S.D.		2.2	2.6	2.1	2.3	3.1	8.9	1.5	2.9	1.9

E_{Slp}, E_{PycA}, E_{GapN}: The reference protein Slp, PycA, or GapN was used for normalization

ND ("not detected"), SC less than or equal to 5 in experimental sample.

NC ("no control"), SC greater than 5 in experimental sample and SC = 0 in control sample. Numbers in parentheses are SCs from experimental sample.

Non-shaded, normalized ratio exceeds the average of the last 13 rows (proteins not enriched in purified his-tagged protein complex) + 3 standard deviations, or NC.

		hydrogen limited								
protein		MM1263			MM1264			MM1265		
		E_{Slp}	E_{PycA}	E_{GapN}	E_{Slp}	E_{PycA}	E_{GapN}	E_{Slp}	E_{PycA}	E_{GapN}
MMP1697	HdrA	167.2	95	53.2	252.1	491.1	160.4	77	127.3	149.5
MMP1155	HdrB1	NC(71)	NC(71)	NC(71)	NC(17)	NC(17)	NC(17)	NC(20)	NC(20)	NC(20)
MMP1053	HdrB2	NC(31)	NC(31)	NC(31)	NC(142)	NC(142)	NC(142)	42.9	70.9	83.3
MMP1154	HdrC1	NC(24)	NC(24)	NC(24)	ND	ND	ND	ND	ND	ND
MMP1054	HdrC2	NC(9)	NC(9)	NC(9)	NC (67)	NC(67)	NC (67)	26.4	43.6	51.3
MMP1298	FdhA	9.7	5.5	3.1	16.7	32.6	10.7	21	34.7	40.8
MMP1297	FdhB	NC(16)	NC(16)	NC(16)	NC(23)	NC(23)	NC(23)	NC(46)	NC(46)	NC(46)
MMP1694	VhuA	NC(12)	NC(12)	NC(12)	NC(29)	NC(29)	NC(29)	NC(20)	NC(20)	NC(20)
MMP1696	VhuD	NC(46)	NC(46)	NC(46)	NC(73)	NC(73)	NC(73)	NC(31)	NC(31)	NC(31)
MMP1695	VhuG	ND	ND	ND	ND	ND	ND	NC(6)	NC(6)	NC(6)
MMP1693	VhuU	ND	ND	ND	ND	ND	ND	ND	ND	ND
MMP1248	FwdA	18.2	10.3	5.8	19.3	37.5	12.3	18.2	30	35.3
MMP1691	FwdB	8.4	4.8	2.7	20.1	40.7	13.3	2.8	4.7	5.5
MMP1249	FwdC	NC(29)	NC(29)	NC(29)	NC(96)	NC(96)	NC(96)	NC(42)	NC(42)	NC(42)
MMP1247	FwdD	NC(9)	NC(9)	NC(9)	NC(23)	NC(23)	NC(23)	NC(14)	NC(14)	NC(14)
MMP1245	FwdF	NC(15)	NC(15)	NC(15)	NC(8)	NC(8)	NC(8)	NC(7)	NC(7)	NC(7)
MMP1520	unknown	1.5	0.9	0.5	1.8	3.6	1.2	0.6	1	1.3
MMP1370		0.9	0.5	0.3	ND	ND	ND	ND	ND	ND
MMP0658	unknown	0.9	0.5	0.3	0.9	1.8	0.6	1	1.7	2
MMP0164	CbiX	4.4	1.1	0.6	0.9	4.8	0.5	0.7	1.2	1.4
MMP0383	Slp	ND	ND	ND	1	1.9	0.6	1	1.7	1.9
MMP0269	unknown	1.8	1	0.6	ND	ND	ND	ND	ND	ND
MMP1515	hsp60	ND	ND	ND	ND	ND	ND	ND	ND	ND
MMP0477	unknown	ND	ND	ND	ND	ND	ND	ND	ND	ND
MMP0133	guaB	ND	ND	ND	ND	ND	ND	ND	ND	ND
MMP0258	rpl12p	ND	ND	ND	ND	ND	ND	ND	ND	ND
MMP0548	hisB	ND	ND	ND	ND	ND	ND	ND	ND	ND
MMP0341	pycA	1.8	1	0.6	0.5	1	0.3	0.6	1	1.2
MMP1487	gapN	3.1	1.8	1	1.6	3	1	0.5	0.9	1
Average of rows MMP1520 – MMP1487		2.1	1.0	0.6	1.1	2.7	0.7	0.7	1.3	1.5
Average + 3 S.D.		5.9	2.3	1.3	2.6	6.9	1.7	1.4	2.3	2.7

E_{Slp}, E_{PycA}, E_{GapN}: The reference protein Slp, PycA, or GapN was used for normalization

ND ("not detected"), SC less than or equal to 5 in experimental sample.

NC ("no control"), SC greater than 5 in experimental sample and SC = 0 in control sample. Numbers in parentheses are SCs from experimental sample.

Non-shaded, normalized ratio exceeds the average of the last 13 rows (proteins not enriched in purified his-tagged protein complex) + 3 standard deviations, or NC.

		Formate								
protein		MM1263			MM1264			MM1265		
		E_{Slp}	E_{PycA}	E_{GapN}	E_{Slp}	E_{PycA}	E_{GapN}	E_{Slp}	E_{PycA}	E_{GapN}
MMP1697	HdrA	NC(64)	NC(64)	NC(64)	NC(142)	NC(142)	NC(142)	47.3	12.9	24.9
MMP1155	HdrB1	NC(31)	NC(31)	NC(31)	NC(12)	NC(12)	NC(12)	NC(14)	NC(14)	NC(14)
MMP1053	HdrB2	NC(18)	NC(18)	NC(18)	NC(61)	NC(61)	NC(61)	NC(61)	NC(61)	NC(61)
MMP1154	HdrC1	NC(29)	NC(29)	NC(29)	NC(8)	NC(8)	NC(8)	NC(9)	NC(9)	NC(9)
MMP1054	HdrC2	NC(11)	NC(11)	NC(11)	NC(32)	NC(32)	NC(32)	NC(20)	NC(20)	NC(20)
MMP1298	FdhA	NC(19)	NC(19)	NC(19)	NC(55)	NC(55)	NC(55)	NC(128)	NC(128)	NC(128)
MMP1297	FdhB	NC(16)	NC(16)	NC(16)	NC(15)	NC(15)	NC(15)	NC(33)	NC(33)	NC(33)
MMP1694	VhuA	NC(49)	NC(49)	NC(49)	NC(53)	NC(53)	NC(53)	NC(65)	NC(65)	NC(65)
MMP1696	VhuD	NC(22)	NC(22)	NC(22)	NC(35)	NC(35)	NC(35)	NC(26)	NC(26)	NC(26)
MMP1695	VhuG	NC(9)	NC(9)	NC (9)	NC(12)	NC(12)	NC(12)	NC(6)	NC(6)	NC(6)
MMP1693	VhuU	ND	ND	ND	ND	ND	ND	ND	ND	ND
MMP1248	FwdA	NC(36)	NC(36)	NC(36)	NC(52)	NC(52)	NC(52)	NC(20)	NC(20)	NC(20)
MMP1691	FwdB	NC(16)	NC(16)	NC(16)	NC(41)	NC(41)	NC(41)	NC(13)	NC(13)	NC(13)
MMP1249	FwdC	NC(30)	NC(30)	NC(30)	NC(75)	NC(75)	NC(75)	9.7	2.6	5.1
MMP1247	FwdD	ND	ND	ND	NC(10)	NC(10)	NC(10)	NC(7)	NC(7)	NC(7)
MMP1245	FwdF	NC(14)	NC(14)	NC(14)	NC(11)	NC(11)	NC(11)	NC(6)	NC(6)	NC(6)
MMP1520	unknown	0.4	1.1	1.1	1.3	3.6	4.7	NC(19)	NC(19)	NC(19)
MMP1370		0.3	0.9	0.9	ND	ND	ND	ND	ND	ND
MMP0658	unknown	ND	ND	ND	ND	ND	ND	ND	ND	ND
MMP0164	CbiX	0.2	0.5	0.5	0.4	1.1	1.5	NC(13)	NC(13)	NC(13)
MMP0383	Slp	1	2.7	2.6	ND	ND	ND	1.5	0.4	0.8
MMP0269	unknown	ND	ND	ND	ND	ND	ND	ND	ND	ND
MMP1515	hsp60	ND	ND	ND	ND	ND	ND	2	0.5	1
MMP0477	unknown	ND	ND	ND	ND	ND	ND	ND	ND	ND
MMP0133	guaB	ND	ND	ND	ND	ND	ND	1.1	0.3	0.6
MMP0258	rpl12p	ND	ND	ND	ND	ND	ND	6	1.6	3.2
MMP0548	hisB	0.7	1.9	1.9	1	2.7	3.6	ND	ND	ND
MMP0341	pycA	0.4	1	1	ND	ND	ND	3.7	1	2
MMP1487	gapN	0.4	1	1	0.3	0.8	1	1.9	0.5	1
Average of rows MMP1520 – MMP1487		0.5	1.3	1.3	0.8	2.1	2.7	2.7	0.7	1.4
Average + 3 S.D.		1.3	3.5	3.4	2.2	6.0	7.9	8.2	2.2	4.4

E_{Slp}, E_{PycA}, E_{GapN}: The reference protein Slp, PycA, or GapN was used for normalization

ND ("not detected"), SC less than or equal to 5 in experimental sample.

NC ("no control"), SC greater than 5 in experimental sample and SC = 0 in control sample. Numbers in parentheses are SCs from experimental sample.

Non-shaded, normalized ratio exceeds the average of the last 13 rows (proteins not enriched in purified his-tagged protein complex) + 3 standard deviations, or NC.

Table 2.3. Proteins enriched in purified complexes.

	H_2-excess[a]			H_2-limited			formate		
	MM1263[b]	MM1264	MM1265	MM1263	MM1264	MM1265	MM1263	MM1264	MM1265
$HdrA_u$	+[c]	+	-	+	+	+	+	+	+
HdrB1	+	+	ND[d]	+	+	+	+	+	+
HdrB2	+	+	ND	+	+	+	+	+	+
HdrC1	+	+	ND	+	ND	ND	+	+	+
HdrC2	+	+	ND	+	+	+	+	+	+
FdhA1	-	-	ND	+	+	+	+	+	+
FdhB1	ND	ND	ND	+	+	+	+	+	+
FwdA	+	+	-	+	+	+	+	+	+
FwdB	+	+	-	+	+	+	+	+	+
FwdC	+	+	ND	+	+	+	+	+	+
FwdD	+	+	ND	+	+	+	ND	+	+
FwdF	+	+	ND	+	+	+	+	+	+
VhuA	+	+	ND	+	+	+	+	+	+
VhuD	+	+	ND	+	+	+	+	+	+
VhuG	+	+	ND	ND	ND	+	+	+	+
VhuU	+	ND	ND	ND	ND	ND	ND	ND	ND

[a] growth condition

[b] experimental strain. MM1263, His-tagged HdrB1; MM1264, His-tagged HdrB2; MM1265, His-tagged FdhA1.

[c] + or -. + = SC values relative to control samples support enrichment in protein complex (unshaded squares in Table S2). - = SC values relative to control samples do not support enrichment in protein complex (shaded squares in Table S2).

[d] ND = not detected (SC less than or equal to 5 in experimental sample).

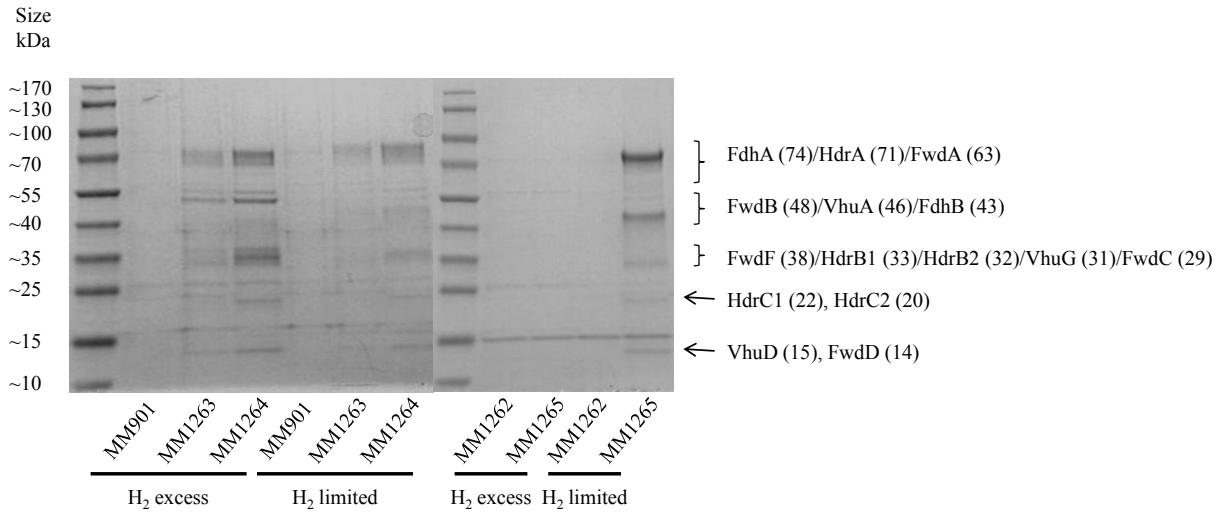

Figure 2.1. SDS/PAGE for purifications of the complex from cultures grown with either excess or limiting H_2. Approximate positions of the purified bands are indicated with their predicted molecular weight in kDa in parentheses. MM901 and MM1262, controls; MM1265, FdhA1-6xHis; MM1263, HdrB1-6xHis; MM1264, HdrB2-6xHis.

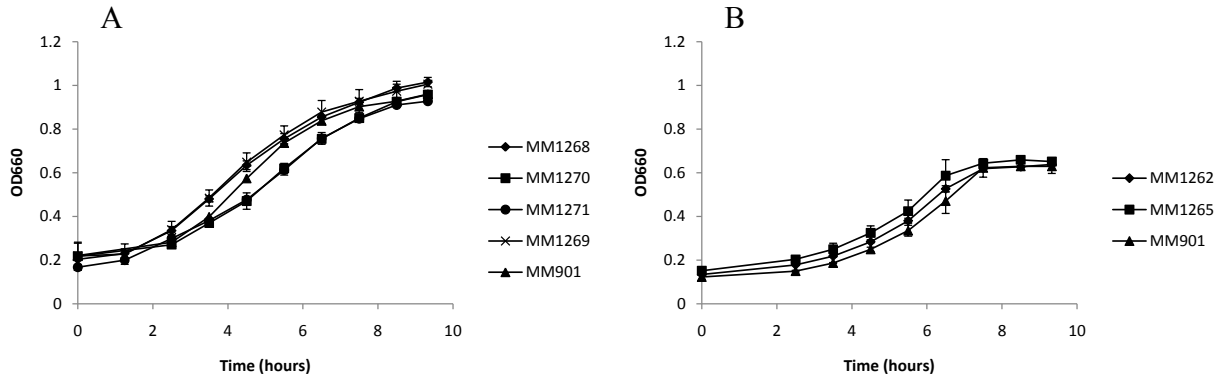

Figure 2.2. Growth curves of strains with a His-tagged protein and the redundant copy inactivated compared to wild-type. OD_{660}, optical density at 660nm. Data is from duplicate cultures with error bars representing one standard deviation. A. Growth on H_2: MM901, wild type; MM1268, wild-type *hdrB2* with *hdrB1::pac*; MM1269, His-tagged HdrB2with *hdrB1::pac*; MM1270, wild-type *hdrB1* with *hdrB2::pac*; MM1271, His-tagged HdrB1with *hdrB2::pac*. B. Growth on formate: MM901, wild-type; MM1262, Δ*fdh2*; MM1265, His-tagged FdhA1 with Δ*fdh2*.

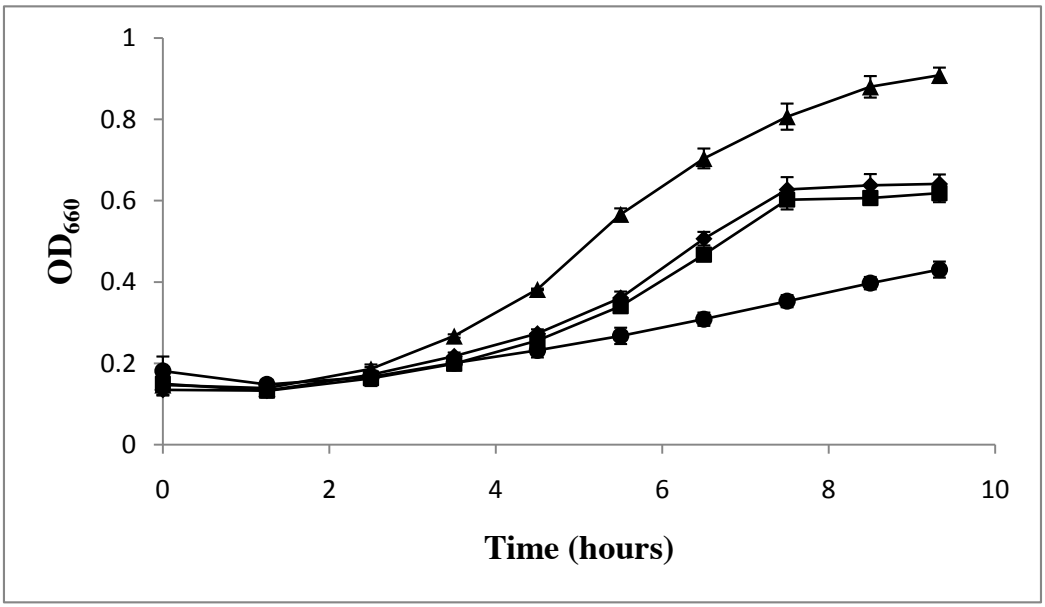

Figure 2.3. Growth of Δ*vhu* Δ*vhc* strain vs. wild type strain on formate or H_2. OD_{660}, optical density at 660 nm. (■) MM1272 (Δ*vhu* Δ*vhc*) grown on formate. (◆) MM901 (wild type) grown on formate. (●) MM1272 grown on H_2. (▲) MM901 grown on H_2. Data is from three independent cultures and error bars represent one standard deviation around the mean.

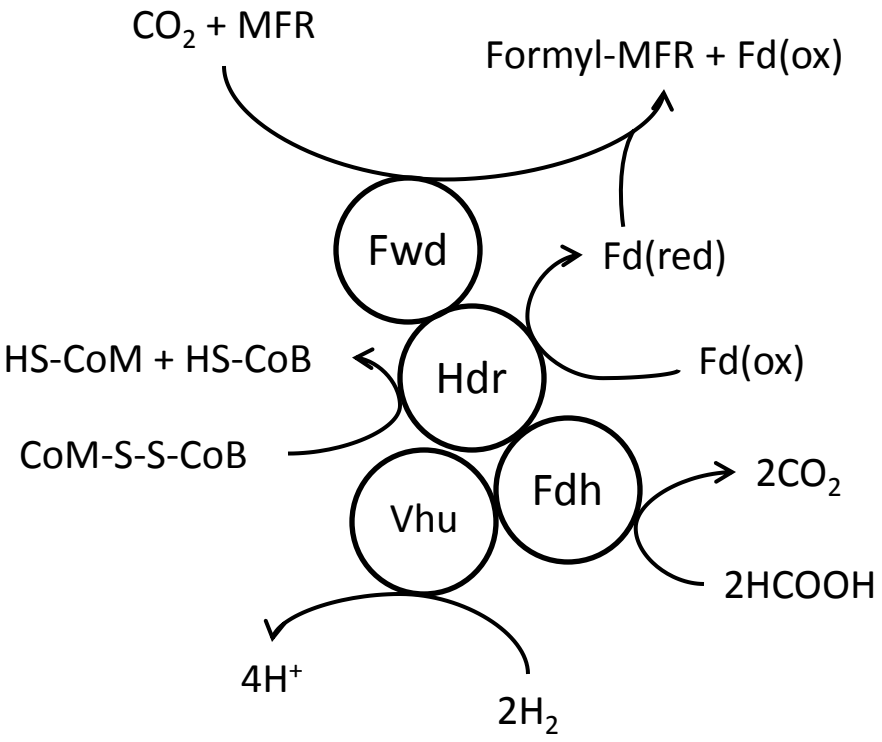

Figure 2.4. Model of complex of proteins that interact with Hdr. When H_2 is used as the electron donor for methanogenesis, electrons are transferred to Hdr via Vhu. Flavin-mediated electron bifurcation at HdrA then results in reduction of the CoM-S-S-CoB heterodisulfide and a ferredoxin that is used by Fwd for the first step in methanogenesis. When hydrogen is limiting or is replaced by formate, Fdh is highly expressed and incorporates into the complex. When formate is used as the electron donor for methanogenesis, electrons are transferred to Hdr from formate via Fdh. Fd(red), reduced ferredoxin; Fd(ox), oxidized ferredoxin.

CHAPTER 3

A biochemical model for methanogenesis

Originally published as an article in *Proceedings of the National Academy of Sciences*:

Lie, Thomas J.*, Kyle C. Costa*, Boguslaw Lupa, Suresh Korpole, William B. Whitman, and John A. Leigh (2012) Essential anaplerotic role for the energy converting hydrogenase Eha in hydrogenotrophic methanogenesis. *Proc Natl Acad Sci USA*. 109 (38) 15473-15478.
*These authors contributed equally.

Summary

Despite decades of study, electron flow and energy conservation in methanogenic archaea are still not thoroughly understood. For methanogens without cytochromes, flavin-based electron bifurcation has been proposed as an essential energy-conserving mechanism that couples exergonic and endergonic reactions of methanogenesis. However, an alternative hypothesis posits that the energy-converting hydrogenase Eha provides a chemiosmosis-driven electron input to the endergonic reaction. In vivo evidence for both hypotheses is incomplete. By genetically eliminating all nonessential pathways of H_2 metabolism in the model methanogen *Methanococcus maripaludis* and using formate as an additional electron donor, we isolate electron flow for methanogenesis from flux through Eha. We find that Eha does not function stoichiometrically for methanogenesis, implying that electron bifurcation must operate in vivo. We show that Eha is nevertheless essential, and a sub-stoichiometric requirement for H_2 suggests that its role is anaplerotic. Indeed, H_2 via Eha stimulates methanogenesis from formate when intermediates are not otherwise replenished. These results fit the model for electron bifurcation, which renders the methanogenic pathway cyclic, and as such requires the replenishment of intermediates. Defining a role for Eha and verifying electron bifurcation provide a complete model of methanogenesis where all necessary electron inputs are accounted for.

Introduction

Methanogenesis is an anaerobic respiration carried out by a phylogenetically related group of archaea within the phylum Euryarchaeota. Methanogens are divided into two metabolic types, those without and those with cytochromes (136). Methanogens without cytochromes use H_2 as an electron donor and are termed hydrogenotrophic. Some species can substitute H_2 with formate, and a few can use secondary alcohols. CO_2 is the electron acceptor and is reduced to methane. Methanogens with cytochromes reduce certain methyl compounds or the methyl carbon of acetate to methane and are called methylotrophic. Many can also utilize H_2 and CO_2 as can hydrogenotrophic methanogens.

Although the pathways of methanogenesis have long been known, an understanding of energy conservation has been slower to emerge. Methanogens with and without cytochromes both export Na^+ when a methyl group is transferred from the carrier tetrahydromethanopterin (H_4MPT) to coenzyme M (CoM, see Fig. 1.1). The Na^+ gradient across the membrane is used directly for ATP synthesis or is converted by an antiporter to a proton gradient. However, for methanogenesis from CO_2, the initial reduction of CO_2 to a formyl group attached to methanofuran (MFR) is endergonic. How energy is provided to drive this reaction is not well understood. Methanogens with and without cytochromes have membrane-associated energy-converting hydrogenases that couple the reduction of low-potential ferredoxins (Fd) to a chemiosmotic membrane gradient (53). If such a Fd donates electrons for CO_2 reduction, an energy-converting hydrogenase is the conduit of energy for this reaction. Indeed, for methanogens with cytochromes, an energy-converting hydrogenase is required for CO_2 reduction (97). However, the energy requirement for the first step in the pathway results in a need for additional energy conservation. This could be provided by the final step of methanogenesis, which involves an exergonic reduction of a heterodisulfide of two methanogenic cofactors (CoM-S-S-CoB) by heterodisulfide reductase (Hdr). Methanogens with cytochromes harvest the energy yielded in heterodisulfide reduction with a proton-exporting electron transport chain. However, methanogens without cytochromes lack this electron transport chain and an alternative explanation is required.

Here we present results supporting an emerging view of methanogenesis without cytochromes. The new model diverges from the conventional picture of a linear pathway of CO_2 reduction to methane. Instead, a cyclical pathway involving electron bifurcation has been proposed (136) (Fig. 1.1). The reductions of the heterodisulfide and CO_2 are coupled in the flavin-containing

enzyme complex centered around Hdr. For each pair of electrons accepted, one electron is used for the exergonic reduction of CoM-S-S-CoB, and one is used to reduce a low-potential ferredoxin that in turn donates electrons for the reduction of CO_2 to formyl-MFR. Hence, electron bifurcation, a non-chemiosmotic form of energy conservation, couples the exergonic and endergonic steps of methanogenesis and allows for the net availability of chemiosmotic energy for ATP synthesis. The electron bifurcation model renders methanogenesis a cyclic process, in which late steps are coupled by electron flow to the initial step, and explains why in cell extracts, CH_4 production from CO_2 requires an input of C-1 intermediates (48). Electron bifurcation is supported by experiments with whole cells (88), with purified enzymes (70), and by the characterization of an enzyme complex in which it could take place (25). However, these studies do not explain the presence in most methanogens without cytochromes of the energy-converting hydrogenase Eha that is apparently linked to the first step (53). Electron flux from this hydrogenase would appear to compete with flux from electron bifurcation as well as to consume chemiosmotic energy, leaving a deficit for ATP synthesis.

Whatever the correct model for energy conservation, it likely centers around reactions that reduce low-potential ferredoxins. Three such reactions are proposed to occur in methanogens without cytochromes. Two of these reactions are those mentioned above, the concomitant reduction of Fd and CoM-S-S-CoB that occurs in electron bifurcation, and the H_2-dependent reduction of Fd by the energy-converting hydrogenase Eha, both of which are proposed to lead to the endergonic reduction of CO_2 to formyl-MFR. A third such reaction, which reduces a Fd with another energy-converting hydrogenase, Ehb, functions in anabolic CO_2 fixation reactions and does not appear to be involved in methanogenesis (90, 110).

Here we present an analysis of electron flow in methanogens without cytochromes, focusing on the role of H_2 when formate is the electron donor for methanogenesis. We show that there are two pools of electrons that are distinguished by their substrate origins, their carriers, and their functions. One pool of electrons feeds into methanogenesis via coenzyme F_{420} as well as directly to Hdr from electron-donating growth substrates. Surprisingly, these electrons need not come from H_2, even in hydrogenotrophic methanogens, but instead can come directly from formate. Another pool of electrons supports critical biosynthetic or anaplerotic steps, are carried by low-potential ferredoxins, and come only from H_2. We show that only one hydrogenase, Eha, is the essential conduit of electrons from H_2 and that Eha supports methanogenesis, but it does so in an anaplerotic and not a stoichiometric manner. Eha is needed only to replenish

intermediates that are removed from the methanogenesis cycle by diversion to biosynthetic pathways, dilution of intermediates due to growth, or imperfect coupling in electron bifurcation as proposed previously (136). Electron bifurcation still accounts for the stoichiometric flow of electrons for methanogenesis. Our results therefore support the electron bifurcation model in vivo as well as demonstrating the function of Eha.

Methods

Construction and growth of strains. Unless otherwise stated, strains were grown in medium containing casamino acids and acetate, with H_2 or formate as the electron donor (59). Strains, plasmids, and primers are shown in Table 3.1. Strain Mm901 was used as the wild type strain unless otherwise stated. To construct plasmids pCRupt∆*fru*neo, pCRupt∆*frc*neo, and pCRupt∆*hmd*neo, insert DNA from plasmids pCRprt∆*fru*neo, pCRprt∆*frc*neo, and pCRprt∆*hmd*neo (59) was recloned into pCRuptneo (25). To construct plasmids pCRupt∆*fruGB*neo, pCRupt∆*frcGB*neo, and pCRupt∆*ehbN*neo, approximately 0.5 kb of DNA upstream and downstream of the designated loci were obtained by PCR from genomic DNA and cloned into pCRuptneo. In each case, the resulting plasmid contained an in-frame deletion consisting of a start codon and a stop codon with intervening codons contained within an AscI site. Plasmid DNA was used to make deletions using a markerless mutagenesis method with neomycin for positive selection and 6-azauracil for negative selection as described (25, 98). When formate was present as electron donor, neomycin was increased to 5 mg mL^{-1} on liquid or solid medium (25). MM1290 (Mm901∆*fruAGB*∆*frcAGB*∆*hmd*, ∆3H_2ase) was constructed by sequential deletion of *frcA*, *hmd*, *fruA*, *fruG* and *B*, and *frcG* and *B*. The first deletion was constructed using H_2 as the growth substrate, and the remaining deletions used formate. MM1313 (MM901∆*fruA*∆*frcA*∆*vhuAU*∆*vhcA*, ∆4H_2ase) was constructed from Mm1272 (MM901∆*vhuAU*∆*vhcA*) (25) by deletion of *fruA* and *frcA* using formate. MM1289 (MM901∆*fruA*∆*frcA*∆*hmd*∆*vhuAU*∆*vhcA*, ∆5H_2ase) was then constructed by deleting *hmd*. Finally, MM1284 (MM901∆*fruA*∆*frcA*∆*hmd*∆*vhuAU*∆*vhcA*∆*ehbN*, ∆6H_2ase) was constructed by deleting *ehbN*. During construction of the ∆5H_2ase and ∆6H_2ase mutants, cultures were grown with formate and H_2. All deletions were confirmed by PCR.

Essentiality of Eha. Merodiploids were constructed containing deletions of the *ehaHIJ* genes and *ehbF* (Fig. 3.1 and Table 3.1), and the generation of deletion mutants by recombination-based resolution of the merodiploids was attempted using wild type strain Mm900 as described

(98). Among the resulting clones, those containing deletion mutations and wild type alleles were distinguished by PCR. A *trans*-complementing plasmid (pMEV1*nif*::*ehaHIJ*, Table 3.1) was constructed on a replicative vector with *ehaHIJ* under control of the nitrogen-regulated *nif* promoter (31, 83). To test the effect of *trans*-complementation, merodiploids containing this plasmid were plated with alanine or ammonia, and the merodiploids were resolved. In preliminary experiments, *ehaHIJ* deletion strains could be obtained with either nitrogen source, and ammonia was used henceforth.

H_2 and CH_4 production. To measure H_2 production by cell suspensions, cultures (5 mL) were grown on formate to OD_{660} between 0.5 to 0.6, and cells were pelleted, washed, and resuspended anaerobically in the same volume of assay buffer (modified from (88), 50 mM MOPS pH 7.0, 400 mM NaCl, 20 mM KCl, 20 mM $MgCl_2$, 1 mM $CaCl_2$, 5 mM dithiothreitol, and 1 mM bromoethanesulfonate). Tubes were then flushed with N_2 for 10 - 30 min to remove residual H_2. At time = 0 min, an initial gas sample was taken, then the assay was initiated by addition of 40 mM (final concentration) sodium formate (pH 7) or NaCl and incubated at 37°C with shaking. At 15-min and 30-min time points, the headspace was sampled and transferred to butyl-rubber stoppered 5 ml vials, mouth ID 13 mm x OD 20 mm (Wheaton; catalog number 223685) pre-flushed with N_2. H_2 was analyzed with a SRI Instruments GC model 8610C equipped with a 6'x1/8" S.S. Molecular Sieve 5A packed column and a Reduced Gas Detector. The carrier gas was He (20 mL min^{-1}), oven temperature was 130°C, and detector temperature was 290°C. CH_4 production by cell suspensions was measured as above except cells were grown to mid log phase (OD_{660} ~0.25), bromoethanesulfonate was omitted from the assay buffer, and the headspace was directly analyzed on a Buck Scientific Model 910 GC equipped with a Flame Ionization Detector provided with air (16 mL min^{-1}) and H_2 (26 mL min^{-1}). The carrier gas was He (24 mL min^{-1}). To measure CH_4 production by cell-free extracts, cells were washed and suspended in buffer (modified from (48), 100 mM Trizma base, 15 mM $MgCl_2$, 5 mM ATP, 2 mM 2-mercaptoethanol, 500 µM FAD^+, with or without 50 mM formic acid, and pH adjusted to 7.1 with 1 M HCl). The suspension was sonicated with a Misonix XL-2000 series sonicator to disrupt the cells. Debris was removed by centrifugation at 16,000xg, and 200 µL supernatant was placed in a 5-mL serum vial and pre-incubated for 10 minutes at room temperature. To start the assay, the headspace was flushed with N_2:CO_2 (80:20, for formate) or H_2:CO_2 (80:20), and 1.5 mM CH_3-S-CoM was added (48). Methanogenesis was monitored as described above.

Results

Identification of a novel H_2:F_{420} oxidoreductase activity and demonstration of a H_2 requirement for growth. Our initial question was whether H_2 is a necessary substrate or intermediate for growth of hydrogenotrophic methanogens. *Methanococcus maripaludis* was an ideal species for addressing this question because it can substitute formate for H_2 and mutations are easily generated (75). In the conventional view, during growth on formate, H_2 generated from formate serves as the electron donor. Indeed, H_2 is generated from formate and recycled in a poorly understood manner (59, 88). However, if there is no direct requirement for H_2 in methanogenesis (25, 88), most of the hydrogenases encoded in the genome ought to be dispensable during growth on formate. The Hdr-associated hydrogenases (Vhu and Vhc, Fig. 1.1), which provide electrons to the last reductive step of methanogenesis and potentially the first step via electron bifurcation (25, 70, 136), can be substituted by formate dehydrogenase (Fdh) during growth on formate (25). The F_{420}-reducing hydrogenases (Fru and Frc) generate $F_{420}H_2$ for the second and third reductive steps of methanogenesis, but the Fdh is also F_{420}-reducing (121, 155). The hydrogenase Hmd catalyzes the third reductive step directly with H_2, but its function is redundant with Mtd which uses reduced F_{420} for the same purpose (59). Finally, the anabolic energy-converting hydrogenase Ehb is non-essential in the presence of fixed carbon and is not required for methanogenesis (90, 110). Only Eha remains as possibly essential.

Based on the above considerations, we expected that H_2 would not be needed as an intermediate for methanogenesis from formate. Indeed, experiments with cell suspensions have already shown that rates of methanogenesis can substantially exceed rates of H_2 production from formate (88). As a further test, our approach here was to genetically remove formate-hydrogen lyase activity, so that H_2 would not be produced from formate. If growth still occurred on formate without added H_2, then H_2 was not a required intermediate. Since Fdh is F_{420}-reducing, removal of formate-hydrogen lyase activity amounts to the removal of F_{420}-H_2 oxidoreductase activity. Two such activities are known, the direct Fru or Frc activity and the Hmd-Mtd cycle (Fig. 1.1) (59). Therefore, deletion of *fru*, *frc*, and *hmd* should eliminate both modes of formate-hydrogen lyase activities. However, cell suspensions of a Δ*fru*Δ*frc*Δ*hmd* mutant (MM1290, henceforth designated Δ3H_2ase) still produced substantial H_2 from formate (Fig. 3.2). Furthermore, the mutant grew not only on formate as predicted, but also on H_2, albeit poorly (Fig. 3.3A). Because $F_{420}H_2$ is essential for methanogenesis, a third pathway must exist for F_{420} reduction by H_2.

In a further attempt to remove F_{420}-H_2 oxidoreductase activity, *vhu* and *vhc* were deleted in the Δ3H_2ase background, resulting in strain MM1289 containing deletions in five hydrogenases (Δ*fru*Δ*frc*Δ*hmd*Δ*vhu*Δ*vhc*, Δ5H_2ase). This strain required both formate and H_2 for growth (Fig. 3.3B). This result suggested that H_2-F_{420} oxidoreductase activity had been reduced to below the level needed to support growth on H_2 alone. The low level of F_{420}-H_2 oxidoreductase activity in Δ5H_2ase was verified by low H_2 production from formate compared to wild type and Δ3H_2ase in cell suspensions (Fig. 3.2). The third F_{420}-H_2 oxidoreductase activity is evidently Vhu/Vhc-dependent and represents a previously uncharacterized electron flow pathway in methanogenic archaea. Although further experiments are needed to characterize this pathway, it could involve Vhu/Vhc, Hdr, and Fdh, which is F_{420}-reducing and like Vhu/Vhc is Hdr-associated. The H_2 requirement of the Δ5H_2ase mutant demonstrates that, contrary to our initial expectation, H_2 is a required intermediate during growth on formate and H_2 is indeed required for growth of hydrogenotrophic methanogens.

The H_2 requirement is quantitatively low. It was unclear whether the H_2 that is required for growth of the Δ5H_2ase mutant supports the catabolic process of methanogenesis or the anabolic process of CO_2 fixation. Cultures of *M. maripaludis* grown on our formate medium utilize 1 mmol of formate (59). Therefore, if H_2 were required for just one reductive step of methanogenesis, the amount of H_2 needed would be ~0.33 mmol. However, we observed maximum growth with H_2 as low as 10-15 µmol (Fig. 3.4). At this level, H_2 cannot be a substantial electron donor for methanogenesis. Instead, the H_2 requirement may be anabolic and/or anaplerotic (see below). In fact, during autotrophic growth, about 35 µmol of H_2 were required for each mg of cell dry weight formed in the Δ5H_2ase mutant (Fig. 3.4). (For *M. maripaludis*, mg dry weight/OD_{660}/ml = 0.34,(88)). Under these conditions, cells require 10.7 µmol of pyruvate and 3.9 µmol of acetate per mg of cell dry weight for autotrophic growth (160). In methanogens, acetate biosynthesis requires two pairs of low potential electrons, one for formation of formyl-MFR and one by the acetyl-CoA synthase. Pyruvate is formed from acetyl-CoA and requires one additional pair of low potential electrons. Thus, about 40 µmol of low potential electron pairs per mg of cell dry weight are required for autotrophic growth, close to the value observed. If the H_2 was required for generation of low potential electrons for anabolism, the addition of carbon sources to the medium should decrease the amount of H_2 needed for growth. In fact, in the presence of acetate and acetate plus casamino acids, the amount of H_2

required decreased to 17 and 8 µmol of H_2 per mg of cell dry weight, respectively (Fig. 3.4). Therefore, the H_2 requirement appears at least partially anabolic.

H_2 is not required for methanogenesis in vitro but stimulates methanogenesis in cell suspensions. We performed two additional experiments to further examine the nature of the H_2 requirement. For both experiments, first Ehb was genetically eliminated from the $\Delta 5H_2$ase mutant background to generate strain MM1284, which contained deletions in six hydrogenases (Δ*fruA*Δ*frcA*Δ*hmd*Δ*vhuAU*Δ*vhcA*Δ*ehbN*, $\Delta 6H_2$ase). Eha was the sole remaining hydrogenase. Similar to the $\Delta 5H_2$ase mutant, $\Delta 6H_2$ase required H_2 as well as formate for growth (Fig. 3.5). In the first experiment, in vitro CH_4 production assays were performed (Fig. 3.6). These assays followed published reports (13, 48), which show that CH_4 production from CO_2 in vitro requires stimulation by the intermediate CH_3-S-CoM and that the yield of CH_4 is limited by the CH_3-S-CoM added. In our assays, CH_3-S-CoM was added and CH_4 production continued presumably until CH_3-S-CoM was depleted. CH_4 production was measured in extracts of $\Delta 6H_2$ase mutant or wild type cells with either H_2 or formate as electron donor. Extract of wild type *M. maripaludis* produced substantial CH_4 from CO_2 with either electron donor. In contrast, the mutant extract produced substantial CH_4 only from formate. H_2 had no stimulatory effect on CH_4 production from formate (Fig. 3.7).

Next, we assayed CH_4 production by cell suspensions of the $\Delta 6H_2$ase mutant. With cell suspensions, stimulation by an intermediate in the pathway was not needed and CH_3-S-CoM was not added. Methanogenesis occurred with formate but not with H_2. Significantly, methanogenesis was greatly enhanced by H_2, either present initially or added during the course of the assay (Fig. 3.8). Hence, H_2 did not contribute to methanogenesis in vitro where the pathway intermediate CH_3-S-CoM was added, but H_2, presumably acting through Eha, stimulated methanogenesis in cell suspensions.

Eha is essential for growth of M. maripaludis. To test whether Eha is essential, mutagenesis of *ehaHIJ* was attempted. The genes *ehaH, I,* and *J* encode the presumed cation translocator of the enzyme complex. Each is homologous to a portion of *ehbF*, for which a null allele has a strong phenotype (110). In preliminary experiments, the construction of an *ehaHIJ* allelic replacement with a puromycin resistance cassette was unsuccessful. An additional test of essentiality was sought. As before (59), our strategy was to determine if negative selection to resolve a merodiploid would result in a deletion allele. All other things equal, if there is no

growth disadvantage for a null allele, deletion mutants should arise with roughly the same frequency as wild type alleles, and this occurred in a control experiment where a *ehbF*$^+$-Δ*ehbF* merodiploid was resolved (Table 3.2). However, resolution of the *ehaHIJ*$^+$-Δ*ehaHIJ* merodiploid in standard medium with H_2 resulted in only wild type clones. Similar results were obtained when formate rather than H_2 was used. Eha could be involved in 2-ketoglutarate biosynthesis, since 2-ketoglutarate oxidoreductase depends on Fd (110), and high levels of glutamate in the medium (10 mM) could provide sufficient 2-ketoglutarate and remove the requirement for Eha. Alternatively, Eha might be involved in NAD^+ reduction, and alanine dehydrogenase in methanococci generates NADH (164). However, when glutamate or alanine was added, still no mutations were obtained. In contrast, when the *ehaHIJ* mutagenesis experiment was performed in the presence of *trans* complementation (P*nif*-*ehaHIJ*), the majority of clones contained the deletion. These results strongly suggest that Eha is essential, consistent with the H_2 requirement for growth of the Δ6H_2ase mutant.

Discussion

Distinct electron pools function in hydrogenotrophic methanogens. Until recently it was not known if any of the hydrogenase activities in hydrogenotrophic methanogens could be eliminated. However, in past work we reported that some of these hydrogenases were unnecessary under some conditions. Thus, in separate strains we deleted genes encoding the F_{420}-reducing hydrogenases (59), the Hdr-associated hydrogenases (25), and the hydrogen-utilizing methylene-H_4MPT dehydrogenase (59). Here we eliminated all three of these hydrogenase activities in a single strain (Δ5H_2ase) and found that both formate and H_2 were required for growth, the former in quantities stoichiometrically sufficient for methanogenesis, and the latter in much smaller quantities. The mutant effectively separates two pools of electrons that ordinarily exchange via H_2. One pool of electrons provides a stoichiometric supply of electrons for methanogenesis and flows through F_{420} and Hdr (Fig. 1.1). In the wild type strain, either formate or H_2 functions as electron donor for this pool. The Δ5H_2ase and Δ6H_2ase mutants, by eliminating H_2-F_{420} oxidoreductase activities, disrupt electron flow from H_2 and, as a result, formate is required as the stoichiometric electron donor for methanogenesis. The other pool of electrons supports biosynthesis, and as demonstrated here, anaplerotically replenishes methanogenesis (see below). This pool is carried by ferredoxins, and only H_2 functions as electron donor. In the wild type strain, H_2 produced from formate allows the latter to function as

sole electron donor. However, in the $\Delta 5H_2$ase and $\Delta 6H_2$ase mutants where electron flow between the two pools is blocked, H_2 must be provided.

The function of Eha is essential, anaplerotic, and ancillary to electron bifurcation. In the $\Delta 5H_2$ase mutant, two hydrogenases remain, Eha and Ehb. Previous work has suggested that the role of Ehb is the reduction of Fd for anabolic CO_2 fixation via acetyl-CoA synthase, pyruvate oxidoreductase, 2-ketoglutarate oxidoreductase, indole-pyruvate oxidoreductase, and 2-oxoisovalerate oxidoreductase (90, 110). Eha may play a role analogous to a related energy conserving hydrogenase, Ech, which in methanogens with cytochromes generates reduced Fd for CO_2 reduction to formyl-MFR (53). Because Eha and Ehb have different functions, they may reduce different ferredoxins. Although not yet proven biochemically, Eha could have specificity for a polyferredoxin associated with formylmethanofuran dehydrogenase (Fwd), the enzyme that catalyzes CO_2 reduction to formyl-MFR (63), while Ehb could reduce a Fd associated with anabolic CO_2 fixation reactions.

In methanogens without cytochromes, if the role of Eha is to reduce CO_2 to formyl-MFR, how is this reconciled with electron bifurcation as the main pathway for delivery of electrons for the same step? Our data show that Eha needs to provide only a small portion of the electrons for this reaction. In the $\Delta 5H_2$ase mutant, formate provided nearly all electrons for methanogenesis and the H_2 requirement accounted for only up to 4% of the electrons for growth, much of this apparently for anabolic purposes. We propose that Eha functions in the reduction of CO_2 to formyl-MFR, but does so anaplerotically. In the electron bifurcation model, hydrogenotrophic methanogenesis is a cyclic pathway where the first step is dependent on the last step (136). However, this model presents a dilemma. A constant pool of CoM-S-S-CoB is required, yet intermediates in methanogenesis will inevitably be diluted by growth and cell division, or lost due to a leaky electron bifurcating Hdr complex (70, 136). In addition, intermediates will diminish when methyl-H_4MPT is diverted from methanogenesis to generate acetyl-CoA for autotrophic CO_2 fixation (8). Our results show that Eha solves this dilemma by priming or recharging the cycle: it anaplerotically restores intermediates to the methanogenic pathway at the level of formyl-MFR. This model accounts for all of the following observations. First, only small amounts of H_2 are required for growth. Second, Eha is essential even though electron bifurcation can account for a stoichiometric supply of electrons for methanogenesis. Third, even though H_2 and Eha are essential, there is no need for H_2 for methanogenesis in an in vitro assay

where the intermediate CH_3-S-CoM is added. Finally, for methanogenesis in cell suspensions where no intermediate is provided, H_2 is stimulatory.

Why do most hydrogenotrophic methanogens, including *M. maripaludis*, maintain two ion-translocating energy-converting hydrogenases that reduce Fd and provide electrons to fix CO_2? One such hydrogenase could suffice, and indeed, Eha can apparently recognize the Ehb-type ferredoxin and substitute for Ehb, albeit inefficiently (90, 110). Having both hydrogenases separates the recharging of methanogenesis from other anabolic activities and may optimize control over the separate processes. When conditions limit growth, anabolic CO_2 fixation is unimportant but CO_2 reduction to formyl-MFR for methanogenesis and ATP synthesis are still necessary for survival. Under these conditions, functional Eha is essential, and a functional Ehb could be detrimental.

A new view of electron flow and energy conservation in hydrogenotrophic methanogens. Electron bifurcation at Hdr explains a decades-old dilemma regarding methanogenesis: how is net energy conservation achieved in hydrogenotrophic methanogens (136)? The results presented here verify that electron bifurcation must function in vivo and elaborate on the mechanisms that allow this to be the case, filling in the known gaps of a pathway that has been incomplete since methanogens were first discovered and grown in culture (6). A complete model for electron flow in methanogens without cytochromes can now be described: Methanogenesis is dependent upon F_{420}-reducing enzymes and enzymes that feed electrons to Hdr for electron bifurcation. During growth on H_2, these enzymes are the F_{420}-reducing hydrogenases Fru and Frc and the Hdr-associated hydrogenases Vhu and Vhc. During growth on formate, both kinds of hydrogenases are unnecessary and Fdh performs both functions. Biochemical experiments have demonstrated CoM-S-S-CoB-dependent reduction of a clostridial Fd with H_2 (70), but are still needed to prove that electrons flow from H_2 or formate to Fwd concurrent with flow to Hdr. Nevertheless, in previous work, we showed that in *M. maripaludis*, Fdh as well as Vhu exist in a complex with Hdr, and that Fwd is in this complex as well (25). Hence, an enzyme complex exists that is suited for electron bifurcation with either H_2 or formate. Fdh, either complexed or also existing in an isolated form, also generates $F_{420}H_2$. Through electron bifurcation at Hdr and F_{420} reduction, formate provides the reducing equivalents to all four reductive steps of methanogenesis. A separate electron pool supports anabolism, which depends on electrons from H_2 entering through Ehb and its associated Fd (90, 110). These isolated inputs keep the electron pools for catabolism and anabolism separated and under

different regulatory control. Overlap between the two electron pools occurs when electrons from H_2 enter methanogenesis through Eha. When low CoM-S-S-CoB concentrations limit the reduction of CO_2 to formyl-MFR by electron bifurcation, Eha recharges methanogenesis.

Tables and figures

Table 3.1. Strains, plasmids and primers used in this study.

Strains	Description	Reference
S2	*M. maripaludis* wild type	(154)
Mm900	'Wildtype'; Δ*hpt*	(98)
Mm901	'Wildtype'; Δ*upt*	(25)
MM1272	MM901Δ*vhuAU*Δ*vhcA*	(25)
MM1290	MM901Δ*fruAGB*Δ*frcAGB*Δ*hmd*	This study
MM1313	MM901Δ*fruA*Δ*frcA*Δ*vhuAU*Δ*vhcA*	This study
MM1289	MM901Δ*fruA*Δ*frcA*Δ*hmd*Δ*vhuAU*Δ*vhcA*	This study
MM1284	MM901Δ*fruA*Δ*frcA*Δ*hmd*Δ*vhuAU*Δ*vhcA*Δ*ehbN*	This study
Merodiploid Mm900*eha*up-down IF	Mm900 with integrated vector harboring *ehaHIJ*$^{+}$ and *ehaHIJ*- in frame deletion, Neo^{R}	This study
Merodiploid Mm900*eha*up-down IF + pMEV*nif*::*ehaHIJ*	Merodiploid for in-frame deletion with the complementation plasmid, Neo^{R}, Pur^{R}	This study
D*ehbF*	In-frame deletion of *ehbF* in Mm900	This study
D*ehaHIJ* + pMEV1::*ehaHIJ*	*ehaHIJ* deletion with the compelmantation vector, Pur^{R}	This study
D*ehaHIJ* + pMEV1*nif*::*ehaHIJ*	*ehaHIJ* deletion with the compelmantation vector with regulated promoter, Pur^{R}	This study

Plasmids:	Description:	Reference:
pCRuptΔ*frcA*neo	Deletion of *frcA*	This study
pCRuptΔ*fruA*neo	Deletion of *fruA*	This study
pCRuptΔ*hmd*neo	Deletion of *hmd*	This study
pCRuptΔ*frcGB*neo	Deletion of *frcGB*	This study
pCRuptΔ*fruGB*neo	Deletion of *fruGB*	This study
pCRuptΔ*ehbN*neo	Deletion of *ehbN*	This study
pCRuptneo	Methanococcal integration vector	This study
pIJA03	Methanococcal integration vector, Pur^{R}, Amp^{R}	(81)
p IJA03*ehaHIJ*-up::*pac*::down	Flanking regions of *ehaHIJ* for recombination	This study
pIJAO3::*hpt-pac*	*hpt* cassette next to *pac* in pIJAO3	This study
pIJAO3:: *ehaHIJ*-up::*hpt-pac*::down	*ehaHIJ* flanking regions in the integration vector	This study
pCRprtneo	Methanococcal integration vector	(98)
pCRprtneo::*ehaHIJ*-up::down-IF	Flanking regions fused together deleting *ehaHIJ*	This study
pCRprtneo::*ehbF*-up::down-IF	Flanking regions fused together deleting *ehbF*	This study
pMEV1::*lacZ*	Replicative vector for *M. maripaludis*	W.Whitman
pMEV1::*ehaHIJ*	*ehaHIJ* in expression vector	This study
pMEV1*nif*::*lacZ*	*lacZ in* vector for *M. maripaludis* with *nif* promoter	This study
pMEV1*nif*::*ehaHIJ*	*ehaHIJ* in regulated expression vector	This study

Primer sequence	Restr. site	Rationale
AAGCGGCCGCCGGAAATATTCTATTTGGGGATG	*NotI*	Amplify upstream *frcG*
AAGGCGCGCCTCTTACCACTATATCACCATTATTCG	*AscI*	Amplify upstream *frcG*
AAGGCGCGCCATACTAATCCATTCCTTTAATTTTTG	*AscI*	Amplify downstream *frcB*
AATCTAGAAAGGAGTTTCACTTAATTTTGGCC	*XbaI*	Amplify downstream *frcB*
AAGCGGCCGCAGGAAAATATGGTTCTTGCATGCGG	*NotI*	Amplify upstream *fruG*
AAGGCGCGCCCATGGTATTCTCCTCCCTTAGTTG	*AscI*	Amplify upstream *fruG*
AAGGCGCGCCAGGATTACCTGTTCCATACTAACTTC	*AscI*	Amplify downstream *fruB*
AATCTAGAAAATTCCAATAGATGCAACAACCGCAGC	*XbaI*	Amplify downstream *fruB*
AAGCGGCCGCTGATCAGTTATTTTTACTTCCCTTGG	*NotI*	Amplify upstream *ehbN*
AAGGCGCGCCGAAGCGTACATGATTTTTCCC	*AscI*	Amplify upstream *ehbN*
AAGGCGCGCCGAACCCTTTAAAAAATAATCAC	*AscI*	Amplify downstream *ehbN*

AATCTAGACTTAATTTATAGTATATCTC	*Xba*I	Amplify downstream *ehbN*
CTAATAGCTAGCCAACCCCTGGGGGAATA	*Nhe*I	*ehaH* up region for pIJAO3
GGCTTATAGCATTCATTGTGGCACTAGTCTTGAT	*Spe*I	
ATAACGTCTAGAGCCCGGTATTGACTTTGCTTG	*Xba*I	*ehaJ* down region for pIJAO3
AGTAATCTCGAGGCCTGTTCAACGTATGCG	*Xho*I	
CCCCCCAGATCTTTGCATATATCATTGTTAGACC	*Bgl*II	*hpt* cassette for pIJAO3
CCCCCCTCTAGATTATTCTAAAATGTTTACTTTTCC	*Xba*I	
CCCCCCGGATCCGGAATCACTGACTTTGCTCCTC	*Bam*HI	*ehaH* up region for
CCCCCCAGATCTAACGAGCATTTTAATCACCTTTG	*Bgl*II	pIJAO3::*hpt-pac*
CCCCCCGGTACCGCCACTACTTGCTCCAAATCAC	*Kpn*I	*ehaJ* down region for
CCCCCCGCTAGCGACGGTAAGTAGCCTGCCTTC	*Nhe*I	pIJAO3::*hpt-pac*
ACAATAGGGCCCGGAATCACTGACTTTGCTCCT	*Apa*I	*ehaH* up region for
CCCCCCAGATCTAACGAGCATTTTAATCACCTTTG	*Bgl*II	cloning into pCRprtneo
CCCCCCAGATCTGCCACTACTTGCTCCAAATCAC	*Bgl*II	*ehaJ* down region for
CCCCCCTCTAGAGACGGTAAGTAGCCTGCCTTC	*Xho*I	cloning into pCRprtneo
CCCCATGCATGCTCGTTGAATATATCGCAGGAAACTTT	*Nsi*I	*ehaHIJ* for cloning into
GGGGGTCTAGACTAATGGATGATTCTGTATGCCAGATCAATA	*Xba*I	pMEV1*nif*
GTTTAACGGACTTATGT*ATGCGT*TGTATGCCTTTTTAGTTGGCGG		Site directed, removal of
CCGCCAACTAAAAAGGCATACA*ACGCAT*ACATAAGTCCGTTAAAC		*Nsi*I site from *ehaJ*
CAACTTGGATCCGGAATCACTGACTTT GCTCCTC		Determination
GCCGCATAAAACGGAGCAACGCCT		presence of *ehaH*
CAAAAGATGCGATACAGGGCCAGG		*eha* fragment with
TTTCCCAAGCTCCGGTTACAGGAC		flanking regions
GCACCTGATTTTCCGATAATGCCCAA		Detects the
CACCGACTATTCCCTGACGATGTAGTC		presence of *ehbF*

Table 3.2. Clones resulting from resolution of merodiploids

Merodiploid	No. of clones	
	wt	mutant
Δ*ehbF*	26	34
Δ*ehaHIJ*	108	0
Δ*ehaHIJ*, formate	24	0
Δ*ehaHIJ*, glu	12	0
Δ*ehaHIJ*, ala	38	0
Δ*ehaHIJ* + P_{nif}-*ehaHJI*	5	52

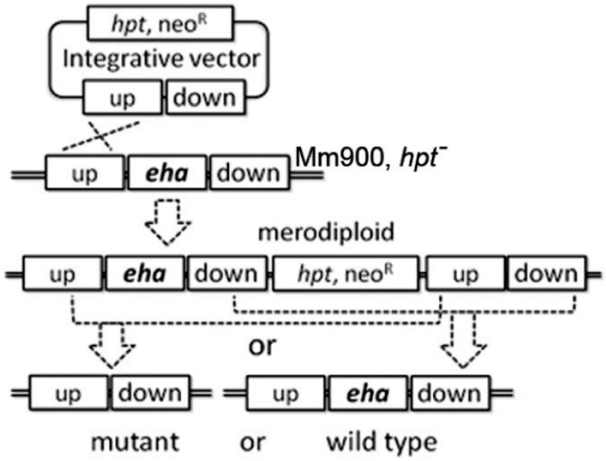

Figure 3.1. In-frame deletion method for generation of the *ehaHIJ* mutation (98). The integrative vector contained DNA fragments upstream and downstream of *ehaHIJ*, fused together deleting the *ehaHIJ*. After transformation into strain Mm900, homologous recombination and selection with neomycin resulted in the merodiploid, which contained both mutated and wild type copies of the genes (confirmed by Southern blot). Depending on which homologous fragment undergoes recombination, two different merodiploids can be generated and only one is shown for clarity. A second homologous recombination event results in removal of the plasmid backbone, and the resulting clone is obtained by negative selection for *hpt*. Depending on which fragment undergoes recombination, either wild type or mutant is produced. Dashed lines indicate possible homologous recombination sites. In the merodiploid, the downstream genes in the *eha* operon are transcribed from the neo promoter. Even though the continuity of the *eha* operon was disrupted, the genes were expressed at sufficient levels to sustain cell viability. The mRNA levels estimated by RT-PCR of *ehaH* and *ehaN* in merodiploid, which were located downstream of the vector were comparable to their levels in wt strain Mm900. The mRNA levels of *ehaH* compared to the DNA primase were 0.5±0.05 (means of triplicates of two independent cultures ± one standard deviation) for both merodiploid and the wt. Corresponding values for *ehaN* were 0.6±0.3 and 1.0±0.1. These results clearly demonstrated that genes downstream of vector in the merodiploid were expressed and that these mutations do not necessarily yield loss of function.

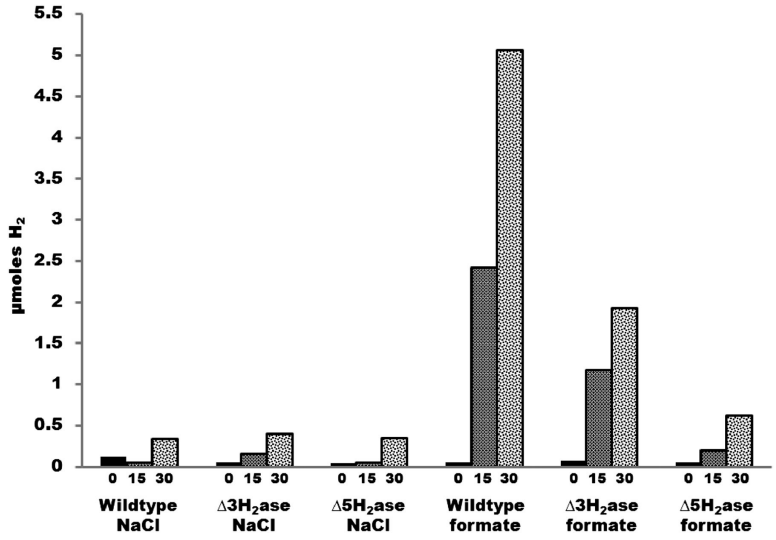

Figure 3.2. H_2 production by cell suspensions. Values in x-axis are in minutes.

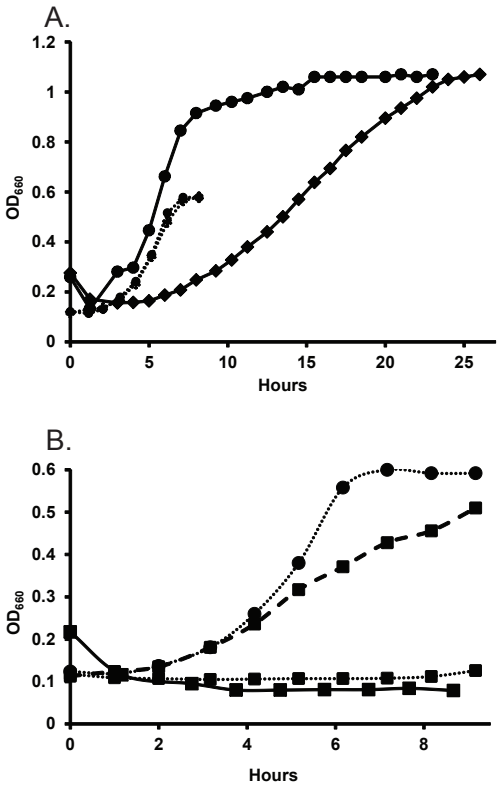

Figure 3.3. Growth of strains. (A) Δ3H_2ase mutant (black diamonds) or wildtype (black circles) on formate (dotted line) or H_2 (solid line). Note: growth kinetics of wildtype and Δ3H_2ase are identical during growth on formate. (B) Δ5H_2ase mutant (black squares) or wildtype (black circles) on formate (dotted line), hydrogen (dashed line), or on formate plus H_2 (14.28 μmoles) (solid line).

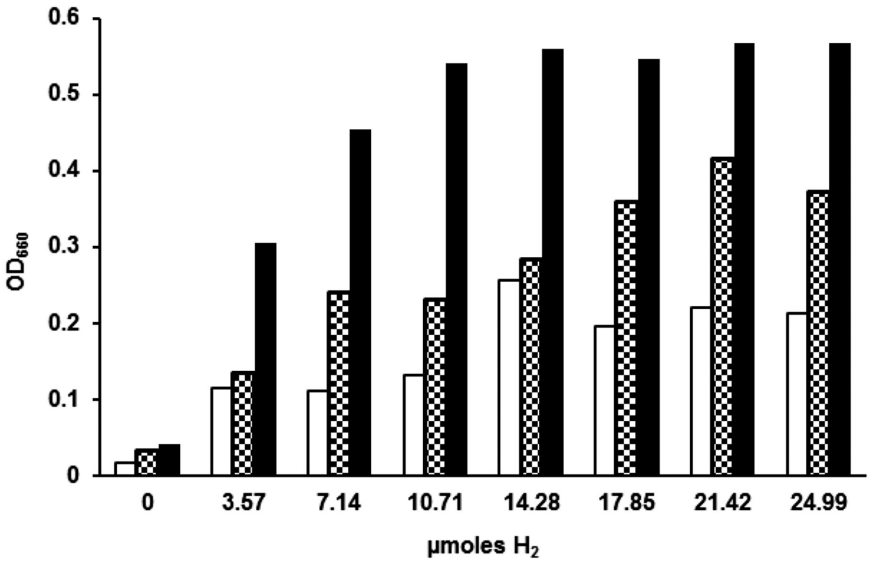

Figure 3.4. H_2 dose-response of $\Delta 5H_2$ase mutant. Clear bars, mineral medium; checkered bars, 10 mM acetate added; solid bars, 10 mM acetate and casamino acids (0.2% w/v) added. All cultures contained 200 mM formate. 5 mL cultures were incubated until stationary phase and OD_{660} was measured.

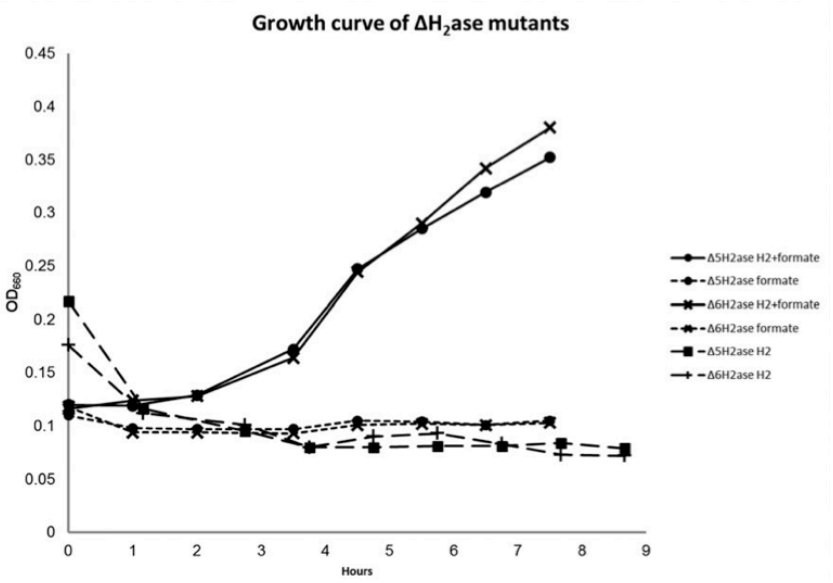

Figure 3.5. Growth of ΔH_2ase mutants with H_2.

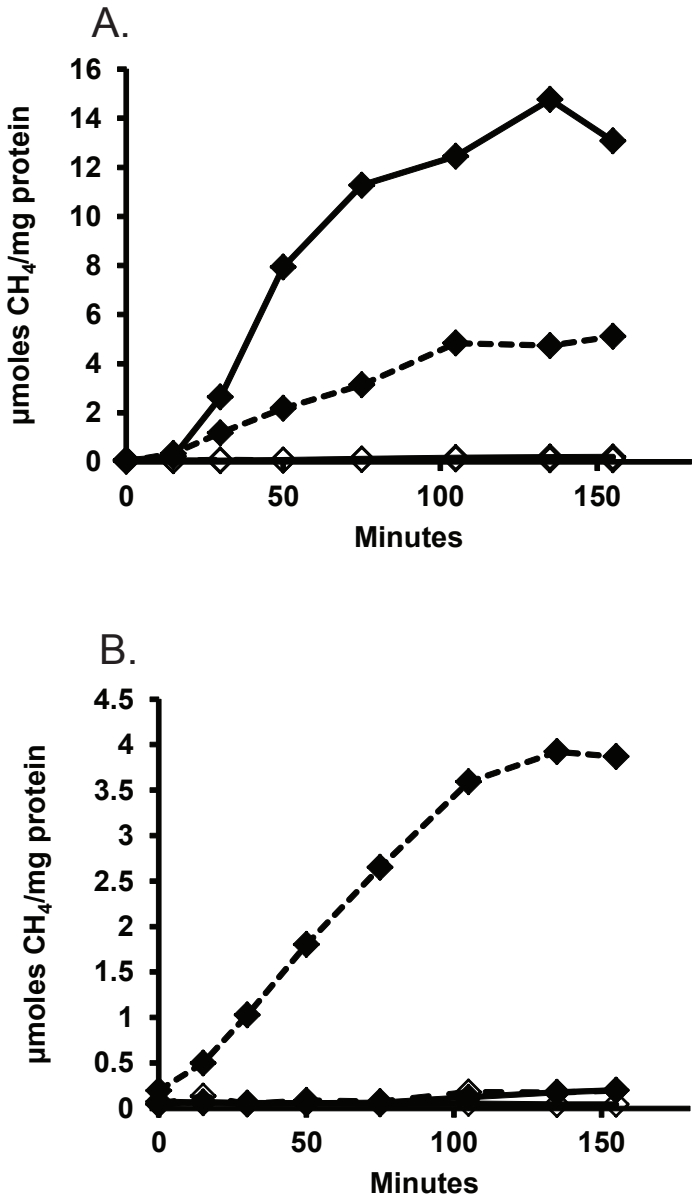

Figure 3.6. Methanogenesis in cell extracts using H_2 (solid line) or formate (dotted line) as the electron donor in cell extracts from A) wild-type or B) Δ6H_2ase mutant. Extracts with no methyl-CoM added are represented by clear diamonds. Each reaction contained 300 µmoles of methyl-CoM and 200-350 mg of protein.

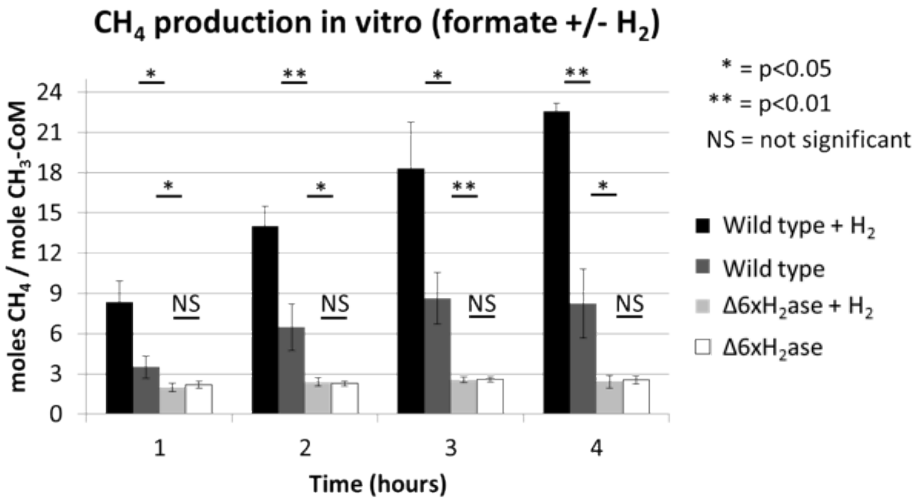

Figure 3.7. CH_4 production in vitro by wild type and $\Delta 6H_2$ase mutant.

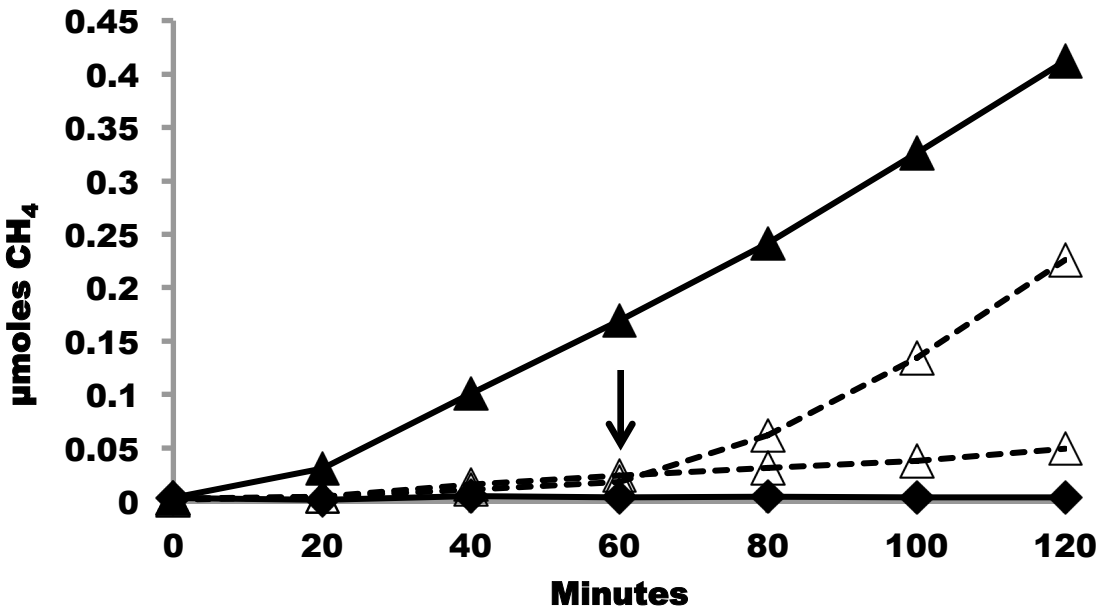

Figure 3.8. CH_4 production by in cell suspensions of the $\Delta 6H_2$ase mutant. Black diamonds, H_2 alone; clear triangles, formate alone with (arrow) or without H_2 addition (8% final concentration) at 60 min; black triangles, H_2 and formate.

CHAPTER 4

H_2-independent growth of *M. maripaludis*

Originally published as an article in *mBio*:

Costa, Kyle C., Thomas J. Lie, Michael Jacobs, and John A. Leigh. H_2-independent growth of the hydrogenotrophic methanogen *Methanococcus maripaludis*. *mBio.* 4: e00062-13.

Summary

Hydrogenotrophic methanogenic archaea require reduced ferredoxin as an anaplerotic source of electrons for methanogenesis. H_2 oxidation by Eha hydrogenase provides these electrons consistent with a H_2 requirement for growth. Here we report the identification of alternative pathways of ferredoxin reduction in *Methanococcus maripaludis* that operate independently of Eha to stimulate methanogenesis. A suppressor mutation that increased expression of the glycolytic enzyme glyceraldehyde-3-phosphate:ferredoxin oxidoreductase resulted in a strain capable of H_2-independent ferredoxin reduction and growth with formate as the sole electron donor. In this background, it was possible to eliminate all seven hydrogenases of *M. maripaludis*. Alternatively, carbon monoxide oxidation by carbon monoxide dehydrogenase could also generate reduced ferredoxin that fed into methanogenesis. In either case, the reduced ferredoxin generated was inefficient at stimulating methanogenesis, resulting in a slow growth phenotype. As methanogenesis is limited by the availability of reduced ferredoxin under these conditions, other electron donors, such as reduced coenzyme F_{420}, should be abundant. Indeed, when F_{420}-reducing hydrogenase was reintroduced into the hydrogenase-free mutant, the equilibrium of H_2 production via a F_{420}-dependent formate:H_2 lyase activity shifted markedly toward H_2 compared to wild type.

Introduction

Methanogenic archaea can be grouped into two physiologically distinct groups: the methylotrophs and the hydrogenotrophs (136). Methylotrophic methanogens are relatively versatile, their substrate repertoire for methanogenesis including H_2 and CO_2, acetate, methyl compounds such as methanol and methylamines, and CO. Hydrogenotrophic methanogens are more restricted, using H_2, formate, or (a few species) certain alcohols as electron donors for CO_2 reduction to CH_4.

Hydrogenotrophic methanogens are distinct from methylotrophic methanogens in their use of electron bifurcation as an energy-conserving step in methanogenesis from CO_2 (25, 70, 79, 136). Two pairs of electrons enter the methanogenic pathway at a protein complex that contains two key enzymes, heterodisulfide reductase (Hdr) and formylmethanofuran dehydrogenase (Fwd). One pair of electrons is used by Hdr in an exergonic reaction to reduce the heterodisulfide CoM-S-S-CoB to the sulfhydryl coenzymes HS-CoB and HS-CoM, which in turn serve as reductants for reduction of the methyl group on coenzyme M (CH_3-S-CoM) to CH_4. The other pair of electrons is used in an endergonic reaction by Fwd to reduce CO_2 to the formyl group of formyl-methanofuran (formyl-MFR). For a diagram of the methanogenic pathway, see Fig. 1.1.

By coupling the final, methane-producing step to the initial, CO_2-reducing step, electron bifurcation renders the pathway cyclic. The cyclic model of methanogenesis was recently named the Wolfe cycle in honor of the contributions of Ralph S. Wolfe (134). The cyclic nature of the pathway can explain in part why hydrogenotrophs have not evolved the metabolic versatility of the methylotrophs. The latter organisms use acetate by oxidizing the carbonyl to provide electrons for reduction of the methyl to methane, and they use methyl compounds by disproportionation where some of the substrate is oxidized and some is reduced to methane. However, in hydrogenotrophs the stoichiometric coupling of the methane-producing step to the recruitment of CO_2 into the pathway prohibits the input of additional intermediates. Furthermore, in the case of acetate, only one pair of electrons is available from the oxidation of the carbonyl, yet electron bifurcation requires that two pairs of electrons must feed into the heterodisulfide reductase complex. Although many hydrogenotrophic methanogens contain acetyl-CoA synthase/CO dehydrogenase (ACS/CODH) (the essential enzyme for aceticlastic methanogenesis), they appear to use it only anabolically for CO_2 fixation and not catabolically for acetate utilization.

Either H_2 or formate donates electrons to all four reduction steps in methanogenesis from CO_2. Both substrates supply electrons directly to the Hdr complex via an Hdr-associated hydrogenase or an Hdr-associated formate dehydrogenase (Fdh) (25), thus providing for the first and last reduction steps in the pathway. The two intermediate reduction steps use the coenzyme F_{420} as direct electron donor, and H_2 or formate directly reduces F_{420} via an F_{420}-reducing hydrogenase or Fdh. Hence, H_2 or formate alone can provide the stoichiometric reducing requirements for CO_2 reduction to methane. However, as another consequence of the Wolfe cycle, the levels of intermediates in methanogenesis must be anaplerotically maintained in order to avoid decaying flux in the pathway (134). In the model species *Methanococcus maripaludis* we showed how this occurs by genetically eliminating six of the seven hydrogenases encoded in the genome (79). The resulting mutant, designated $\Delta 6H_2$ase, was unable to use H_2 as the stoichiometric electron donor for methanogenesis. The mutant also lacked a formate-H_2 lyase activity found in the wild type strain. As a result of these two deficiencies, the $\Delta 6H_2$ase mutant required both formate and H_2 for growth and methanogenesis. While formate was needed stoichiometrically for the four reduction steps of methanogenesis, H_2 was required only in low amounts sufficient to support the anaplerotic needs of methanogenesis. In the $\Delta 6H_2$ase mutant, only one hydrogenase remained: the membrane-bound energy-converting hydrogenase Eha, which harvests chemiosmotic energy to drive the reduction of a low-potential ferredoxin which in turn is thought to reduce CO_2 to formyl-MFR. Hence, during growth on H_2 or formate, Eha is essential in wild type *M. maripaludis* to anaplerotically replenish methanogenesis at the first reduction step. Indeed, a knockout of the genes encoding Eha was not successful. Consistent with these results, H_2 stimulated methanogenesis from formate in cell suspensions (79).

Here we show that the essentiality of H_2 and Eha does not always hold, and that in *M. maripaludis* there are at least two additional pathways by which the anaplerotic requirements of methanogenesis can be satisfied. We delete genes encoding Eha in a strain derived from the $\Delta 6H_2$ase mutant that expresses one of these pathways, thus eliminating all H_2 metabolism in a hydrogenotrophic methanogen. These findings show that hydrogenotrophic methanogens are metabolically more versatile than previously thought. Finally, by re-introducing a single hydrogenase - the F_{420}-reducing hydrogenase - into the hydrogenase-free strain, we characterize the electron flux through an isolated formate:H_2 lyase activity that is essential for the growth of wild type on formate.

Methods

Growth conditions. All strains were grown as described in McCas medium containing 200 mM sodium formate and 200 mM MOPS pH7 buffer (59, 98). H_2:CO_2 (20:80, 40 psi) or N_2:CO_2 (20:80, 15 psi) was added to culture headspace unless otherwise indicated. Antibiotics (neomycin sulfate (5 mg mL^{-1}), puromycin (2.5 µg mL^{-1}), or metronidazole (50 µg mL^{-1})) were used where appropriate. For growth with CO in the culture headspace, 50% CO was injected to a final concentration of 5% (V/V). For growth curves, triplicate cultures were inoculated with a 10% inoculum and optical density was monitored at 660 nm.

For growth under continuous culture, a modified version of a previously established chemostat system was employed (52, 57, 74). $\Delta 7H_2ase_{sup}$-*frc* was grown under steady state with 380 mM sodium formate. NaCl was removed to maintain osmotic balance. 0.2% w/v casamino acids and ampicillin (100 µg mL^{-1}) were included in the growth medium. A gas mixture containing Ar/CO_2/1% H_2S (29:8:3) was used. Medium and gas flow rates are indicated in the text. The pH of steady state samples was monitored and maintained at 6.95 with automated addition of 10% H_2SO_4. Agitation in the vessel was maintained at 50 rpm throughout steady state growth.

For continuous culture, $\Delta 7H_2$ase-*frc* was grown to a maximum OD of 0.7 with a medium dilution rate of 0.083 L hr^{-1} and a gas flow rate of 26 mLs min^{-1}. Medium dilution was changed to 0.125 L hr^{-1} until culture OD dropped to 0.28 at which point the first sample was taken. The low OD ensured the culture was constantly growing with excess formate. When medium dilution rate was changed throughout the course of sampling, culture was given at least 24 hours to equilibrate before samples were collected. For changes in gas flow rate, the gas phase was allowed at least 1 hour to equilibrate before sample collection.

Generation of mutants and plasmids. Strains, plasmids, and primers used in this study are listed in Table 4.1. Strain MM901, a derivative of *M. maripaludis* S2 that lacks uracil phosphoribosyl transferase (*upt*), was used as the wild type strain (25, 154). Mutants were constructed using methods described in (98) and modified in (25). Briefly, to generate deletion mutants, a PCR product containing an in-frame deletion of the gene of interest was ligated into the vector pCRuptneo (25). This was then transformed into MM901. Neomycin sulfate (5mg mL^{-1}) was used to select for a merodiploid and 6-azauracil (250µg mL^{-1}) was used as negative

selection to isolate the mutant of interest. To place genes onto a replicative vector, PCR products were cloned directly into pLW40 or pLW40neo and transformed into the strain of interest. Either neomycin sulfate (5mg mL^{-1}) or puromycin (2.5µg mL^{-1}) was included as appropriate. Suppressor strains of $\Delta 6H_2$ase capable of growth in the absence of H_2 were grown in formate medium either with our without addition of 100µM or 1mM ammonium 2-(methylthio)ethanesulfonate (CH_3-S-CoM); however, CH_3-S-CoM was found to have no stimulatory effect on growth and was excluded from all subsequent experiments. All mutants were confirmed by PCR screen, and deletion of *ehaNO* was also confirmed by Southern blot and Illumina sequencing (see below).

Genome sequencing. Genome sequencing was carried out for $\Delta 6H_2$ase (MM1284), $\Delta 7H_2ase_{sup}$ (MM1310), and six of the $\Delta 6H_2$ase strains that had developed suppressor mutations (MM1315, MM1316, MM1317, MM1318, MM1319, MM1320). $\Delta 6H_2$ase strains were isolated by dilution to extinction before processing. High molecular weight DNA for sequencing was extracted using the Qiagen PureGene kit according to the manufacturer's instructions. Genomes were sequenced as described in (51) using unpaired 36 bp reads with the Illumina Genome Analyzer GA IIX according to manufacturer's instructions (Illumina, San Diego, CA). For each genome, a random-fragment library was constructed using a custom protocol. Briefly, gDNA samples were sheared using a Bioruptor UCD-200 (Diagenode Inc. Denville, NJ), and end-repaired a using the End-It DNA End Repair Kit (Epicentre). Repaired fragments were subjected to A-Tailing using Taq DNA polymerase (Roche Inc USA, Chicago, IL), and custom adaptors ligated to A-tailed fragments using T4DNA Ligase (New England Biolabs Beverly, MA). Libraries were size selected using automated electrophoresis on a Pippen Prep (Sage Science, Beverly MA), and assessed for size range and concentration using a Qubit (Invitrogen Inc, Carlsbad CA) and a Bioanalyzer (Agilent Inc, San Diego, CA).

Raw sequence data were compared directly to the *M. maripaludis* strain S2 reference genome (NCBI reference NC_005791.1) to identify possible suppressor mutations allowing for H_2 independent growth (Table 4.2). Putative mutations upstream of the gene encoding glyceraldehyde-3-phosphate:ferredoxin oxidoreductase (GAPOR) were identified and verified in $\Delta 6H_2$ase and $\Delta 7H_2ase_{sup}$ with Sanger sequencing (GeneWiz, South Plainfield, NJ).

CH_4 and H_2 measurements. To measure H_2 from batch culture, 2.5 mL of culture headspace was collected and stored for no longer than 24 hours in a 5mL serum vial pre-flushed with 100%

N_2. To measure gas concentration from chemostat-grown cells, gas was collected directly into 5 mL serum vials after flushing with at least 350 mLs of chemostat gas outflow. For batch culture measurements, the headspace contained a pressure of 2 atm. H_2 and CH_4 concentrations were measured by gas chromatography as described (79). To completely oxidize ferredoxin, metronidazole (50 μg mL^{-1}) was used. Upon addition of metronidazole, gas flow through the chemostat vessel was allowed to equilibrate for one hour prior to collection and analysis. Rates of H_2 production were calculated assuming a liter of cell material at OD 1.0 yields 0.34 grams dry weight (88).

Results

CO stimulates growth of Δ6H_2ase in the absence of H_2. Eha provides anaplerotic input to the methanogenic pathway by acting as a supplement to electron bifurcation for the reduction of a ferredoxin that in turn is used to reduce CO_2 to formyl-MFR (79). However, other pathways of ferredoxin reduction/oxidation exist in methanogenic archaea. The ACS/CODH enzyme complex converts CO_2 to CO, which ultimately becomes the carbonyl carbon of acetyl-CoA (8, 38). This reduction is dependent on reduced ferredoxin as an electron donor.

To test whether the reverse reaction of ACS/CODH – CO oxidation to CO_2 with the production of reduced ferredoxin – can stimulate methanogenesis in an H_2 independent manner, the Δ6H_2ase mutant was grown on formate medium with or without the addition of H_2 or CO to the culture headspace. As expected, H_2 promoted robust growth. In addition, CO promoted growth in the absence of H_2 (Fig. 4.1). Growth rates were much slower with CO in place of H_2 suggesting that ferredoxin reduction by Eha is preferred. Growth promoted by CO was directly attributable to ACS/CODH since, when the CO_2-reducing subunits were genetically eliminated (Δ6H_2ase-Δ*cdh*), growth no longer occurred with CO and formate as the only electron donors (Fig. 4.1).

Isolation of a suppressor mutant that allows growth of Δ6H_2ase on formate alone. The growth of Δ6H_2ase with formate and CO suggests that ferredoxin reduction by Eha is not necessary for growth provided alternative mechanisms to anaplerotically stimulate methanogenesis are present. CH_3-S-CoM addition to cell extracts stimulates methanogenesis (12, 48), and methanogenic archaea are capable of CH_3-S-CoM uptake via a poorly characterized and very inefficient activity (5, 37). Therefore, we tried to grow Δ6H_2ase on

formate in the absence of H_2 in the presence and absence of CH_3-S-CoM. Surprisingly, regardless of the presence or absence of CH_3-S-CoM, after prolonged incubation of nine independent cultures, all nine grew (Fig. 4.2). Upon transfer to new medium, each strain tested routinely grew to maximum OD within 24 hours. These results suggested that independent suppressor mutations ($\Delta 6H_2ase_{sup}$) were generated that allowed for growth on formate alone. Suppressor strains that were generated in the presence of CH_3-S-CoM grew well in its absence. Hence, although CH_3-S-CoM failed to stimulate growth, mutants developed that had a novel mechanism to anaplerotically stimulate methanogenesis.

Deletion of *eha* is possible due to a suppressor mutation. A suppressor mutation that allows growth of $\Delta 6H_2ase_{sup}$ on formate alone could have produced a novel H_2 production activity or it could have generated a new ferredoxin reducing activity that is independent of H_2. If a novel H_2 production pathway were responsible, *eha* would still be essential (79). We attempted deletion of the genes encoding the active site subunits of Eha (*ehaNO*) in one of the $\Delta 6H_2ase_{sup}$ strains (58, 133). Deletion of *ehaNO* was indeed possible suggesting another ferredoxin reduction activity is present in the suppressor background. The new strain ($\Delta 7H_2ase_{sup}$) lacks the genes encoding the active sites for all genomically encoded hydrogenases: Δ*vhuAU*Δ*vhcA*Δ*fruA*Δ*frcA*Δ*hmd*Δ*ehbN*Δ*ehaNO*. $\Delta 7H_2ase_{sup}$ grew in the absence of H_2, and H_2 did not stimulate growth (Fig. 4.3A).

CO is a potent inhibitor of nickel-containing hydrogenases (105, 112). 5% CO inhibited wild type *M. maripaludis* grown on formate, but had no inhibitory effect on $\Delta 7H_2ase_{sup}$. In fact, $\Delta 7H_2ase_{sup}$ grew better on formate in the presence of 5% CO than it did on formate alone (Fig. 4.3B), suggesting that in $\Delta 7H_2ase_{sup}$, like $\Delta 6H_2ase$, CO was oxidized to CO_2 leading to the production of reduced ferredoxin. The growth of $\Delta 7H_2ase_{sup}$ is apparently limited by the availability of reduced ferredoxin, and CO oxidation partially relieves its slow growth phenotype. The reduced ferredoxins generated by the suppressor activity and ACS/CODH appear additive in stimulating methanogenesis. $\Delta 7H_2ase_{sup}$ grew faster with formate and CO than either $\Delta 7H_2ase_{sup}$ with formate alone or $\Delta 6H_2ase$ with formate and CO.

Genome sequencing reveals a suppressor mutation allowing for growth of $\Delta 6H_2ase_{sup}$ and $\Delta 7H_2ase_{sup}$ on formate alone. To determine the genetic background that allowed growth of $\Delta 6H_2ase_{sup}$ and $\Delta 7H_2ase_{sup}$ on formate in the absence of H_2 or CO, we performed Illumina sequencing on $\Delta 7H_2ase_{sup}$ and six of the isolated suppressors and compared the sequence to

the $\Delta 6H_2$ase parent (Table 4.2). Four out of six of the $\Delta 6H_2ase_{sup}$ mutants, as well as $\Delta 7H_2ase_{sup}$, shared a common insertion (AT at position 931341) in an intergenic region directly upstream of the gene for glyceraldehyde-3-phosphate (G3P):ferredoxin oxidoreductase (GAPOR) (Fig. 4.4). The insertion generated the sequence AATATATA upstream of GAPOR which is very similar to the consensus methanogen promoter TTTA(T/A)ATA (114). Therefore, it appears that generation of a promoter upstream of GAPOR increases expression of this ferredoxin-reducing enzyme to allow for H_2-independent growth. Sanger sequencing confirmed the presence of this mutation in $\Delta 7H_2ase_{sup}$ and its absence in $\Delta 6H_2$ase. The nature of the suppressor mutations allowing growth in the other two $\Delta 6H_2ase_{sup}$ strains was not readily apparent from the genome sequencing data.

Overexpression of GAPOR in $\Delta 6H_2$ase allows growth without H_2. Although the generation of a putative promoter sequence upstream of GAPOR suggests overexpression of this gene leads to growth, the nature of the mutation could also result in a promoter reading in the opposite direction (Fig. 4.4). Therefore, instead of engineering the mutation on the chromosome of $\Delta 6H_2$ase to test its efficacy at stimulating growth, we chose to overexpress GAPOR on a replicative vector to recapitulate the effect and avoid possible overexpression of a second operon. GAPOR was placed under control of the *Methanococcus vanneilii* histone promoter on the replicative vector pLW40neo (32) and introduced into the $\Delta 6H_2$ase background. The resulting strain displayed moderate growth in the absence of H_2 and robust growth in the presence of H_2, verifying that either GAPOR or Eha could be used to generate the reduced ferredoxin required for growth (Fig 4.5).

$\Delta 7H_2ase_{sup}$ expressing F_{420}-reducing hydrogenase can produce substantial amounts of H_2. $\Delta 7H_2ase_{sup}$ grows more slowly than wild type on formate, suggesting that reduced ferredoxin is limiting. Reduced ferredoxin limitation of methanogenesis implies that other reduced cofactors that feed into the pathway, such as $F_{420}H_2$, are present in excess. Wild type *M. maripaludis* possesses a F_{420}-dependent formate:H_2 lyase activity that is catalyzed by Fdh and F_{420}-reducing hydrogenase. The wild type strain grown on formate can accumulate H_2 in the culture headspace to a concentration of 0.16 ± 0.02% of the gas phase at 2 atm pressure (average ± SD for three biological replicates) (59, 88). An excess of $F_{420}H_2$ should drive the equilibrium of this activity towards increased H_2 production. *frc* encoding F_{420}-reducing hydrogenase was placed on the replicative vector pLW40 (32) and reintroduced into $\Delta 7H_2ase_{sup}$ to restore formate:H_2 lyase activity. When grown with formate as the only electron donor for

methanogenesis, $\Delta 7H_2ase_{sup}$-*frc* was capable of producing H_2 up to a concentration of 2.32 ± 0.79% (Fig. 4.6A). When cultures entered stationary phase, H_2 reuptake occurred, presumably due to depletion of formate and an equilibrium shift back towards $F_{420}H_2$ production from H_2. $\Delta 7H_2ase_{sup}$, which lacks formate:H_2 lyase activity, was incapable of H_2 production.

We also attempted continuous culture of $\Delta 7H_2ase_{sup}$-*frc* to assess how additional factors effect the equilibrium of formate:H_2 lyase activity. $\Delta 7H_2ase_{sup}$-*frc* was maintained at a low OD under conditions where the medium dilution rate (0.125 L hr^{-1}) slightly exceeded the growth rate to ensure that the culture was continuously growing. Under these conditions, $\Delta 7H_2ase_{sup}$-*frc* produced between 100 and 500 µmol H_2 gdw^{-1} (gram dry weight) hr^{-1} (Fig. 4.6B). The higher production rates were observed when the gas flow rate was increased from 25 to 230 mLs min^{-1} demonstrating that increased removal of H_2 results in an equilibrium shift towards even greater H_2 production. When the growth rate was allowed to exceed the medium dilution rate (0.031 L hr^{-1}), H_2 production was not greatly affected.

As reduced ferredoxin limitation of growth appears to lead to increased H_2 production, we sought to take this to the extreme case of the absence of reduced ferredoxin. Metronidazole, an antibiotic capable of oxidizing ferredoxin (87), was added to the chemostat and after one hour, H_2 production was found to have increased five-fold to ~2.5 mmol gdw^{-1} hr^{-1}. With increased gas flow, this rate approached 5 mmol gdw^{-1} hr^{-1}. Robust H_2 production upon metronidazole addition verifies that limiting reduced ferredoxin leads to an excess of $F_{420}H_2$.

Discussion

Hydrogenotrophic methanogens have unappreciated metabolic versatility. Although they do not share pathways of methylotrophic methanogens, hydrogenotrophic methanogens have a different kind of metabolic versatility. We have shown previously that this is due in part to the ability of hydrogenotrophs to use either formate or H_2 as electron donor to all four reduction steps of methanogenesis (25, 79). In addition, we have shown here that hydrogenotrophs also have versatility in their pathways of ferredoxin reduction for the anaplerotic electron input to methanogenesis. First, our results show clearly that H_2 is not the only possible reductant for this purpose. The $\Delta 6H_2ase$ mutant grows in the complete absence of H_2 as long as CO is present along with formate. In the case of the $\Delta 7H_2ase_{sup}$ strain, even CO was not needed and formate was the sole electron donor. H_2 addition to cultures of $\Delta 7H_2ase_{sup}$ grown on formate had no

stimulatory effect confirming that H_2 uptake did not occur (Fig. 4.3B). CO, a hydrogenase inhibitor, also had no inhibitory effect in the $\Delta 7H_2ase_{sup}$ background but did in wild type (105, 112). Additionally, $\Delta 7H_2ase_{sup}$ lacked all formate:H_2 lyase activity (Fig. 4.6A). Taken together, these data confirm that all hydrogenase activity had been eliminated. The $\Delta 6H_2ase$, $\Delta 6H_2ase_{sup}$ and $\Delta 7H_2ase_{sup}$ strains represent, to our knowledge, the first examples of hydrogenotrophic methanogens capable of growth in the complete absence of H_2.

H_2-independent growth occurs via novel electron flow pathways. Here we have demonstrated two pathways by which H_2 may be replaced as the anaplerotic electron donor for methanogenesis. Like Eha with H_2, both pathways reduce ferredoxin, which then presumably reduces CO_2 to formylmethanofuran. First, CO served this purpose in the $\Delta 6H_2ase$ and $\Delta 7H_2ase_{sup}$ strains. To our knowledge only one other study reported the use of CO for methanogenesis in a hydrogenotrophic methanogen. In that report, CO as sole substrate supported slow growth of *Methanothermobacter thermautotrophicus* by disproportionation to CO_2 and CH_4, and a F_{420}-reducing carbon monoxide dehydrogenase activity was found (27). This differs from our results in which formate as well as CO was present. In addition, our $\Delta 6H_2ase$ and $\Delta 7H_2ase_{sup}$ mutants are capable of producing $F_{420}H_2$ directly from formate, so a F_{420}-reducing carbon monoxide dehydrogenase activity is likely of little importance. Instead, the oxidation of CO leads to reduced ferredoxin. CO formation from H_2 and CO_2 with reduced ferredoxin as an intermediate has been observed in cell suspensions of hydrogenotrophic methanogens possessing ACS/CODH (17, 38), and the process we observed here, which depended on ACS/CODH, appears to be the reverse.

The CO utilization demonstrated here for *M. maripaludis* contrasts with methylotrophic methanogens. First, in methylotrophic methanogens CO can be converted to methane and CO_2 or to formate and acetate with the concomitant generation of ATP (77, 115). In contrast, 5% CO, as was used in our growth experiments, is insufficient as a stoichiometric electron donor for the amount of growth observed, and functioned only anaplerotically. In both kinds of methanogens CO oxidation results in reduced ferredoxin, but only the methylotrophs are known to use reduced ferredoxin as a stoichiometric source of electrons for methanogenesis. Second, methylotrophic methanogens can carry out methanogenesis solely from acetate by using ACS/CODH to cleave acetyl-CoA. *M. maripaludis* can utilize acetate anabolically (110), and can also use ACS/CODH anabolically for CO_2 fixation to acetyl-CoA (8). Nevertheless, although CO utilization as an anaplerotic stimulant of methanogenesis in *M. maripaludis* occurred via

ACS/CODH, *M. maripaludis* is apparently unable to use acetate for methanogenesis, even anaplerotically. Thus, our $\Delta 6H_2$ase mutant, which was always grown in the presence of acetate and casamino acids, would not grow on formate in the absence of H_2 without a suppressor mutation occurring.

As an additional novel pathway, overexpression of GAPOR could substitute for Eha and H_2. GAPOR is found throughout the Archaea (101, 106, 124, 140) and functions in glycolysis, catalyzing the oxidation of G3P to 3-phosphoglycerate (3-PG) with the concomitant reduction of ferredoxin (101, 106). The corresponding gluconeogenic reactions are catalyzed by G3P dehydrogenase (GAPDH), a NADPH dependent enzyme, and phosphoglycerate kinase (PGK), an ATP dependent enzyme (Fig. 4.7). Running both pathways simultaneously would result in:

$$NADPH + ATP + Fd_{ox} \rightarrow NADP^+ + ADP + Pi + Fd_{red}$$

M. maripaludis also encodes a $F_{420}H_2$:$NADP^+$ oxidoreductase (Fno) and the F_{420}-dependent Fdh (10, 58). When these activities are taken into account, an ATP-dependent $F_{420}H_2$:ferredoxin oxidoreductase activity is possible (Fig. 4.7):

$$F_{420}H_2 + ATP + Fd_{ox} \rightarrow F_{420} + ADP + Pi + Fd_{red}$$

This pathway evidently operates in the $\Delta 6H_2ase_{sup}$ strains and the $\Delta 7H_2ase_{sup}$ strain, as well as in $\Delta 6H_2$ase with GAPOR overexpressed on a plasmid.

Reduced ferredoxin abundance vs. inefficient electron transfer. The CO-dependent and GAPOR-dependent pathways of ferredoxin reduction appear less efficient than Eha in supplying anaplerotic electrons to methanogenesis, since the $\Delta 6H_2$ase strain with formate and CO and the $\Delta 7H_2ase_{sup}$ strain with formate alone grew more slowly than Eha^+ strains with formate and H_2. Indeed, combining the two pathways by including CO with formate for growth of the $\Delta 7H_2ase_{sup}$ strain increased growth in an additive manner. The low efficiency of the alternative pathways may be due to low concentrations of reduced ferredoxin produced compared to what can be produced by Eha, or the reduced ferredoxin could be abundant but inefficient at transferring electrons to Fwd. The latter interpretation is consistent with the proposal that the ferredoxin pools for anabolism and catabolism are normally separated in *M. maripaludis* (79), since the anabolic ferredoxin-reducing hydrogenase Ehb and the anaplerotic ferredoxin-reducing Eha reduce ferredoxins that substitute inefficiently for each other (79, 110).

Robust H_2 production by $\Delta 7H_2ase_{sup}$-*frc* is consistent with abundant $F_{420}H_2$. Growth limitation by the availability of reduced ferredoxin resulted in a buildup of $F_{420}H_2$ and a robust

production and accumulation of H_2 when F_{420}-reducing hydrogenase was reintroduced into the $\Delta 7H_2ase_{sup}$ strain. In batch-grown $\Delta 7H_2ase_{sup}$-*frc*, H_2 buildup in culture headspace was ~13-fold higher than in wild type and accounted for ~2% of the gas phase. Additionally, continuous culture of $\Delta 7H_2ase_{sup}$-*frc* saw robust H_2 production. Maximal production rates approaching 5 mmol gdw^{-1} hr^{-1} were observed when metronidazole was added further supporting the idea that a dearth of reduced ferredoxin, and, by extension, an excess of $F_{420}H_2$ shifts the equilibrium of formate:H_2 lyase activity towards H_2 production.

Tables and figures

Table 4.1. Strains, plasmids and primers used in this study.

Strain	Description	Locus	Reference
MM901	Wild type *M. maripaludis* with an in-frame deletion of *upt*	See Reference	(25)
MM1284	Δ6H_2ase, MM901 Δ*vhuAU*Δ*vhcA*Δ*fruA*Δ*frcA*Δ*hmd*Δ*ehbN*	See Reference	(79)
MM1310	Δ7H_2ase$_{sup}$, MM1316 Δ*ehaNO*	Mmp1461,Mmp1462	This study
MM1315	Δ6H_2ase with a suppressor allowing for growth without H_2	-	This study
MM1316	Δ6H_2ase with a suppressor allowing for growth without H_2	-	This study
MM1317	Δ6H_2ase with a suppressor allowing for growth without H_2	-	This study
MM1318	Δ6H_2ase with a suppressor allowing for growth without H_2	-	This study
MM1319	Δ6H_2ase with a suppressor allowing for growth without H_2	-	This study
MM1320	Δ6H_2ase with a suppressor allowing for growth without H_2	-	This study
MM1327	MM1284 with a deletion of CO dehydrogenase (*cdh*)	Mmp0983-0985	This study
MM1338	MM1284 with GAPOR overexpressed on pLW40neo	Mmp0945	This study
MM1339	MM1310 with F_{420}-reducing hydrogenase (*frc*) on pLW40	Mmp0817-0820	This study

Primer	Sequence 5' to 3'	Notes
EhaNO-Us-F-NotI	AAAAGCGGCCGCCATTTCCACTTGGAATGAGGCCAGG	NotI
EhaNO-Us-R-AscI	AAAAGGCGCGCCCATCAAGATCATCTCCAAATTAAGTC	AscI
EhaNO-Ds-F-AscI	AAAAGGCGCGCCATAATAAATAAACCTGATTGCAGGTG	AscI
EhaNO-Ds-R-XbaI	AAAATCTAGAGTAACTATTGCATTTTCCACAGGAC	XbaI
cdhA_us_F_NotI	AAAAGCGGCCGCGAAATAAACTTCACAATTATCC	NotI
cdhA_us_R_AscI	AAAAGGCGCGCCCCATGACCATCACCGATTTGTCATG	AscI
cdhB_ds_R_XbaI	AAAATCTAGATTAAAATTCCTCTTTTTGATGAATCAG	XbaI
cdhB_Ds_F_AscI	AAAAGGCGCGCCTAGGCTGTTAAAAATGATTATTGCAGTTACTGG	AscI
GAPOR-F-pstI	AAAACTGCAGATGAACATTTTGATTGATGGATCAAGAC	PstI
GAPOR-R-AscI	TTTTGGCGCGCCTTATTCTTTTAATTTCCAGTCAATTTCTAACAATTCGC	AscI
FrcA-F-Phos	ATGGGTAAGACGGTAGAGATAAATCCTACAAC	5'-Phos
FrcB-R-AscI	AAAAGGCGCGCCTTAGTATGGAACTGGAAGGCCTATTTCTTTTCTGTGGGC	AscI
pHMV-F	TTAACGCTTTTATTTCCCTTATCTTGTGGG	SpeI
pHMV-R	ATGCATTTCACCTATTAGTTATCTATAAAATTATAATATCAATAGC	

Plasmid	Reference
pCRuptneo	(25)
pLW40	(32)
pLW40neo	(32)
pCRuptneoΔeha	This study
pCRuptneoΔcdh	This study
pLW40neo-GAPOR	This study
pLW40-frc	This study

Table 4.2. Genome sequencing results for Δ6H_2ase, Δ7H_2ase$_{sup}$, and Δ6H_2ase$_{sup}$. Mutations due to the upt and hydrogenase deletions are not shown.

Strain	base position	reference base	sequence change	locus tag	gene	change
MM1284						
Δ6H_2ase	24070	*	*/+AT	MMP0014	truD	
	98165	T	A	MMP0087	hmgA	142:I->F
	353523	*	*/-T	MMP0356		
	563785	*	*/+TA			
	687745	A	G	MMP0697	leuS	331:I->V
	920059	T	G	MMP0930	cheR	60:T->P
	1150379	*	*/+G	MMP1165		
	1153734	*	+AT/*	MMP1169		
	1438687	*	-G/*	MMP1478	cbiA	
	1495457	*	-A/*			
MM1310						
Δ7H_2ase$_{sup}$	98165	T	A	MMP0087	hmgA	142:I->F
	313616	C	T	MMP0317		216:S->L
	687745	A	G	MMP0697	leuS	331:I->V
	931341	*	+AT/*			
	952444	A	G	MMP0964		
	1153734	*	+AT/*	MMP1169		
	1438687	*	-G/*	MMP1478	cbiA	
MM1315						
Δ6H_2ase$_{sup}$	98165	T	A	MMP0087	hmgA	142:I->F
	269003	*	*/-TG	MMP0269		
	471448	*	*/+G	MMP0475		
	543786	*	*/-T			
	687745	A	G	MMP0697	leuS	331:I->V
	931341	*	*/+AT			
	1104513	A	T	MMP1114	rpe	91:V->D
	1153734	*	+AT/*	MMP1169		
	1171264	*	*/+AT			
	1438687	*	-G/*	MMP1478	cbiA	
	1530524	*	*/+CC	MMP1580		
MM1316						
Δ6H_2ase$_{sup}$	98165	T	A	MMP0087	hmgA	142:I->F
	458790	*	*/-AT	MMP0462		
	687745	A	G	MMP0697	leuS	331:I->V
	920059	T	G	MMP0930	cheR	60:T->P
	931341	*	*/+AT			
	1153734	*	+AT/*	MMP1169		
	1201528	*	*/+G			
	1288613	*	*/+TT			
	1438687	*	-G/*	MMP1478	cbiA	
	1497389	*	*/-TT			
MM1317						
Δ6H_2ase$_{sup}$	98165	T	A	MMP0087	hmgA	142:I->F
	687745	A	G	MMP0697	leuS	331:I->V
	760695	A	G	MMP0769		246:M->T
	778723	*	*/-T			
	931341	*	*/+AT			
	1153734	*	+AT/*	MMP1169		
	1318753	*	*/-CT			
	1438687	*	-G/*	MMP1478	cbiA	
	1495457	*	-A/*			

MM1318						
$\Delta 6H_2ase_{sup}$	42925	*	*/+C	MMP0027		
	98165	T	A	MMP0087	hmgA	142:I->F
	449397	T	C			
	675485	C	T	MMP0687	tpiA	59:P->L
	687745	A	G	MMP0697	leuS	331:I->V
	730220	*	*/+TG			
	920059	T	G	MMP0930	cheR	60:T->P
	931333	*	-AA/*			
	1153734	*	+AT/*	MMP1169		
	1173018	*	*/-AT			
	1438687	*	-G/*	MMP1478	cbiA	
	1495457	*	-A/*			
MM1319						
$\Delta 6H_2ase_{sup}$	98165	T	A	MMP0087	hmgA	142:I->F
	675485	C	T	MMP0687	tpiA	59:P->L
	687745	A	G	MMP0697	leuS	331:I->V
	753643	*	*/+CG	MMP0762		
	835554	*	*/+AC			
	920059	T	G	MMP0930	cheR	60:T->P
	931056	*	+A/*	MMP0944		
	1153734	*	+AT/*	MMP1169		
	1438687	*	-G/*	MMP1478	cbiA	
MM1320						
$\Delta 6H_2ase_{sup}$	354970	*	*/-T	MMP0358		
	675485	C	T	MMP0687	tpiA	59:P->L
	687745	A	G	MMP0697	leuS	331:I->V
	931341	*	+AT/*			
	1043580	*	*/-A			
	1153734	*	+AT/*	MMP1169		
	1438687	*	-G/*	MMP1478	cbiA	

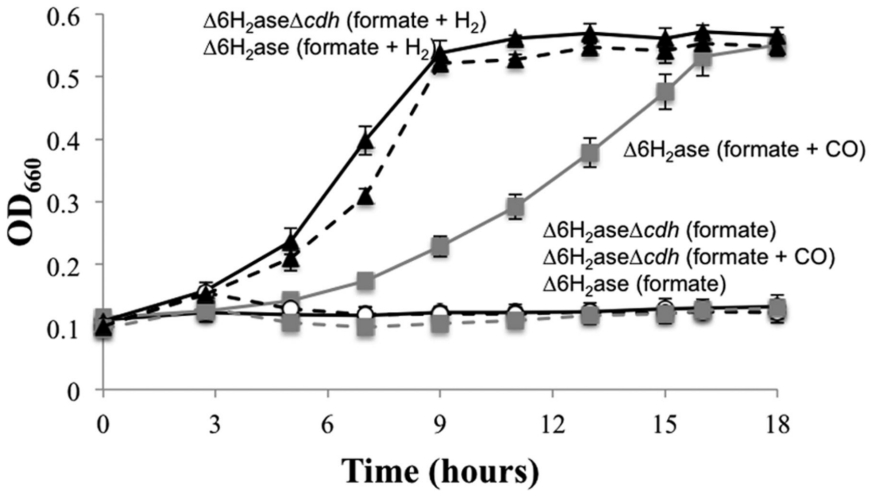

Figure 4.1. Growth of Δ6H_2ase with CO and formate. Δ6H_2ase and Δ6H_2aseΔ*cdh* grown with formate + H_2 (black symbols), formate + 5% CO (grey symbols), or formate alone (white symbols). Solid lines, Δ6H_2ase; dashed lines, Δ6H_2aseΔ*cdh*. Data points are averages of three cultures and error bars represent one standard deviation around the mean.

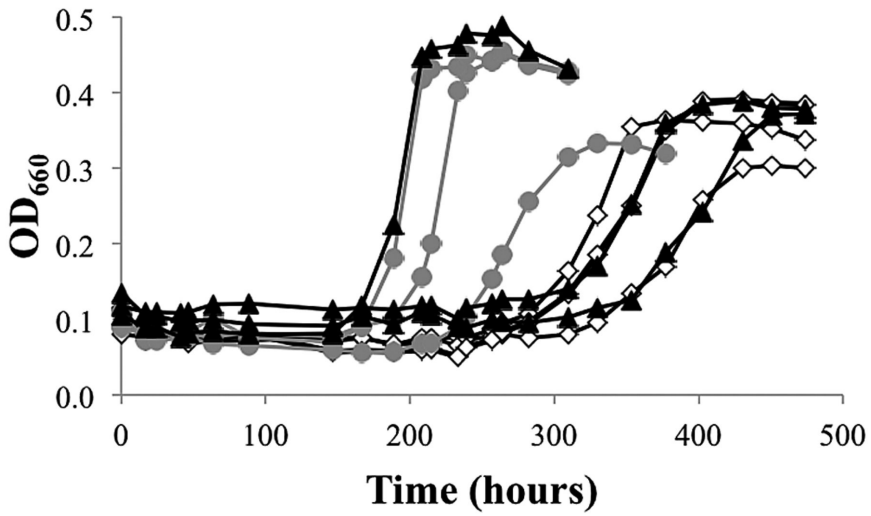

Figure 4.2. Generation of suppressor strains of Δ6H_2ase capable of H_2-independent growth. Δ6H_2ase was grown in formate-containing medium without H_2 or CO. Medium contained 1000 μM (black), 100 μM (grey), or 0 μM (white) CH_3-S-CoM (three replicates each); however, CH_3-S-CoM had no stimulatory effect on growth. Each curve represents growth in a single tube.

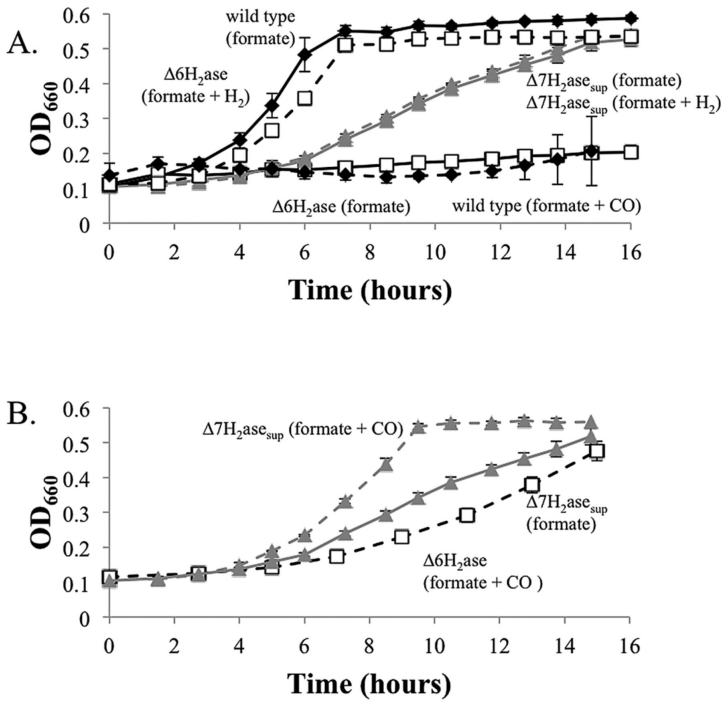

Figure 4.3. Growth characteristics of $\Delta 7H_2ase_{sup}$. Black symbols, growth of wild-type strain MM901; grey symbols, $\Delta 7H_2ase_{sup}$; white symbols, $\Delta 6H_2ase$. Dashed lines indicate cultures with H_2 or 5% CO in culture headspace. A) Growth of $\Delta 7H_2ase_{sup}$ with formate alone or formate + H_2. B) Growth of $\Delta 7H_2ase_{sup}$ with formate + CO. $\Delta 7H_2ase_{sup}$ grown on formate (from Fig. 3A) and $\Delta 6H_2ase$ grown on formate + CO (from Fig. 1) are shown for comparison. Data points are averages of three cultures and error bars represent one standard deviation around the mean.

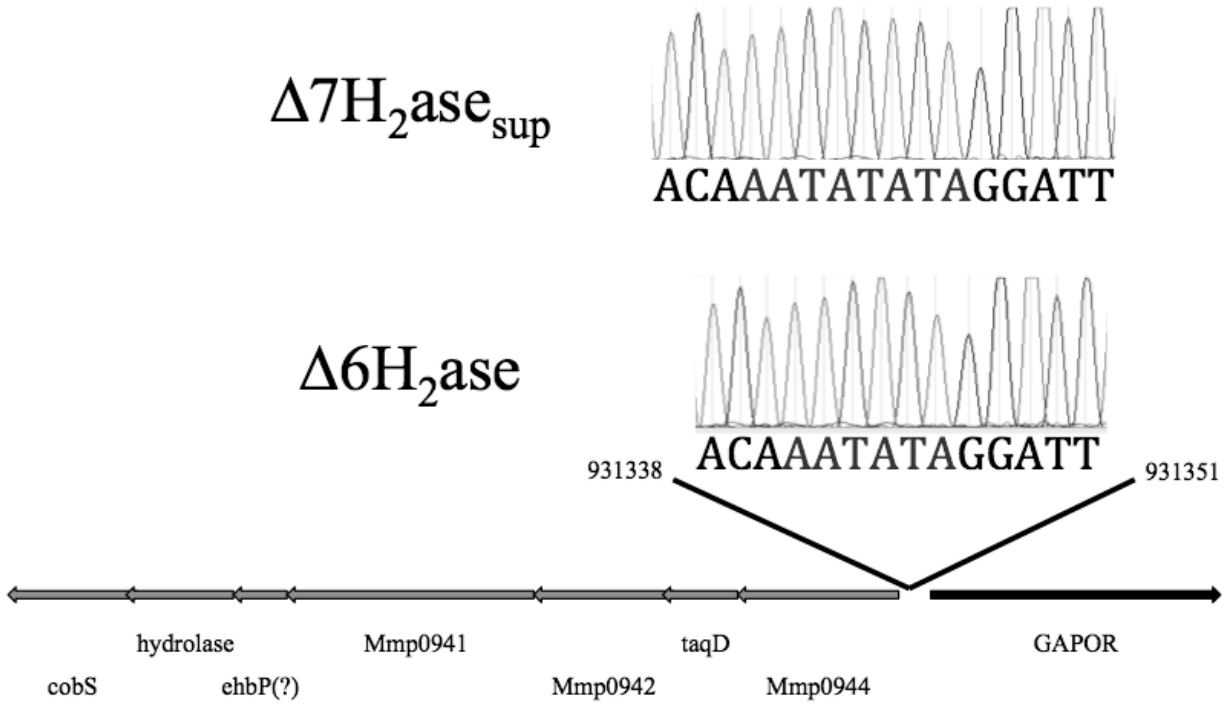

Figure 4.4. Genomic context of a suppressor mutation allowing for H_2-independent growth of $\Delta 7H_2ase_{sup}$.

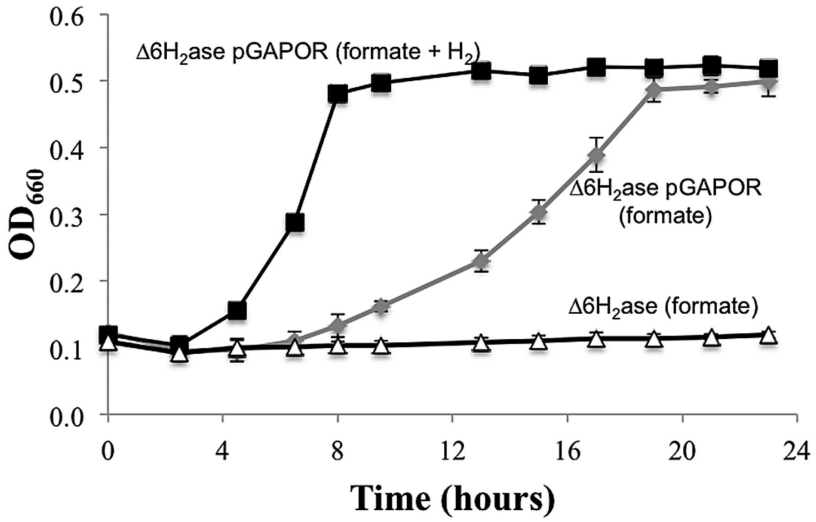

Figure 4.5. Growth of $\Delta 6H_2$ase overexpressing GAPOR in the presence and absence of H_2. Black symbols, $\Delta 6H_2$ase overexpressing GAPOR grown on formate + H_2; grey symbols, $\Delta 6H_2$ase overexpressing GAPOR grown formate alone; white symbols, $\Delta 6H_2$ase on formate alone.

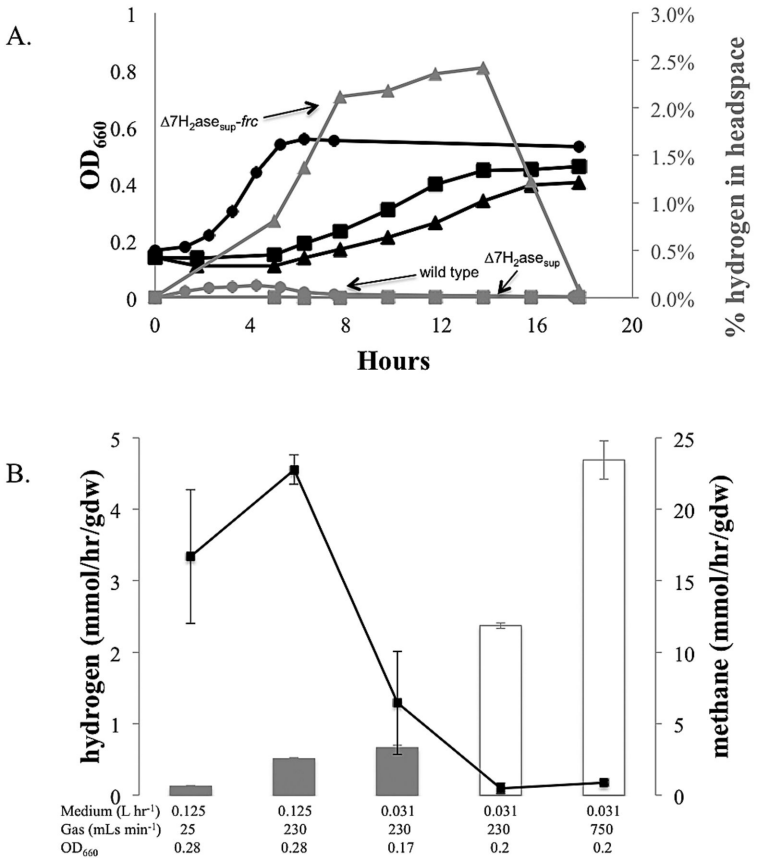

Figure 4.6. Growth and H_2 production by $\Delta 7H_2ase_{sup}$ expressing F_{420}-reducing hydrogenase ($\Delta 7H_2ase_{sup}$-*frc*). A) Growth on formate (black) and H_2 production (grey) by wild-type strain MM901 (circles), $\Delta 7H_2ase_{sup}$ (squares), and $\Delta 7H_2ase_{sup}$-*frc* (triangles) in batch culture. Data are from a single representative experiment, but two replicate experiments gave similar results (Fig. S2). B) CH_4 (black curve) and H_2 production (bars) of $\Delta 7H_2ase_{sup}$-*frc* in continuous culture. Grey bars indicate where culture was actively growing. White bars indicate culture where metronidazole (50 µg mL-1) was added to completely oxidize ferredoxin. X-axis indicates medium dilution rate, gas flow rate, and culture optical density (top to bottom, respectively).

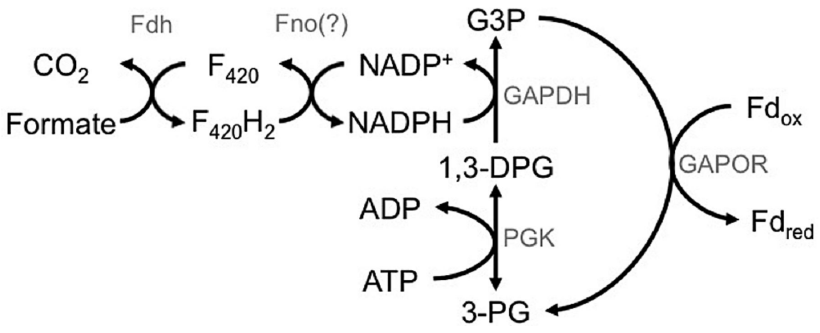

Figure 4.7. Glyceraldehyde-3-phosphate:ferredoxin oxidoreductase cycle for ATP dependent ferredoxin reduction. The GAPOR cycle of *M. maripaludis* as originally described by (30) with potential input from $F_{420}H_2$. Fdh, formate dehydrogenase; Fno, $F_{420}H_2$:$NADP^+$ oxidoreductase; GAPDH, glyceraldehyde-3-phosphate dehydrogenase; GAPOR, glyceraldehyde-3-phosphate:ferredoxin oxidoreductase; PGK, phosphoglycerate kinase. G3P, glyceraldehyde-3-phosphate; 1,3-DPG, 1,3-diphosphoglycerate; 3-PG, 3-phosphoglycerate.

CHAPTER 5

The importance of VhuD for heterodisulfide reduction

Originally published as an article in *Journal of Bacteriology*:

Costa, Kyle C., Thomas J. Lie, Qin Xia, and John A. Leigh. 2013. VhuD facilitates electron flow from H_2 or formate to heterodisulfide reductase in *Methanococcus maripaludis*. *J. Bacteriol*. 195: 5160-5165.

Summary

Flavin-based electron bifurcation has recently been characterized as an essential energy conservation mechanism utilized by hydrogenotrophic methanogenic archaea to generate low potential electrons in an ATP-independent manner. Electron bifurcation takes place at the flavin associated with the α subunit of heterodisulfide reductase (HdrA). In *Methanococcus maripaludis* the electrons for this reaction come from either formate or H_2 via formate dehydrogenase (Fdh) or Hdr-associated hydrogenase (Vhu) respectively. However, how these enzymes bind to HdrA to deliver electrons is unknown. Here we demonstrate that the δ subunit of hydrogenase (VhuD) is central to the interaction of both enzymes with HdrA. When *M. maripaludis* is grown under conditions where both Fdh and Vhu are expressed, these enzymes compete for binding to VhuD, which in turn binds to HdrA. Under these conditions, both enzymes are fully functional and are bound to VhuD in sub-stoichiometric quantities. Surprisingly, in the absence of Vhu, growth on hydrogen still occurs; we show that this involves F_{420}-reducing hydrogenase. The data presented here represent an initial characterization of specific protein interactions centered on Hdr in a hydrogenotrophic methanogen that utilizes multiple electron donors for growth.

Introduction

Energy conservation in hydrogenotrophic methanogenic archaea is interesting in that hydrogenotrophs lack cytochromes yet still rely on the generation of chemiosmotic membrane potential for ATP synthesis. One critical step that makes this possible is the coupling of the exergonic reduction of a terminal heterodisulfide (CoM-S-S-CoB) to the endergonic reduction of CO_2 to formyl-methanofuran (formyl-MFR) rendering methanogenesis a cycle (25, 70, 79, 136). Central to these coupled reactions is the recent discovery of flavin-based electron bifurcation in the α subunit of heterodisulfide reductase (Hdr): an energy conservation mechanism that generates low potential electrons in an ATP-independent manner (70, 136). Although it has become apparent that electron flow is bifurcated at the flavin of HdrA, how electrons arrive at the flavin is still unclear.

Hdr from *Methanothermobacter* spp. co-purifies with a three-subunit hydrogenase known as the methyl-viologen reducing hydrogenase (Mvh) (125, 130). In the model species *Methanococcus maripaludis* two methyl-viologen reducing hydrogenases are present, one containing selenocysteine (Vhu) and one cysteine (Vhc), encoded in two separate operons (58). It has long been assumed that the δ subunit (VhuD or VhcD in *M. maripaludis*) is the site of binding to Hdr. This assumption is based on the presence of HdrA-MvhD fusion proteins encoded in the genomes of *Methanosarcina* spp. and *Archaeoglobus fulgidus* (130). Additionally, methanogens that lack genes for the active site of Mvh, such as *Methanospirillum hungatei*, still encode MvhD suggesting that although Mvh is not used for heterodisulfide reduction in these organisms, MvhD is still essential for electron flow to Hdr (135). MvhD contains a 2Fe-2S cluster, further implicating it as an electron transfer protein (136).

We have shown that, in the hydrogenotroph *M. maripaludis*, H_2 oxidation by Vhu or Vhc is not essential for heterodisulfide reduction with cultures grown on formate and that both formate dehydrogenase (Fdh) and Vhu bind Hdr (25). A Δ*vhuAU* Δ*vhcA* mutant retains wild-type growth rates with formate as an electron donor, but has a growth defect specifically on H_2. However, in this mutant background, the *vhuD* and *vhcD* genes were left intact; therefore, it is still unclear whether this subunit is essential for electron flow to Hdr when cultures are grown with formate. Additionally, how Vhu and Fdh bind to Hdr remains unclear. We investigated the interactions of these proteins by analyzing the subunit composition of the Hdr protein complex in cells grown under conditions when formate dehydrogenase (Fdh) is either expressed or repressed. Our results suggest the active site subunits of Vhu (VhuAGU) and Fdh (FdhAB) compete for binding

to VhuD under conditions where Fdh is present. Additionally, we show evidence that in the Δ*vhuAU* Δ*vhcA* strain, slow growth on H_2 involves a cryptic electron flow pathway involving F_{420}-reducing hydrogenase.

Methods

Growth conditions. Strains used in this study are listed in Table 1. For batch culture, strains were grown with McCas medium with 276 kPa H_2:CO_2 (80:20) in the headspace or with formate medium with 207 kPa N_2:CO_2 (80:20) (59, 98). Growth curves were done in triplicate and optical density was monitored at 660 nm. For continuous culture under H_2-limitation/phosphate excess or H_2-excess/phosphate limitation, a previously described chemostat system was employed (25, 52, 74).

Protein purification. Cell material from strains containing oligo-His tagged proteins grown under defined nutrient limitation was used for protein purification. All procedures were done in a Coy™ anaerobic chamber. Solutions were de-gassed and then allowed to equilibrate with the chamber atmosphere (5% H_2:95%N_2). Frozen cell paste was thawed on ice and sonicated (Misonix™ Sonicator model XL-2000) at a setting of 11 in short 3-second bursts. Unbroken cell debris was pelleted and the cell-free extract was subjected to nickel affinity purification. A modified version of our previous protocol was used for purification (25): Binding buffer contained 25 mM HEPES (pH 7.5), 12.5 mM $MgCl_2$, 100 mM NaCl, 10 mM imidazole and 0.5 mM dithionite. Wash and elution buffers were the same as the binding buffer except that they contained 30 mM and 100 mM imidazole respectively. The eluted protein was concentrated with a Vivaspin™ 500 centrifugal concentrator (polyethersulfone membrane , 5 kDa molecular weight cut off) before further purification by FPLC (AKTA purifier UPC10 system with a UV and Conductivity cell from General Electric life sciences) using a Hiprep 16-60 Sephacryl S300HR sizing column run at 0.5 mLs min^{-1} flow rate. The FPLC running buffer was the same as the binding buffer but without the imidazole. The retention time of protein molecular weight standards for the Hiprep column provided in the literature was used as reference (32). Specific 1 mL fractions were identified, pooled, and concentrated.

Subunit composition analysis of purified proteins. Pooled and concentrated fractions from FPLC purification were subjected to SDS-PAGE using 4-20% Precise™ Protein Gels and stained with Gelcode™ Blue Safe Protein Stain (Thermo Scientific). Gels were subjected to

densitometry analysis using the ImageJ suite (113, 122) and band intensity was normalized to predicted protein mass. Stoichiometry of subunits was determined by calculating the ratio of normalized band intensity between two proteins.

In vitro methane production assays. Methane production was assayed using cell material from strain MM901 grown with either formate or H_2 (25). For each assay, 10-20 mLs of culture was collected and anaerobically lysed by sonication (Misonix™ Sonicator model XL-2000) on setting 2 in 10-second bursts. Insoluble cell material was removed by centrifugation and the supernatant was mixed in methane assay buffer composed of 100 mM trizma base (pH7.1), 15 mM $MgCl_2.6H_2O$, 5 mM ATP, 2 mM 2-mercaptoethanol, and 500 µM FAD. Formic acid (50 mM) was included, or H_2 was added to the headspace. Headspace was pressurized to 138 kPa with N_2:CO_2 (80:20) for assays performed with formic acid or H_2:CO_2 (80:20) for assays with H_2 (79). Methane production was initiated by addition of 1 mM (final concentration) CoM-S-S-CoB (13). Methane production was monitored using a Buck Scientific model 910 GC equipped with a flame ionization detector (79). Protein concentration was determined using Bradford assays (18).

CoM-S-S-CoB was synthesized as described previously using thiol exchange chemistry with CoB-S-S-CoB homodisulfide and HS-CoM (13) and purified by HPLC. CoB-S-S-CoB homodisulfide was a gift from William B. Whitman. HPLC was performed using a Magic 2002 HPLC with a Magic C18AQ 5µ 100Å (2.0 x 150mm) column equipped with a C1 (silica) RP MICRO guard column (MICHROM Bioresources Inc.) using a 0.3 mL min^{-1} flow rate and buffer containing 25 mM ammonium bicarbonate with a MeOH gradient (0-80%).

Results

Size exclusion chromatography of purified His tagged heterodisulfide reductase. In previous work, we found that in cells of *M. maripaludis* grown under H_2-excess, Hdr, Vhu, and formylmethanofuran dehydrogenase (Fwd) formed a super-complex that presumably catalyzes the electron bifurcation-based reductions of CO_2 and CoM-S-S-CoB (25). (In the presence of selenium, *vhc* is repressed, so only Vhu is observed (25, 103)). In the present work, we used a 6x-His tag on the β subunit of Hdr to purify the protein by nickel affinity chromatography as before, but additionally subjected the protein to gel filtration chromatography by FPLC. A peak eluted of approximately 500 kDa (Fig. 5.1A), consistent with a dimer of HdrABC-VhuAUGD

(predicted mass of ~450 kDa). This size is consistent with the Hdr-Mvh complex from *Methanothermobacter marburgensis*, which was reported to have an apparent molecular weight of 500 kDa with a 1:1 stoichiometry of hydrogenase to Hdr (125). This subunit composition was confirmed by SDS-PAGE (Fig. 5.1B). In contrast to our previous results (25), Fwd was not present. Fwd may have dissociated during gel filtration chromatography, or have been destabilized due to the use of a much lower concentration of sodium dithionite, which at high concentration interfered with UV detection in the FPLC.

Fdh and hydrogenase compete for binding to the protein complex. When *M. maripaludis* is grown under H_2-limitation, *fdh* is derepressed and Fdh is incorporated into the Hdr-Vhu protein complex (25). We sought to determine if Fdh binds to a separate site on the complex or if Fdh displaces Vhu as the electron-donating enzyme. Nickel affinity purification followed by size exclusion chromatography of a HdrB-His expressing strain grown with H_2-limitation revealed that the apparent molecular mass of the Vhu-Fdh-Hdr complex was similar to the mass of a Vhu-Hdr complex (Fig. 5.1A) despite the additional presence of Fdh (Fig. 5.1B). This suggested that Fdh displaced Vhu, as additional binding of two molecules of Fdh would increase the apparent mass of the protein complex by 234 kDa.

Densitometry analysis confirmed that Fdh binding to the protein complex displaced the hydrogenase (Figure 5.1C and Table 5.2). The relative subunit stoichiometry of VhuA to HdrC decreased from 1:1 in cells grown with H_2-excess to 0.37:1 in cells grown with H_2-limitation, while the relative stoichiometry of FdhB to HdrC increased from 0.10:1 to 0.77:1 (Table 5.2). In contrast, the VhuD subunit remained bound to the protein complex at an approximate 1:1 ratio under both growth conditions. Furthermore, the ratio of VhuA to to VhuD decreased from 1.01:1 with H_2-excess to 0.39:1 with H_2-limitation, while the ratio of FdhB to VhuD increased from 0.10:1 to 0.82:1. As VhuD is known to interact with HdrA, we hypothesized that Fdh bound the same site of VhuD as VhuAGU leading to displacement of the hydrogenase. This would make *vhuD* an essential gene. Consistent with this, we have been unable to generate a *vhuD* deletion in *M. maripaludis* (data not shown).

VhuD co-purifies with Fdh. To assess the binding associations of Fdh, a His-tagged version of this protein was also purified. Cell extracts of a FdhA-His expressing strain were subjected to nickel affinity purification followed by FPLC. A large peak eluted consistent with the size of the Hdr protein complex (Fig. 5.2A, P1), and was found to comprise proteins from Hdr and Fdh (Fig.

5.2B). VhuD was also present, consistent with a role in binding Fdh. Bands for other subunits of the hydrogenase were not visible despite their purification with Fdh-His in previous studies (25). This is likely due to a more stringent wash (30 mM imidazole) than what was used previously (10 mM) and the fact that a Hdr dimer can bind either one Fdh and one VhuAGU or two Fdh molecules. Two Fdh molecules with two His-tags would remain bound more tightly to the nickel resin resulting in an enrichment in 2:2:2 Fdh:VhuD:Hdr complexes over 1:1:2:2 Fdh:VhuAGU:VhuD:Hdr complexes.

Interestingly, a small peak was also visible after FPLC purification (P2 in Fig. 5.2A) composed of FdhA, FdhB, and VhuD (Fig. 5.2B). The calculated mass of this peak was ~125 kDa consistent with a 1:1:1 stoichiometry of the subunits. P2 comprised a very small fraction of the total protein purified; therefore, it was likely a dissociation product generated during the purification. However, the fact that VhuD remained bound to Fdh upon dissociation verifies that Fdh binds VhuD while competing with VhuAGU for binding to the complex.

M. maripaludis maintains functional hydrogenase and Fdh when both are present in the Hdr protein complex. The presence of both hydrogenase and Fdh bound to Hdr when cells are grown on formate or under H_2-limitation (25) suggests that *M. maripaludis* is poised to rapidly switch between these two electron donors. Batch culture *M. maripaludis* experiences H_2-limitation when culture optical density (OD) reaches values greater than ~0.4 as H_2 utilization becomes limited by the rate of H_2 transfer into the aqueous phase (88). We therefore tested the ability of cell extracts from batch grown *M. maripaludis* to switch electron donors using a previously established in vitro methane production assay (13, 48, 79). Cultures were grown to maximum OD on H_2 (OD ~1.0) or formate (OD ~0.6) and whole cell protein was assayed for the ability to generate methane from the alternative electron donor. Thus H_2-grown cell extract was assayed with formate and formate-grown extract was assayed with H_2. Cell extracts generated methane with both electron donors regardless of which was used for growth (Fig. 5.3A and B) suggesting that both hydrogenase and Fdh bound to Hdr are functional regardless of the actual electron donor being used for growth.

F_{420}-reducing hydrogenase plays a role in heterodisulfide reduction in the ∆vhuAU ∆vhcA mutant background. Surprisingly, a ∆*vhuAU* ∆*vhcA* mutant of *M. maripaludis* grows on H_2, albeit slowly (25) (Fig. 5.4). In addition to utilizing H_2 as an electron donor for heterodisulfide reduction, *Methanococcus voltae* was reported to possess an inefficient, membrane-associated

$F_{420}H_2$:heterodisulfide oxidoreductase activity that was dependent on F_{420}-reducing hydrogenase (108). We hypothesized that the growth of the *M. maripaludis* Δ*vhuAU* Δ*vhcA* mutant on H_2 may depend on F_{420}-reducing hydrogenase. To test this hypothesis, we assayed the ability of a Δ*vhuAU* Δ*vhcA* Δ*fruA* Δ*frcA* mutant to grow with H_2 as an electron donor. This mutant showed little or no growth on H_2, but had similar kinetics to Δ*vhuAU* Δ*vhcA* on formate (Fig. 5.4).

Discussion

A picture of how the proteins in the Hdr complex interact is starting to emerge (Fig. 5.5). Results presented here show that VhuD is the primary electron conduit to Hdr from either Fdh or hydrogenase. Thus, VhuD sits at the intersection of the substrate oxidizing enzymes and the active site of electron bifurcation, regardless of whether formate or hydrogen is the electron donor. Additional interactions can be inferred. Contact between VhuD and Hdr probably occurs at HdrA, since the homologous proteins are fused in some organisms (130). However, which subunit of Fdh or VhuAGU interact directly with VhuD is still unknown. From HdrA, electron flow is bifurcated to the active sites of CO_2 reduction and heterodisulfide reduction. Fwd, the five-subunit enzyme that reduces CO_2 to formyl-MFR, has been purified alone or as part of the Hdr-Vhu-Fdh super complex (25, 147), and likely binds near the electron bifurcating center of HdrA. Although HdrA, B, and C interact (54), it is unclear between HdrB and HdrC which binds to HdrA. HdrC likely binds to HdrB, the site of heterodisulfide reduction, since these are fusion proteins in *Methanosarcina* spp. (49).

Our results show either Fdh or hydrogenase can bind to VhuD. Cultures grown with H_2 excess do not maintain high levels of Fdh (26, 57, 159), but when H_2 is growth limiting, Fdh is abundant and competes with the Hdr-associated hydrogenase for binding to VhuD. When H_2 is growth limiting there is evidently an advantage for *M. maripaludis* to be poised to alternate between H_2 and formate as substrates for methanogenesis, and indeed, both substrates were functional in cell extracts. (Fig. 5.3A and B). Mvh from *M. marburgensis* was found to exist in both Hdr-bound and free forms, suggesting that hydrogenase displaced from the Hdr complex by Fdh is maintained by the cell rather than degraded (130).

We also found that the F_{420}-reducing hydrogenase (Fru/Frc) plays a role in heterodisulfide reduction when Vhu and Vhc are not functional, since a Δ*vhuAU* Δ*vhcA* mutant grows slowly on H_2 but a Δ*vhuAU* Δ*vhcA* Δ*fruA* Δ*frcA* did not grow (Fig. 5.4). This suggests three possibilities.

First, $F_{420}H_2$ generated by Fru/Frc could be an electron donor to Hdr via an $F_{420}H_2$ dehydrogenase. This is the case in the methylotrophic methanogens from the order *Methanosarcinales*, where electron flow from F_{420} to heterodisulfide is coupled via an electron transport chain to a chemiosmotic membrane gradient (136). However, neither a homologous F_{420} dehydrogenase, nor components of the electron transport chain is present in hydrogenotrophic methanogens. Second, $F_{420}H_2$ generated by Fru/Frc could donate electrons to Hdr via Fdh, which uses F_{420} as an electron acceptor. However, the existence of the Hmd-Mtd cycle, an alternative pathway for F_{420} reduction with H_2, argues against the first two possibilities, both of which rely on the known role of Fru/Frc to generate free $F_{420}H_2$. In the Hmd-Mtd cycle, a combination of the H_2-dependent methylene-H_4MPT dehydrogenase (Hmd) and the F_{420}-dependent methylene-H_4MPT dehydrogenase (Mtd) acting in reverse result in F_{420} reduction with H_2 (3, 59). The Hmd-Mtd cycle is adequate for F_{420} reduction since a Δ*fruA* Δ*frcA* mutant has no growth defect on H_2 (3, 59). Therefore, $F_{420}H_2$ should be abundant even in a Δ*fruA* Δ*frcA* mutant. These data suggest a third possibility, that direct electron flow occurs from Fru/Frc to Hdr without free $F_{420}H_2$ as an intermediate, as suggested in *M. voltae* (19).

Tables and figures

Table 5.1. Strains used in this study.

Strain	Description	Reference
MM901	*M. maripaludis* S2 with an in frame deletion of uracil phosphoribosyltransferase	(25, 154)
MM1264	MM901 with a 6x-His tag on HdrB2	(25)
MM1265	MM901 Δ*fdhA2B2* with a 6x-His tag on FdhA1	(25)
MM1272	MM901 Δ*vhuAU* Δ*vhcA*	(25)
MM1313	MM901 Δ*vhuAU* Δ*vhcA* Δ*fruA* Δ*frcA*	(79)

Table 5.2. Ratios of proteins identified in purified complexes.

Condition	VhuA : HdrC[a]	FdhB : HdrC	VhuD : HdrC	HdrA : HdrC	VhuA : VhuD	FdhB : VhuD
High H_2	1.0 : 1	0.10 : 1	0.99 : 1	0.96 : 1	1.0 : 1	0.10 : 1
Low H_2	0.37 : 1	0.77 : 1	0.94 : 1	ND[b]	0.39 : 1	0.82 : 1

[a]Data are based on densitometry plots from Fig. 1C.
[b]Not determined; HdrA and FdhA bands overlap, so it was not possible to quantify HdrA under H_2 limitation.

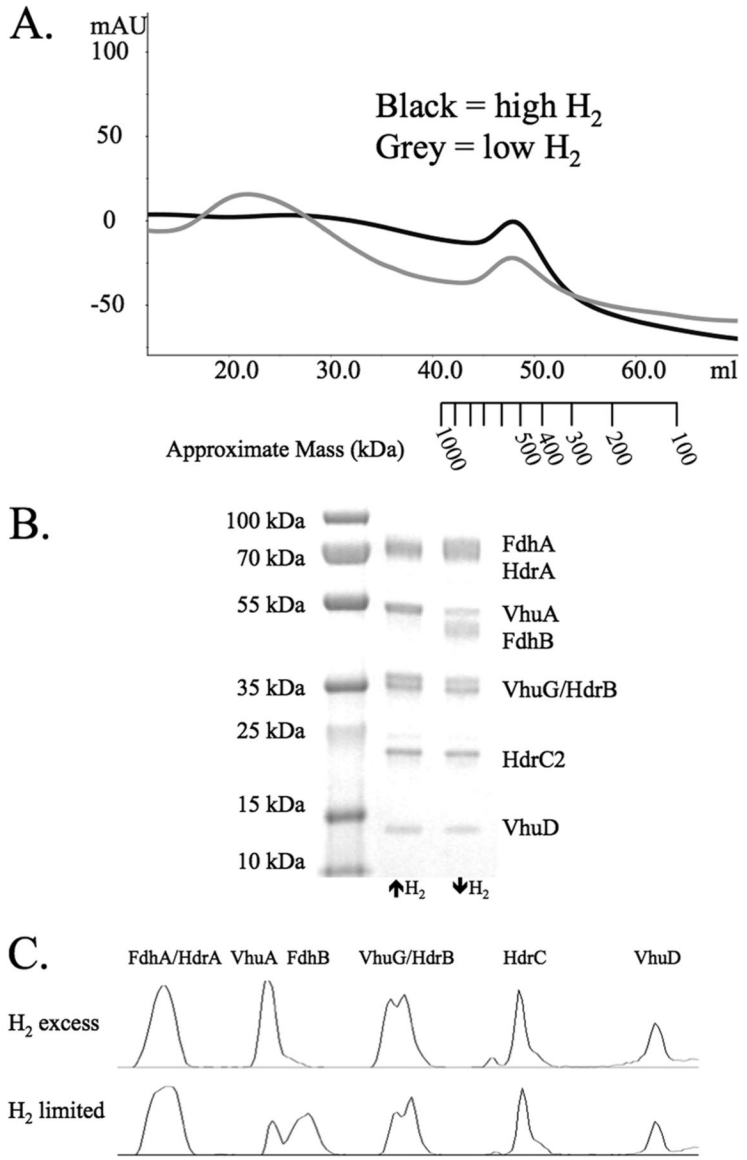

Figure 5.1. Purification of His-tagged HdrB2. A) Gel filtration of the Hdr protein complex from *M. maripaludis* grown under H_2-excess (black) or H_2-limitation (grey). B) SDS-PAGE gel of stained protein collected from the peaks shown in A. C) Densitometry plots for the lanes from the SDS-PAGE gel.

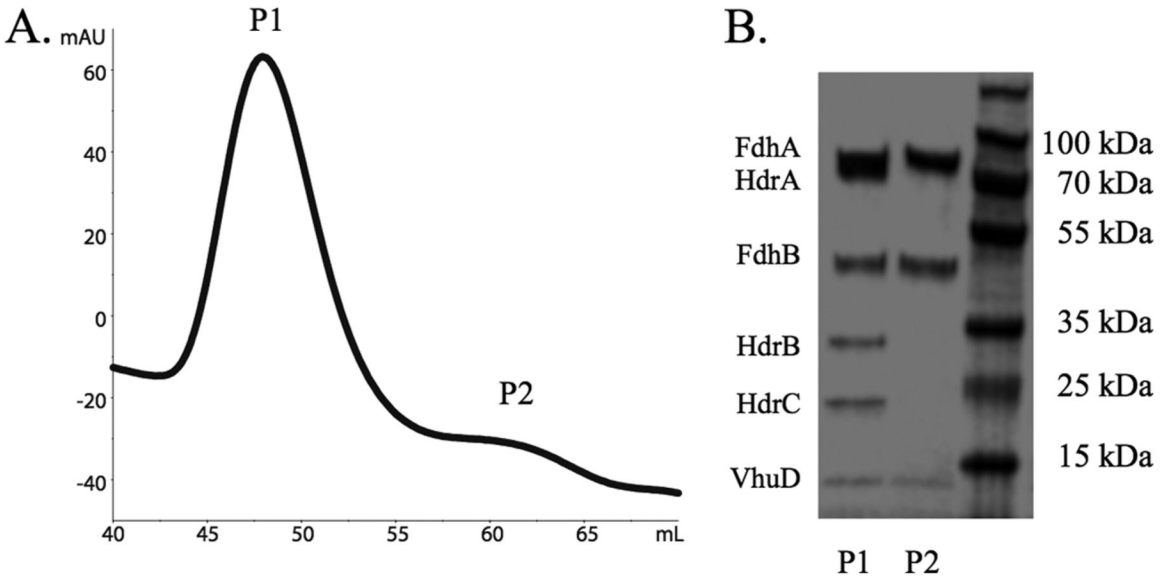

Figure 5.2. Purification of His-tagged A1. A) Gel filtration of the purified protein complex from *M. maripaludis* grown under H_2-limitation. Peaks labeled P1 and P2 were collected and subjected to SDS-PAGE. B) SDS-PAGE gel of protein from P1 and P2.

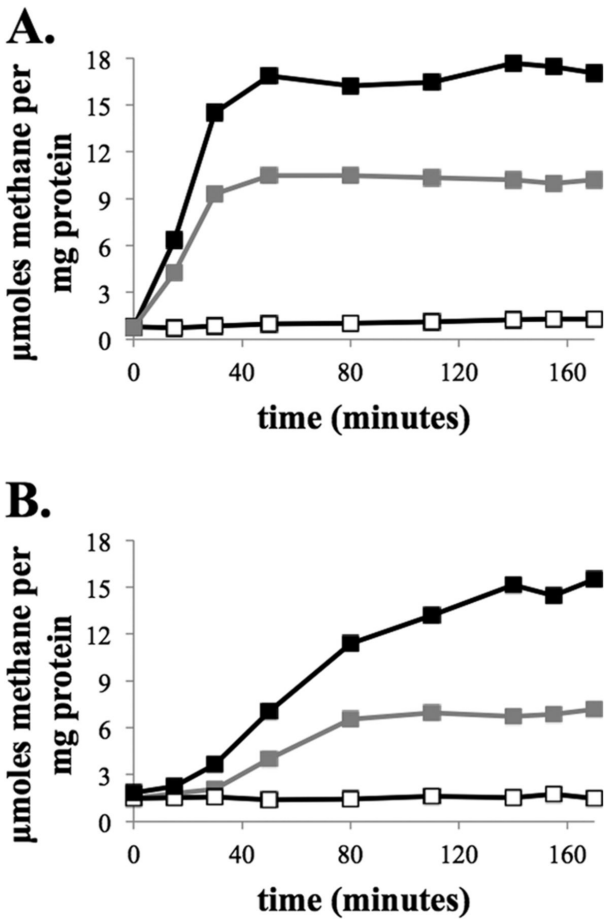

Figure 5.3. CH_4 production from cell extracts of *M. maripaludis* strain MM901 grown with either H_2 (A) or formate (B). Methane production was stimulated by addition of CoM-S-S-CoB. Controls where CoM-S-S-CoB was excluded are shown (white symbols). Black symbols, CH_4 production by cell extracts using H_2 as the electron donor. Grey symbols, CH_4 production by cell extracts using formate as the electron donor.

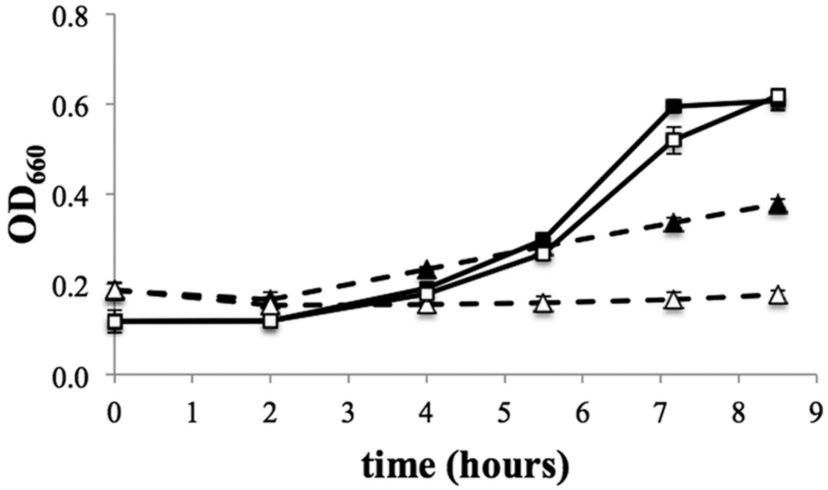

Figure 5.4. Growth of a Δ*vhuAU* Δ*vhcA* strain (black symbols) and a Δ*vhuAU* Δ*vhcA* Δ*fruA* Δ*frcA* strain (white symbols). Solid lines, growth with formate. Dashed lines, growth with H_2. Triplicate cultures grown with a 10% inoculum are shown. Error bars represent one standard deviation around the mean.

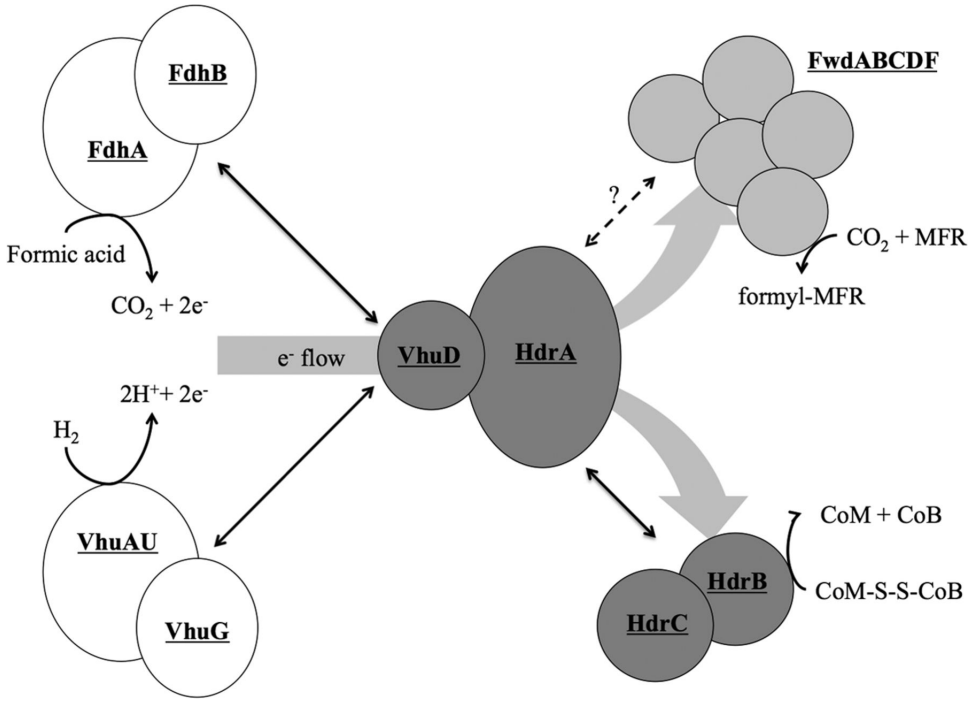

Figure 5.5. Protein interactions in the Hdr super-complex. Formate dehydrogenase (FdhAB) and hydrogenase (VhuAGU) complete for binding to VhuD. VhuA and VhuU are drawn together, since they form the catalytic site of H_2 oxidation (108, 109). Electrons flow to HdrA where their path is bifurcated to both FwdABCDF and HdrBC. Black double arrows indicate known interactions between sub-complexes. The dashed line between HdrA and Fwd signifies a hypothesized site of interaction between these sub-complexes. Reactions catalyzed by the individual enzymes are shown.

CHAPTER 6

Regulation and physiology of methanogenesis on formate

Originally published as an article in *Journal of Bacteriology*:

Costa, Kyle C., Sung Ho Yoon, Min Pan, June A. Burn, Nitin Baliga, and John A. Leigh (2013) Effects of H_2 and formate on growth yield and regulation of methanogenesis in *Methanococcus maripaludis*. *J Bacteriol.* 195: 1456-1462.

Summary

Hydrogenotrophic methanogenic archaea are defined by a H_2 requirement for growth. Despite this requirement, many hydrogenotrophs are also capable of growth with formate as an electron donor for methanogenesis. While certain responses of these organisms to hydrogen availability have been characterized, responses to formate starvation have not been reported. Here we report that during continuous culture of *Methanococcus maripaludis* under defined nutrient conditions, growth yields relative to methane production decreased markedly with either H_2 excess or formate excess. Analysis of the growth yields of several mutants suggests that this phenomenon occurs independently of the storage of intracellular carbon or a transcriptional response to methanogenesis. Using microarray analysis, we show that the expression of genes encoding F_{420}-dependent steps of methanogenesis, including one of two formate dehydrogenases, increased with H_2 starvation, but with formate occurred at high levels regardless of limitation or excess. One gene, encoding H_2-dependent methylene-tetrahydromethanopterin dehydrogenase, decreased in expression with either H_2 limitation or formate limitation. Expression of genes for the second formate dehydrogenase, molybdenum-dependent formylmethanofuran dehydrogenase, and molybdenum transport increased specifically with formate limitation. Of the two formate dehydrogenases, only the first could support growth on formate in batch culture where formate was in excess.

Introduction

Methanogenic archaea (methanogens) play a key role in the anaerobic breakdown of organic matter. Five of six known orders of methanogens, termed "hydrogenotrophic", derive their energy through the use of H_2 to reduce CO_2 to methane. Hydrogenotrophic methanogens lack a cytochrome-containing electron transport chain and are proposed to conserve energy by the mechanism of electron bifurcation (134, 136). H_2 availability has profound physiological and regulatory effects in hydrogenotrophic methanogens. For example, in *Methanothermobacter thermautotrophicus*, when H_2 is present in excess, growth in relation to methane production (Y_{CH4}, grams dry weight of cells per mole methane) decreases (28, 99), suggesting that energy spilling (otherwise known as growth uncoupling or overflow metabolism (118)) occurs. In *M. thermautotrophicus*, *Methanococcus maripaludis*, and other methanogens H_2 availability also alters the expression of key genes of methanogenesis (42, 57, 99, 100, 138, 159). The mechanisms for the effects on growth yield and gene expression are unknown.

In addition to H_2, formate may also be a primary electron donor for methanogenesis in the environment (33, 129), and several hydrogenotrophic species can use formate without the addition of H_2. For the catabolic process of methanogenesis, formate and H_2 are interchangeable electron donors; all four reductive steps can proceed with electrons derived directly from either electron source (25, 59, 79, 88). H_2, however, is essential for the anabolic process of CO_2 fixation (90, 110) and for an anaplerotic input to methanogenesis (79). During growth on formate, a formate:H_2 lyase activity generates the necessary H_2 (59, 79, 88).

Since formate acts independently of H_2 as an electron donor for methanogenesis, we asked whether its availability similarly affects growth yield and gene expression. We identify four different response patterns with regard to four conditions, H_2 limitation and excess and formate limitation and excess. Interestingly, a discrete set of genes responds specifically to formate limitation.

Methods

Strains and batch culture conditions. Strains, plasmids, and primers are listed in Table 6.1. Deletion mutants were either taken from previous studies, or generated in this study as described (25, 98). Briefly, where possible, deletion constructs were digested out of the plasmid pCRprtneo and ligated directly to pCRuptneo (59); otherwise, PCR products containing the

deletion of interest were generated and ligated into pCRuptneo. Strain MM901 was then transformed with the deletion constructs and subjected to a selection/counter selection system dependent on neomycin (1-5 mg mL^{-1}) and 6-azauracil (250 µg mL^{-1}) to generate mutants of interest (25). Strains were grown on McCas medium as before (98). When formate instead of H_2 was supplied as the electron donor, McCas was amended with 200 mM sodium formate (with an equivalent reduction in NaCl to maintain sodium osmolarity) and 200 mM MOPS buffer (pH 7); the headspace was 140 kPa N_2/CO_2 (80:20) (59). For growth curves, a 4% inoculum was used and optical density (OD) was monitored at 660 nm. For all experiments, cultures were grown at 37°C.

Growth and microarray analysis of M. maripaludis grown in a chemostat under defined nutrient limitation. *M. maripaludis* strain MM901 was grown in a chemostat on H_2 as described (52, 57, 74). For the *ehb* mutant, 0.1% (w/v) casamino acids was added to chemostat medium and 100 µg mL^{-1} ampicillin was included to prevent bacterial contamination. For unknown reasons, when casamino acids (Fisher BioReagents catalog number BP1424-500) were used, limitation occurred at a lower phosphate level (0.02 mM vs. 0.12 mM in minimal medium). For growth on formate, the chemostat setup is diagramed in Fig. 6.1. Conditions were modified as follows unless otherwise indicated: Medium contained 380 mM sodium formate in place of NaCl. Although Cl^- is important for cellular function, replacing NaCl with sodium formate is standard practice and has no known deleterious effects on growth (119) suggesting that other Cl^- containing salts in our medium (e.g. $MgCl_2$) are sufficient. MOPS buffer was not included during continuous culture on formate. Formate utilization results in a pH increase by the following equation:

$$4NaCOOH + 2H_2O \rightarrow CH_4 + 3CO_2 + 4NaOH$$

Therefore, a pH probe was used to monitor and maintain pH at 6.95 with the automated addition of 10% (v/v) H_2SO_4. The agitation rate was 250 revolutions per minute. The gas mixture initially supplied to the chemostat was $H_2/Ar/CO_2$/1% H_2S (21/125/40/14 mLs min^{-1}) (57). After the OD increased above 0.6 (24 h), the medium flow was turned on at 0.083 L hr^{-1}. Medium was either non-limiting (described above), formate limiting (modified to contain 200 mM sodium formate and 180 mM NaCl), nitrogen limiting (2 mM NH_4Cl), or phosphate limiting (0.08 mM K_2HPO_4). Also at this point, gas flow through the vessel was shut off, a 7 kPa check valve was installed on the exhaust line to maintain positive pressure within the vessel while also allowing for exhaust of gaseous metabolic byproducts, and a 1% $Na_2S.9H_2O$ feed was started into the vessel at 0.83

mL hr^{-1}. 48 hours later, samples were taken for physiological measurements or microarray analysis. If conditions were nutrient limited, non-limiting medium was then re-introduced. A subsequent increase in OD confirmed that nutrient limitation had been imposed. If the chemostat was allowed to run longer, iron sulfides precipitated several days after the start of Na_2S addition and attached to surfaces within the culture vessel (data not shown).

Samples were collected for microarray analysis as follows: 1.5 mLs of chemostat culture (OD_{660} ~0.65) was centrifuged at 13,000 x g for 30 seconds and supernatant was discarded. The pellet was immediately placed in a dry ice/ethanol bath and stored at -80°C until RNA extraction and microarrays could be performed. Microarrays were run as described previously (162). Microarray data have been deposited, GEO accession number GSE42111.

Growth yield calculations. To calculate growth yield of *M. maripaludis* during H_2 limitation or excess, culture OD_{660}, gas flow rate, and percent methane in the gas outflow were determined. Methane concentrations were measured on a Buck Scientific model 910 GC equipped with a flame ionization detector. Carrier gases were air (110 kPa), H_2 (180 kPa), and He (170 kPa). Growth rate based on the chemostat dilution was one doubling per 499 minutes. Finally, an OD_{660} of 1.0 was assumed to equal 0.34 g dry cell mass per liter (88). The following equation was used to determine dry cell mass produced per mole CH_4 (Y_{CH4}):

$$(OD_{660}/CH_4(mL/min))*(0.34g/OD_{660})*(1/499min)*(22400mL/mole)$$

To determine grams dry mass yield per mole formate consumed, the offset of pH in the chemostat vessel by 10% (v/v) H_2SO_4 addition was monitored (Y_{H2SO4}). H_2SO_4 consumption was monitored over ~18 hours and Y_{H2SO4} was calculated as follows:

$$(OD_{660}/(mL\ acid/hour))*(0.34g/OD_{660})*(1/(499/60))*(543.5mL\ acid/mole)$$

Y_{H2SO4} was converted to Y_{CH4} assuming that each mole of H^+ from H_2SO_4 offsets the pH change from one mole NaOH produced by sodium formate utilization. Therefore, two moles H_2SO_4 corresponds to four moles formic acid and one mole CH_4.

Results

A chemostat system for growth of M. maripaludis with formate. Continuous culture of *M. maripaludis* on formate required modification of our protocol for growth on H_2. Even though the

medium contained formate, it was necessary to first establish a culture in the chemostat vessel by sparging with gas containing H_2. When H_2 was subsequently excluded, culture OD steadily decreased (Fig. 6.2). *M. maripaludis* requires H_2 for methanogenesis and anabolism; normally, formate:H_2 lyase activity generates this H_2 (59, 79, 88, 90, 110). Maintaining H_2-free gas flow likely flushed all H_2 from the vessel, inhibiting growth. We also tried changing the agitation rate of the vessel (Fig. 6.2) as this affects the rate of H_2 removal from the system; however, this had no noticeable effect. We therefore completely stopped gas flow in order to maintain physiologically relevant levels of autochthonous H_2 (Fig. 6.2). A 7 kPa check valve was installed to maintain positive pressure within the vessel while allowing escape of gaseous metabolic products. In addition, *M. maripaludis* requires sulfide as a reducing agent and a sulfur source for growth (86); therefore, a system for the addition of Na_2S, instead of gaseous H_2S, was devised. OD rebounded under these conditions and reliable steady state growth of *M. maripaludis* on formate was achieved with a constant OD of 0.8. (Fig 6.2). Finally, phosphate limitation was introduced and culture OD dropped to steady state value of 0.6, confirming our ability to impose nutrient limitation of *M. maripaludis* grown on formate (Fig. 6.2) similarly to nutrient limitation on H_2 (52).

Changes in growth yield occur with both H_2 and formate as electron donors. Our chemostat system allowed us to determine whether H_2 excess affects growth yield in *M. maripaludis*. We compared three continuous cultures: H_2-limited, phosphate-limited, and ammonia-limited. Growth rate and cell density were held similar under all conditions. Since H_2 was in excess when phosphate or ammonia limited growth, two comparisons yielded information on the effect of H_2 limitation. Y_{CH4} (g cell mass per mole CH_4 produced) under H_2 limitation was 2.86 ± 0.58 (SD) compared to 0.77 ± 0.20 under phosphate or ammonia limitation (Fig. 6.3A). Hence, H_2 excess results in a marked decrease in growth yield in *M. maripaludis*.

We then asked whether formate limitation would have the same effect. A decrease in Y_{CH4} due to H_2 excess has previously been demonstrated in hydrogenotrophic methanogens but whether it occurs with formate excess has not been determined. Again, we compared three continuous cultures: formate-limited, phosphate-limited, and ammonia-limited. Since continuous culture on formate required the cessation of gas flow through the system, we could not accurately measure the rate of CH_4 generation directly. Instead, we used the rate of acid addition, reflecting the rate of formic acid utilization, as an indirect measure for calculating Y_{CH4}. Y_{CH4} under formate limitation was 2.31 ± 0.29 compared to 1.50 ± 0.26 under phosphate or ammonia limitation (Fig.

6.3A). Hence, the lowest Y_{CH4} levels were observed with H_2 excess, intermediate levels occurred with formate excess, and the highest levels occurred with formate limitation or H_2 limitation (H_2 excess vs. formate excess, P = 0.002; H_2 limitation vs. formate limitation, P = 0.218; formate excess vs. formate limitation, P = 0.006).

Changes in mRNA abundance or energy storage capacity cannot account for differences in Y_{CH4}. A variety of hydrogenotrophic methanogens display altered Y_{CH4} values in response to changes in H_2 availability (42, 99, 138) suggesting a mechanism common to all organisms. In all methanogens tested, the F_{420}-dependent steps of methanogenesis are also transcriptionally regulated in response to H_2 (42, 57, 99, 100, 138, 159). Therefore, we tested the importance of these H_2-regualted genes in altering growth yields on *M. maripaludis*. Genes for both of the F_{420}-reducing hydrogenases (*fru* and *frc*) or the F_{420}-dependent methylene-H_4MPT dehydrogenase (*mtd*) were genetically eliminated. The gene for the F_{420}-dependent methylene-H_4MPT reductase (*mer*) is essential and, therefore, was overexpressed from the replicative vector pLW40 (32) rather than genetically eliminated. Each of these mutant strains displayed a marked change in Y_{CH4} upon transition from H_2 excess to H_2 limitation similar to wild type (Fig. 6.3B).

The membrane bound, energy-converting hydrogenase Eha acts to anaplerotically sustain methanogenesis by reducing ferredoxin that can be used by formylmethanofuran dehydrogenase to reduce CO_2 to formyl-methanofuran (79). This reaction consumes membrane potential and could account for differences in growth yields between H_2 excess and H_2 limitation. As *eha* is required for methanogenesis in wide-type *M. maripaludis*, we elected to place it under control of the nitrogenase promotor (P_{nif}) in an effort to control and repress its expression in the presence of ammonium. When grown in batch culture with formate as the electron donor (i.e. low H_2 concentrations), this strain has a slow growth phenotype suggesting Eha levels are indeed repressed (Fig. 6.4). The P_{nif}-*eha* construct also displayed a marked difference in growth yield in response to H_2 availability (Fig 6.3B).

Finally, alterations in growth yield in *M. maripaludis* could be due to changes in cellular composition such that energy storage occurs under H_2 excess. As Y_{CH4} decreases with H_2 excess and phosphate limitation, energy storage as polyphosphates is unlikely despite the fact that this capability has been demonstrated for methanogens from the order *Methanosarcinales* (117). *M. maripaludis* was shown to synthesize glycogen (164); therefore, a deletion mutant for glycogen synthetase (*glgA*) was generated (58). Additionally, deletion mutants for carbon

monoxide dehydrogenase (*cdh*, important for the first step of CO_2 fixation) and the energy-converting hydrogenase *ehb* (important for generating reduced electron carriers for carbon metabolism) were also generated. As expected, the *cdh* and *ehb* mutants were auxotrophic for acetate and casamino acids respectively (90, 110). Like the wild type, all three mutants, disrupting different pathways of carbon metabolism, displayed marked differences in Y_{CH4} between H_2 excess and H_2 limitation (Fig. 6.3B). These data suggest that a diversion of cellular resources towards intercellular carbon and energy storage is unlikely to account for the differences in growth yield observed in wild type. However, as the *cdh* mutant is auxotrophic for acetate, we cannot discount the possibility that some of the 10 mM acetate included in our growth medium was diverted for a change towards a higher energetic content in cellular lipids during H_2 excess.

Transcriptional response of genes encoding F_{420}-dependent steps of methanogenesis. We compared formate-grown cultures to H_2-grown cultures. In addition, we determined if the effect of formate limitation when formate is the electron donor is similar to the effect of H_2 limitation when H_2 is the electron donor. Microarray analysis was performed using samples from the same six nutrient-limited cultures described above. In each case, nutrient supplementation after sampling resulted in an increase in OD, verifying that the nutrient in question had been limiting (Table 6.2). A seventh culture was grown on formate where high levels of all nutrients were provided; in this case OD was continuously high. In addition, expression levels of key genes responded as expected, since transcript levels for genes for nitrogenase (*nifH*), phosphate transporter (*pstB*), and *mtd* increased with ammonia, phosphate, and H_2 limitation respectively (57, 60, 159).

With H_2 limitation, nearly all of the genes for the F_{420}-dependent steps of methanogenesis showed a marked increase in mRNA abundance, in agreement with previous results (57). Thus, *fdh1* encoding formate dehydrogenase, *mtd* encoding F_{420}-dependent methylene-tetrahydromethanopterin (H_4MPT) dehydrogenase, *mer* encoding methylene-H_4MPT reductase, and *fru* encoding F_{420}-reducing hydrogenase, had higher mRNA abundance with H_2 limitation than with either condition of H_2 excess (phosphate limitation or ammonia limitation) (Fig. 6.5 and GEO accession number GSE42111). In contrast, the formate-grown cultures showed a different pattern: Nearly all of the F_{420}-dependent activities that showed increased mRNA abundance under H_2 limitation also had high mRNA abundance during formate growth under all three conditions (Fig. 6.5) as well as in the seventh culture where all nutrients were present at high

levels (GEO accession number GSE42111). *fru* displayed a single exception, showing increased mRNA abundance with formate except when nitrogen was limiting. Hence, growth on formate as the electron donor, whether formate was limiting or not, had a similar effect to H_2 limitation.

Formate limitation leads to increased mRNA levels of a formate dehydrogenase and other molybdenum-associated functions. In contrast to most F_{420}-dependent steps of methanogenesis, certain genes did respond specifically to formate limitation: a second formate dehydrogenase operon *fdh2*, the genes for the molybdenum-containing formylmethanofuran dehydrogenase (*fmd*), and several molybdenum transport genes (GEO accession number GSE42111). In contrast, neither *fdh1* (which followed the pattern of other genes for F_{420}-dependent steps of methanogenesis) nor the tungsten-containing form of formylmethanofuran dehydrogenase genes (*fwd*) showed differences in mRNA abundance during formate limited growth (Fig. 6.5). (Note: *fdhB* transcript abundance (MMP0139, MMP1297) was used to assess *fdh* expression. There is a known artifact where portions of *fdhA2* (MMP0138) sometimes appear highly expressed under H_2 limitation in microarrays, most likely due to probe cross hybridization with *fdhA1* (MMP1298) transcripts which share high (~73%) nucleotide identity (162). However, both gene expression and protein abundance analysis have conclusively demonstrated that *fdhA2* is not differentially expressed between H_2 limitation and excess (57, 159). Due to this documented ambiguity in determining *fdhA2* gene expression using microarray data, *fdhA* was ignored in our analysis in favor of *fdhB*.) Since the two *fdh* operons were expressed differently, we checked the ability of each to support growth on formate. Deletion of *fdhA1* eliminated growth on formate, while deletion of *fdhA2* had no effect in batch culture (Fig. 6.6A). Deletion mutants for *fdhA1* and *fdhA2* should have no polar effects on formate transport (*fdhC*) or carbonic anhydrase (CA) (Fig. 6.6B).

A distinct pattern occurred with *hmd*, which encodes the H_2-dependent methylene-H_4MPT dehydrogenase (Fig. 6.5). Although regulation appeared complex, H_2 limitation clearly resulted in low mRNA abundance in agreement with previous results (158, 159). Formate limitation had a similar effect.

Discussion

We observed four different response patterns with regard to H_2 and formate (Table 6.3). First, mRNA transcript levels for the F_{420}-dependent steps of methanogenesis were high under three conditions, H_2 limitation, formate limitation, and formate excess, and were low only with H_2 excess. One possibility is that the presence of formate could act independently of H_2 limitation. However, since the same set of genes is affected, we favor the hypothesis that the presence of formate or H_2 limitation act through the same set of regulatory signals (see below). The second response pattern, that of growth yield, was similar: Y_{CH4} was high with H_2 limitation or formate limitation, had an intermediate level with formate excess, and was lowest with H_2 excess. The third response pattern was shown with only one gene: *hmd* had decreased expression with H_2 limitation or formate limitation compared to formate excess or H_2 excess. Fourth, one set of genes responded specifically to formate limitation: *fdh2*, *fmd*, and genes for molybdenum transport increased.

During growth on formate, a low level of H_2 is present due to its production and re-utilization (59). It is tempting to speculate that H_2 is a primary signal and that different response thresholds determine the different regulatory patterns. In this model, the highest H_2 levels occur with H_2 excess. The next step down in H_2 occurs with growth on formate supplied in excess; at this point transcript levels for F_{420}-dependent steps in methanogenesis increase and Y_{CH4} increases to an intermediate level. The next lower H_2 level occurs with H_2 limitation, where Y_{CH4} reaches a high level and *hmd* mRNA decreases in abundance. Hmd is an unusual [Fe] hydrogenase that has a low affinity for H_2 (166), so when H_2 levels are low, Hmd is of limited utility.

$F_{420}H_2$ concentrations are directly affected by H_2 concentrations in the growth medium (29); therefore, it was previously suggested that when H_2 limits growth, the genes for F_{420} dependent processes are up regulated to maintain a constant availability of $F_{420}H_2$ (57). When *M. maripaludis* is grown with formate as the electron donor, $F_{420}H_2$-dependent formate:H_2 lyase activity is essential for growth, explaining the need to maintain high levels of F_{420} dependent enzymes under these conditions (59, 79, 88). A previous study that analyzed protein abundance of *M. maripaludis* cultures grown under different H_2 gassing regimes demonstrated that changes in mRNA levels correspond to changes in protein abundance for these enzymes (159).

The remaining set of genes *fdh2*, *fmd*, and molybdenum transport genes, could respond to the

lowest extreme of H_2 or could respond directly to a limiting level of formate. Fdh and Fmd both contain a molybdopterin cofactor (93). However, it is unlikely that these genes responded to molybdenum limitation as a primary signal, since a switch to medium containing higher formate and identical molybdate resulted in an increased OD verifying that formate, not molybdenum, was the limiting nutrient (Table 6.2). We suggest that formate limitation leads to *fdh2* expression and that molybdenum transport and *fmd* expression are secondary and tertiary responses, in which increased demand for molybdenum leads to increased molybdenum transport and increased intracellular molybdenum induces *fmd* transcription. Consistent with this, increased molybdate in cultures of *M. thermautotrophicus* resulted in increased *fmd* expression (62).

The different patterns of mRNA abundance for *fdh1* and *fdh2* suggest different roles for the two formate dehydrogenases. In a previous study by Wood *et al.*, our lab reported that either Fdh was sufficient for growth on formate, whereas a later study by Lupa *et al*. reported that only Fdh1 supported growth on formate unless a Δ*fdh1* mutant was incubated for prolonged periods of ~70 hours (88, 156). This suggests enrichment of a suppressor mutation may have accounted for the initial observations of Wood *et al.*; the data in our present study agree with this interpretation. We propose that Fdh1 functions for sustained growth on formate or for a transition from growth on H_2 to growth on formate as H_2 becomes limiting, while Fdh2 functions only at low formate concentrations. However, since a mutant containing only *fdh2* (the *fdh1* deletion mutant) could not be grown in the lab on formate without a probable suppressor mutation altering its expression pattern, we could not test the growth of this mutant under formate-limited conditions.

The differences in growth yield that occurred in *M. maripaludis* were striking, reflected in Y_{CH4} values that varied as much as four-fold. The fact that mutants for several genes in carbon metabolism (*glgA*, *cdh*, and *ehb*) display this phenotype suggests that energy storage does not account for differences in Y_{CH4} between H_2 excess and limitation or formate excess and limitation. Additionally, mutation of each of the F_{420} metabolizing enzymes of methanogenesis had no impact on the ability of *M. maripaludis* to alter growth yields in response to H_2. Therefore, we tentatively propose that differences in Y_{CH4} values in hydrogenotrophic methanogens are due to energy spilling, or the dissipation of energy when the metabolic electron donor is present in excess. The energy yield of hydrogenotrophic methanogens relies on electron bifurcation at the heterodisulfide reductase complex (136), where exergonic and

endergonic electron flows are coupled via reduced ferredoxin (Fig. 6.5). One possibility is that this coupling partially breaks down. To make up for the endergonic requirement, electron flow through the energy-converting hydrogenase Eha, which normally functions anaplerotically (79), could increase with a concomitant consumption of membrane potential. However, if this is the case, we saw no evidence in the form of any regulation of Eha or any other steps of methanogenesis at the transcriptional level. Indeed, a promoter switch mutant for *eha* still displayed differences in cell yield in response to H_2 availability. As an alternative, energy spilling in methanogenic archaea may be more commonplace, perhaps involving a futile cycle that consumes ATP or membrane potential. Such cycling has been observed in *Escherichia coli* starved for potassium (21). Indeed, organisms from all three domains of life have documented examples of energy spilling metabolism (118). In methanogenic archaea, energy spilling could be beneficial to maintain low concentrations of H_2 or formate in order to prevent nutrient use by competitors or to maximize the energetics of metabolism during syntrophic growth: rapid nutrient consumption shifts the equilibrium of syntrophic metabolism allowing for robust growth of both partners despite energy spilling on the part of the methanogen.

Tables and figures

Table 6.1. Strains, plasmids, and primers used in this study.

Strain	Description	Reference
MM901	wild type	(25, 154)
Δ*fdhA1*	Δ*fdhA1*	(156)
Δ*fdhA2*	Δ*fdhA2*	(156)
Δ*fdhA1*Δ*fhdA2*	Δ*fdhA1*Δ*fhdA2*	(156)
MM1280	Δ*fru*Δ*frc*	(79)
MM1283	Δ*mtd*	this study
MM1301	Δ*cdh*	this study
MM1311	ΔMmp1447	this study
MM1312	Δ*ehbN*	this study
MM1322	P_{nif}-*eha*	this study
MM1354	pLW40-*mer*	this study
MM1355	Δ*glgA*	this study

Plasmid	Reference
pLW40	(32)
pCRuptneo	(25)
pCRuptneoΔ*mtd*	this study
pCRuptneoΔ*cdh*	(23)
pCRuptneoΔMmp1447	this study
pCRuptneo:P_{nif}-*eha*	this study
pLW40-*mer*	this study
pCRuptneoΔ*glgA*	this study

Primer	Sequence (5'-3')
F2del1447AscI	AAGGCGCGCCATGATTTTCATGGTTTTATTAATTAACTACGCAG
F1del1447AscI	AAGGCGCGCCCATTCTACCACTTTTTGAGGTAATCGG
F2del1447XbaI	AATCTAGACCATGAAATAGCCACCATTGATATTTCC
F1del1447NotI	AAGCGGCCGCTTGAAACGTATGCTTCGGATGCAGGGCCG
Eha-ds-p-F-NsiI	AAAAATGCATATGGTTTTATTAATTAACTAGCGAG
Eha-ds-p-R-BglII	TTTTAGATCTCATCAGGGGAACATACAATGTTTCCC
pNif-Eha-F-XbaI	AAAATCTAGACTCATCTGCCTTTTTCCTTTCATCTTC
pNif-Eha-R-NotI	AAAAGCGGCCGCCATCAGGGGAACATACAATGTTTCCC
mer-F-pstI	AAAACTGCAGATGAAATTTGGTATCGAATTTGTTCCAAACGAACC
mer-R-AscI	TTTTGGCGCGCCTTATTGGAATTCTTTAATGATTTTTCC
glgA-us-F-XbaI	AAAATCTAGAATTAATTCCACCACAACGTCCTCGCTCAGTACTGTG
glgA-us-R-AscI	TTAGGCGCGCCTCATAAAAATACCCCTTCTCATATACTCCC
glgA-ds-F-AscI	ATGAGGCGCGCCTAAATAACCATAACTATTTTTCAGGAGGG
glgA-ds-R-NotI	AAAAGCGGCCGCTTAAATTCCTAACTATAAAGAAATTTGCG

Table 6.2. Nutrient limited conditions for *M. maripaludis* grown in a chemostat.

Sample	Conditions				OD_{660}		log(2) expression			
	formate (mM)	H_2 (mL/min)	phosphate (mM)	ammonia (mM)	limited	non-limited	*mtd*	*fdhB2*	*nifH*	*pstB*
undefined limitation	380	0	0.8	10	0.89		**2.07**	**2.14**	-0.33	-0.1
formate limitation	200	0	0.8	10	0.64	0.87	**1.87**	**3.33**	-0.56	-0.12
formate: P limitation	380	0	0.08	10	0.69	0.86	**0.82**	0.23	-0.47	**4.71**
formate: N limitation	380	0	0.8	2	0.66	0.89	**1.78**	0.28	**5.33**	-0.14
H_2 limitation	0	21	0.8	10	0.68	>1.0	**3.08**	0.41	-0.34	0.05
H_2: P limitation	0	110	0.12	10	0.67	>1.0	-3.84	0.29	0.06	**4.06**
H_2: N limitation	0	110	0.8	2.8	0.59	>1.0	-2.89	0.02	**5.89**	-0.1

Table 6.3. Summary of regulatory and physiological responses to H_2 and formate.

	H_2 excess[b]	formate excess	H_2 limitation	formate limitation
F_{420}-dependent genes[a]	-	↑	↑	↑
hmd	-	-	↓	↓
Y_{CH4}	low	intermediate	high	high
fdh2, *fmd*, molybdenum transport genes	-	-	-	↑

[a]Genes for F_{420}-dependent steps of methanogenesis (except *fdh2*)
[b]-, baseline expression; ↑, increased expression; ↓,decreased expression

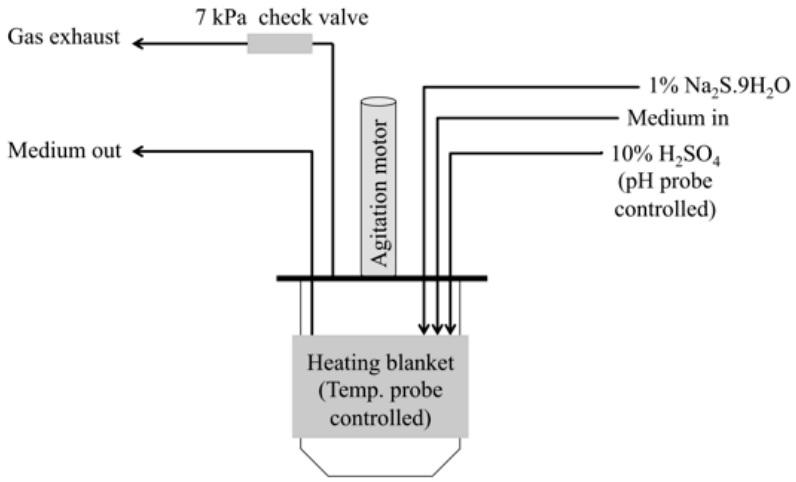

Figure 6.1. Schematic of chemostat setup with formate as the electron donor. A more detailed diagram of the chemostat setup for H_2 based growth can be found in (52).

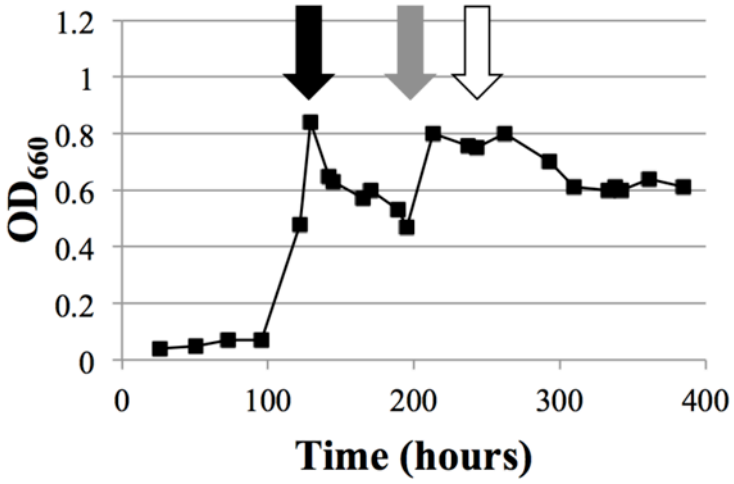

Figure 6.2. Growth behavior of *M. maripaludis* in a chemostat with formate. Plot shows OD over time in response to various perturbations. Initially the vessel was sparged with gas containing H_2 (H_2/Ar/CO_2/1% H_2S (21/125/40/14 mLs min^{-1}). At 121 hours (black arrow), medium flow was started and H_2 was turned off while flow of other gasses was continued (Ar/CO_2/1% H_2S (20/20/6 mLs min^{-1})); these gassing rates were stepped down to 5/20/2 mLs min^{-1} at hour 170. At 195 hours (grey arrow) all gas flow was terminated and 1% Na_2S addition was started. Finally, at 243 hours (white arrow) the medium flowing into the vessel was switched to a limiting level of phosphate. Medium flow was maintained at 0.083 L/h throughout except between hours 165 and 195 when it was 0.062 L/h. Agitation was 250 rpm throughout except after hour 121 when it was maintained between 50-100 rpm.

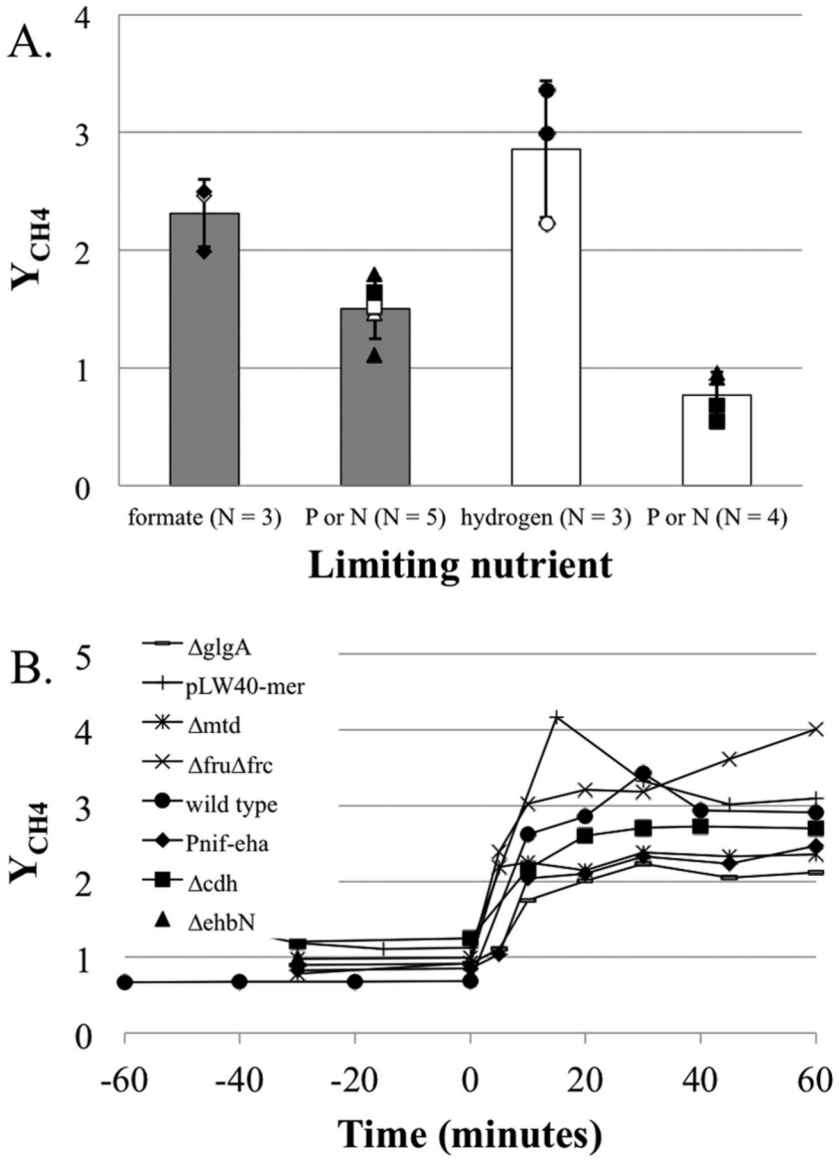

Figure 6.3. Growth yields for *M. maripaludis* under different nutrient limitations. A. Cell yield (g dry weight) per mole CH_4 (Y_{CH4}) in steady state culture grown with H_2 or formate excess or limitation. Error bars represent one SD around the mean. P and N limitation samples were pooled to represent H_2 or formate excess growth. Grey bars, formate growth; white bars, H_2 growth. Diamonds, formate limited samples; circles, H_2 limited samples; squares, N limited samples; triangles, P limited samples. Open symbols indicate samples used for microarray analysis. B. Changes to Y_{CH4} for various mutants upon transition from H_2 excess to H_2 limitation at time point 0.

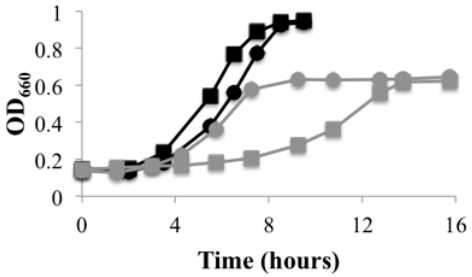

Figure 6.4. Growth of P_{nif}-*eha* on hydrogen and formate. The P_{nif} promoter switch out also resulted in deletion of the gene Mmp1447; therefore, the wild type strain for this figure is a ΔMmp1447 strain. Black, growth of H_2. Grey, growth on formate. Circles, MM901ΔMmp1447. Squares, P_{nif}-*eha*. Curves represent averages of three independent cultures.

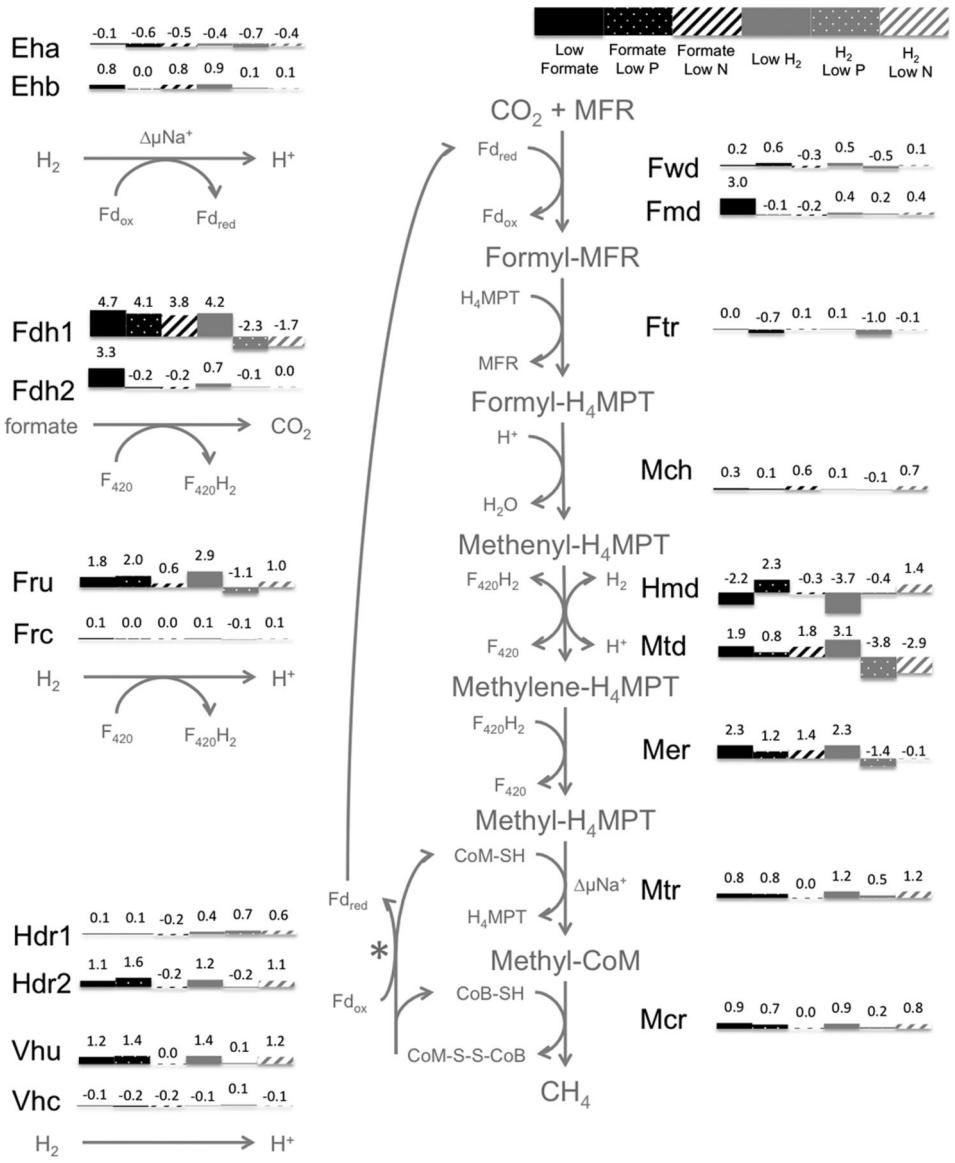

Figure 6.5. Expression of methanogenesis genes in response to nutrient limitations. Bars and numbers show $\log_2$ expression ratios relative to an arbitrary standard (20). Values are for genes encoding active site enzymes (except *fdh*, see text). $\Delta\mu Na^+$, change in Na^+ across membrane; H_4MPT, tetrahydromethanopterin; MFR, methanofuran; CoM-SH, coenzyme M; CoB-SH, coenzyme B; CoM-S-S-CoB, heterodisulfide of CoM and CoB; $F_{420}/F_{420}H_2$, coenzyme F_{420}; Fd_{ox}/Fd_{red}, ferredoxin; Eha/Ehb, energy-converting hydrogenase A or B; Fdh, formate dehydrogenase; Ftr, formyltransferase; Fmd/Fwd, formylmethanofuran dehydrogenase; Fru/Frc, F_{420}-reducing hydrogenase; Hdr, heterodisulfide reductase; Hmd, H_2-dependent methylene-H_4MPT dehydrogenase; Mch, methenyl-H_4MPT cyclohydrolase; Mcr, methyl- CoM reductase; Mer, methylene-H_4MPT reductase; Mtd, F_{420}-dependent methylene-H_4MPT dehydrogenase; Mtr, methyl-H_4MPT:CoM methyltransferase; Vhu/Vhc, Hdr-associated hydrogenase. *Either H_2 or formate acts as the electron donor for these reactions.

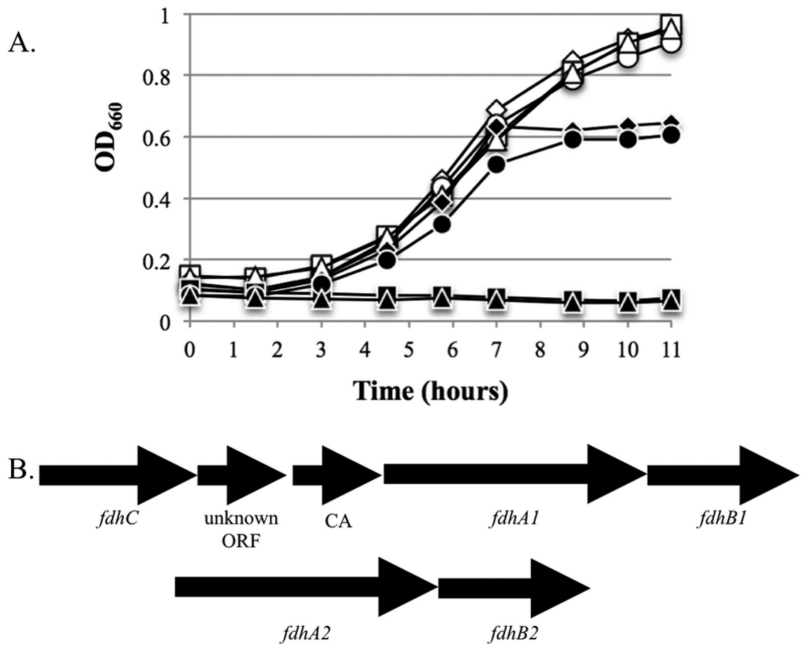

Figure 6.6. Growth of *M. maripaludis fdh* mutants on H_2 or formate. A. Open symbols, growth on H_2; filled symbols, growth on formate; diamonds, wild type; squares, Δ*fdhA1*; circles, Δ*fdhA2*; triangles, Δ*fdhA1*-Δ*fdhA2*. Data are averages of duplicate growth experiments. Similar curves were observed in replicate experiments. B. Structure of the operons for *fdh1* and *fdh2*.

CHAPTER 7

A selection for mutants lacking H_2-based repression of formate dehydrogenase

Summary

How hydrogenotrophic methanogenic archaea regulate metabolic genes in response to the presence and abundance of various electron donors has remained a mystery. The hydrogenotrophic methanogen *Methanococcus maripaludis* utilizes both H_2 and formate as electron donors for growth. Using microarrays, the transcriptional profiles for cells grown under each of these conditions have been determined, but what factors or genes determine these profiles are unknown. Here we attempt to identify some of these factors. We show that a mutant lacking both heterodisulfide reductase associated hydrogenases (Vhu and Vhc) is inhibited specifically by H_2 due to the H_2-dependent repression of formate dehydrogenase (*fdh*) expression. A Δ*vhu* Δ*vhc* mutant grows like wild type on formate, but has a growth defect in the presence of both formate and H_2. We selected for suppressor mutations that alleviated this phenotype, identified the mutations through whole-genome sequencing, and found three genes that appear to be involved in *fdh* regulation: H_2-dependent methylene-tetrahydromethanopterin dehydrogenase and two hypothetical proteins (Mmp 0267 and Mmp 1381). Analysis of gene expression profiles verifies that the H_2-based repression of *fdh* is attenuated when any of these three genes are genetically eliminated.

Acknowledgements

We thank Hillary Hayden and Kyle Hager from Samuel Miller's lab for assisting with the genome sequencing of suppressor mutations and Serdar Turkarslan, Min Pan, and Nitin Baliga for performing microarray analyses on in-frame deletion strains.

Introduction

A series of recent studies has elucidated the final molecular details behind CO_2 reduction to methane (hydrogenotrophic methanogenesis) (25, 70, 79, 134, 136). However, despite our mechanistic knowledge about the pathway, little is known regarding the details behind the regulation of methanogenesis. The model methanogen *Methanococcus maripaludis* is an ideal candidate for the identification and characterization of factors involved in the regulation of methanogenesis and substrate utilization. This organism possesses a fully sequenced and annotated genome (58), a record of peptides and genes expressed under various conditions (26, 57, 158, 159), characterized operon structures across the genome (162), a functional genetic system for the knockout of genes (25, 98, 111, 119, 139), protocols for steady state growth with defined nutrient limitation (52, 74), and a set of mutants lacking genes encoding all hydrogenases and formate dehydrogenases involved in methanogenesis (23, 25, 59, 79, 90, 156).

Previous studies in *M. maripaludis* have investigated physiology and steady state mRNA and protein abundance with cultures grown with excess or limiting concentrations of H_2 and formate (26, 57, 158, 159). These studies showed that several genes involved in hydrogenotrophic methanogenesis are regulated in response to substrate availability. However, this approach is incapable of confidently identifying regulatory factors that lead to differences between these growth states. To date, one study has explicitly focused on identifying transcription factors involved in the regulation of genes related to methanogenesis with H_2 as the electron donor (163). This was done through microarray analysis of several cultures upon transition from excess to limiting H_2 concentrations using an environment and gene regulatory influence network (EGRIN). The EGRIN model prediction relies on grouping genes into clusters to model the transcription factors associated with and influencing the regulation of each cluster. This work identified and phenotypically verified at least two transcription factors important for regulation of numerous methanogenesis genes that formed a cluster containing several hydrogenases and formate dehydrogenases. Although a series of genes required for formate dependent growth have been identified (120), there have been no studies to comprehensively and specifically identify factors involved in the repression of formate dehydrogenase.

The focus of this study is to identify genes important for the regulation of formate dehydrogenase (*fdh*). *M. maripaludis* possesses two *fdh* operons with one regulated specifically in response to H_2 (*fdh1*) (26, 57). Fdh1 is also fully integrated into methanogenesis (79). The

terminal step of methanogenesis is the reduction of a mixed disulfide of coenzyme M and coenzyme B (CoM-S-S-CoB) to the thiol-containing forms (HS-CoM and HS-CoB) by heterodisulfide reductase (Hdr). In *M. maripaludis*, the electrons for this reaction come from either H_2, via an Hdr-associated hydrogenase (Vhu or Vhc), or formate via Fdh1 (25). We identify a growth phenotype in a Δ*vhuAU* Δ*vhcA* background where the mutant is inhibited for growth on formate in the presence of H_2. This suggests *fdh1* expression is repressed under these conditions, and cells are incapable donating electrons to Hdr. The phenotype also provides a selection for mutants that lack H_2-dependent *fdh1* repression. Using this selection, we isolate 11 independent strains with mutants in seven genes. Mutations in three of these were selected for further characterization.

Methods

Strains and growth conditions. Strains, plasmids, and primers used in this study are listed in Table 7.1. Strain MM901 was the wild type strain (25). Mutants were constructed using a selection-counter selection based system for the generation of markerless genomic mutations (25, 98). Briefly, regions upstream and downstream of a gene of interest were PCR amplified and ligated to generate constructs containing in-frame deletions of the gene of interest. These constructs were ligated into the vector pCRuptNeo (25). The vector was transformed into *M. maripaludis* and merodiploids were selected with neomycin (5 mg mL^{-1}). This was followed by counter selection with 6-azauracil (250 μg mL^{-1}) to generate strains with the mutation of interest (25). Mutations were verified via PCR.

Batch culture experiments were conducted as described previously using either McCas medium with 276 kPa H_2:CO_2 (80:20) or formate medium with 207 kPa N_2:CO_2 (80:20) (59, 98). For growth curves, a 1% to 10% inoculum was used and cultures were monitored in triplicate at 660 nm to determine optical density (OD_{660}). For continuous culture, a previously developed chemostat system for the anaerobic cultivation of *M. maripaludis* was employed (52, 57, 74). Gas input contained H_2 (110 mL min^{-1}), CO_2 (40 mL min^{-1}), Ar (35 mL min^{-1}) and 1% H_2S:99% Ar (15 mL min^{-1}) for phosphate limitation (0.12 mM phosphate). For H_2 limitation, phosphate was increased (0.8 mM) and H_2 was decreased (21 mL min^{-1}) with an increase in Ar to maintain 200 mL min^{-1} total gas flow. Cultures were grown to high OD_{660} before continuous culture was initiated with phosphate limiting medium (26, 162). After cultures stabilized with P-limitation, a transition to H_2-limitation was initiated and OD_{660} and methane production rates were monitored

across a series of time points (-30, -10, 0, 5, 10, 20, 30, 45, 60, 90, 120, 180, 240, 300, 420, 600, and 1440 min.). Samples for microarray analysis were also collected at each time point as described (26). Methane was monitored using a Buck Scientific model 910 GC equipped with a flame-ionization detector (79).

Generation of suppressor mutations. 35 independent cultures of MM1272 were grown to maximum OD in liquid medium containing formate (25, 59). Cultures were concentrated 10x by centrifugation, and 0.1 mL was spread onto agar plates with 200 mM formate (25). Plates were placed in an anaerobic incubation vessel gassed with 138 kPa H_2:CO_2 (80:20) and incubated at 37°C for 3 days. After incubation, any colonies were considered possible suppressor mutants and streak purified under the same conditions. Streak purified clones were inoculated into formate medium gassed with N_2:CO_2 (80:20). Finally, putative suppressor mutants were grown in liquid formate medium gassed with 276 kPa H_2:CO_2 to verify the phenotype before being stored in 25% glycerol at -80°C for downstream analysis.

Genome sequencing. DNA for genome sequencing was extracted using the Qiagen Puregene kit for yeast genomic DNA extraction according to manufacturer's protocols. DNA was prepped and sequenced as described (23, 51), except a MiSeq benchtop sequencer (Illumina, San Diego, CA) was used according to manufacturer's recommendations instead of the Illumina Genome Analyzer GA IIX. Sequence data was compared directly to the *M. maripaludis* strain S2 reference genome (NCBI reference NC_005791.1) to identify mutations. A summary of identified mutations can be found in Table 7.2.

Microarray analysis. Microarrays were performed on mutants with either phosphate limitation/H_2 excess or H_2 limitation/phosphate excess (see strains and growth conditions). mRNA for mutants was collected and subjected to microarray analysis as described (26).

Results and Discussion

A hydrogenotropgic methanogen that is inhibited by H_2. *fdh1* was shown to be repressed in the presence of H_2, even when cultures were grown in the presence of both H_2 and formate (156). Additionally, a Δ*vhuAU* Δ*vhcA* mutant was shown to have a growth defect specifically on H_2 but grew like wild type with formate (25). Based on these data, we reasoned that Δ*vhuAU* Δ*vhcA* would grow poorly on formate in the presence of H_2 due to the absence of Vhu and Vhc

and the repression of *fdh* leading to a lack of electron donors to Hdr. Indeed, although the Δ*vhuAU* Δ*vhcA* strain grows in the presence of both formate and H_2, it possesses a growth defect compared to growth with formate alone (Fig. 7.1). As noted previously, Δ*vhuAU* Δ*vhcA* grows poorly on H_2 alone. Wild type *M. maripaludis* showed no growth defect in the presence of formate and H_2 (79). Taken together, these data show that Δ*vhuAU* Δ*vhcA* in the presence of formate and H_2 is specifically inhibited by H_2. This inhibition provides the basis of a selection to alleviate H_2-based repression of *fdh1*.

Isolation of suppressor mutants that are not inhibited by hydrogen. 35-independent cultures of the Δ*vhuAU* Δ*vhcA* mutant were plated on agar medium containing formate and incubated in an atmosphere of H_2:CO_2 (80:20). Of these 35, 11 had colonies form after 3 days; one colony from each independent culture was picked for further characterization. All 11 mutants displayed the ability to grow on formate liquid medium in the presence of a H_2 atmosphere, unlike the Δ*vhuAU* Δ*vhcA* parent (Fig. 7.2). These 11 strains were considered to possess possible suppressor mutations that alleviated the H_2-dependent repression of *fdh1* expression.

Although these strains were isolated for the ability to grow in the presence of formate and H_2, the sup26 strain had an additional phenotype: the ability to grow on H_2 only (Fig. 7.2). This is surprising since sup26, like all mutants generated, lacks the Hdr-associated hydrogenases. Subsequent PCR analysis of sup 26 verified that *vhuAU* and *vhcA* were still genenetically eliminated in this background. Therefore, the mutation in sup26 must be functioning in a novel pathway to provide electrons to Hdr from H_2. The most likely candidate for such an activity is the F_{420}-reducing hydrogenases Fru or Frc. These hydrogenases were found to be important for inefficient, possibly membrane associated, electron transfer to Hdr in both *M. maripaludis and Methanococcus voltae* (19, 24).

Three classes of mutations identified through whole genome sequencing. We performed whole genome sequencing of the 11 suppressor strains using the Illumina platform to identify mutations responsible for growth of Δ*vhuAU* Δ*vhcA* on both formate and H_2. A total of seven genes were mutated in these strains (Table 7.2). Strains sup13 and sup33 had two mutations each. The most commonly mutated gene was Mmp 1381, of which seven strains contained a frame shift (+1 and -1) or a point mutation. In sup 13, both Mmp 1381 and Mmp 1719 were mutated, but we assume the Mmp 1381 mutation is responsible for the phenotype considering

the large number of other suppressor strains with mutations in this gene. In sup33, Mmp 0267 and Mmp 0466 both contained frame shifts. Mmp 0466 is only found in select strains of *M. maripaludis*; whereas, Mmp 0267 is found in all sequenced lineages of hydrogenotrophic methanogens. Therefore, Mmp 0267 was selected for downstream analysis. Finally, sup18, sup20 and sup26 contained mutations within genes or regulatory elements potentially affecting the H_2-dependent methylenete-trahydromethanopterin (H_4MPT) dehydrogenase (Hmd*)*, and were grouped into a third class. Mmp 0034 is a predicted GTP cyclohydrolase and is related to genes involved in folate and tetrahydrofolate (H_4F) biosynthesis; as H_4MPT performs a function similar to H_4F, this gene may be important for H_4MPT synthesis and, by extension, Hmd function. Mmp 0125 is the gene for HcgG, which is essential for Hmd function (80, 135). Therefore, these mutations were classified as possibly impacting Hmd function and were represented in downstream analysis by a Δ*hmd* strain.

It is interesting that Hmd-related genes were mutated in our selection. Hmd has the lowest affinity for H_2 of all methanogenic hydrogenases (137); therefore, Hmd would be the first hydrogenase to experience limitation of substrate. Could Hmd be involved in sensing H_2? There are documented examples of Hmd homologs possessing functions other than hydrogenase activity. For example, HmdII was recently shown to bind tRNA, suggesting a possible regulatory link between energy metabolism and protein synthesis (104).

BLASTp search of Mmp1381 suggests this protein shares similarity to a group of putative RNA metabolizing enzymes (blast.ncbi.nlm.nih.gov). A subsequent BLASTp search against a bacterial database reveals that Mmp 1381 is between 30 – 35% identical, across the entirety of the protein, to beta-lactamase type RNA metabolizing enzymes from clostridia. RNA processing is an important mechanism used by all three domains of life to regulate mRNA abundance or activity (for reviews, see (34, 41, 67, 123)). If Mmp 1381 is a RNA metabolizing enzyme, perhaps it may specifically control transcripts for genes involved in the H_2 response. Mmp 0267 is a hypothetical protein with no known function.

In the previous study of regulation of methanogenesis with the EGRIN model, *fdh* was found to cluster with several genes associated with methanogenesis including hydrogenases and subunits of Hdr (163). Although this study identified and verified two genes that impact regulation of this cluster - Mmp 0719 and Mmp 1100 - these were not spontaneously mutated in our selection. The present study was designed to identify regulatory elements specifically

important for *fdh1*, while Mmp 0719 and Mmp 1100 impact a regulatory cluster containing both *fdh1* and *fdh2*. In addition, the EGRIN study may have identified genes involved in regulation by factors other than H_2. Therefore, it is likely that our screen targeted a different class of genes important for formate dehydrogenase regulation. It is also worth noting that we only isolated and sequenced 11 suppressor strains. It is unlikely that our selection was saturated. Further isolation and identification of suppressor mutations may reveal knockouts of Mmp 0719 and Mmp 1100 to be important for alleviating the H_2-based growth inhibition of the Δ*vhuAU* Δ*vhcA* mutant.

Phenotypic analysis of Mmp 0267, Mmp 1381, and hmd deletion mutants. In the Δ*vhuAU* Δ*vhcA* background, *hmd*, Mmp 0267, and Mmp 1381 deletion mutants all had the ability to grow on formate in the presence of H_2 (Fig 7.3). This confirms these mutants are no longer inhibited by the presence of H_2. Additionally, like the Mmp 0125 mutation in sup26, Δ*hmd* gained the capacity to grow on H_2 alone.

In addition to batch culture analysis in the Δ*vhuAU* Δ*vhcA* background, we sought to analyze the effects of these mutations in a wild type background under continuous culture with either excess or limiting quantities of H_2. All three genes were genetically eliminated in the MM901 background (in the case of Mmp 0267 and Mmp 1381 in the Δ*vhuAU* Δ*vhcA* background growth on H_2 alone is not possible, so continuous culture with H_2 is not possible). Previous continuous culture analysis of wild type and several metabolic gene mutants showed that energy spilling – or formation of excess CH_4 over what is needed to sustain biosynthesis – occurs upon transition from H_2 limitation to H_2 excess. Y_{CH4} (g cell yield per mole methane formed) goes from 2.86 ± 0.58 with H_2 limitation to 0.77 ± 0.22 with H_2 excess (26). ΔMmp 1381 displayed Y_{CH4} values in agreement with what was previously seen in wild type; however, ΔMmp 0267 and Δ*hmd* had more interesting phenotypes (Fig. 7.3). ΔMmp 0267 displayed intermediate Y_{CH4} values ranging from 1.26 to 1.57 regardless of H_2 limitation or excess. In Δ*hmd* Y_{CH4} was similar to ΔMmp 0267 during H_2 limitation and after prolonged H_2 excess; however, between 20 and 300 minutes after transition, Y_{CH4} was similar to wild type under H_2 excess.

Possible mechanisms behind the growth of Δvhu**AU* Δ*vhcA suppressor strains. *M. maripaludis* regulates the expression of *fdh1* in response to H_2 concentrations (26, 57, 156). The simplest explanation for the growth of our mutants is that repression of the *fdh1* operon has been alleviated. There is a second *fdh* encoded in the genome, but it has never been shown to

support growth on formate in wild type (26, 88) and is only expressed in the presence of growth limiting concentrations of formate and the absence of exogenously added H_2 (26). However, a deletion in *fdh1* will eventually gain the ability to grow with formate as an electron donor, presumably due to a suppressor mutation that leads to the de-repression of *fdh2* (88). These data suggest that, in addition to the obvious de-repression of *fdh1*, a second mutation class that may have appeared in our screen is the de-repression of *fdh2*. A last intriguing possibility is that the same regulatory network controls expression of all the F_{420}-dependent steps of methanogenesis. All of the genes encoding for the F_{420}-dependent steps of methanogenesis are highly expressed under similar growth conditions, suggesting they may be regulated together (26, 57). In an effort to determine which of these three possibilities leads to growth of our mutants, we preformed microarray analysis of our mutants grown under both H_2-excess and H_2-limiting conditions.

Microarray analysis of ∆hmd, ∆Mmp 0267, and ∆Mmp 1381. Microarrays of each of the deletion mutants revealed distinct regulatory patterns. In all three mutant backgrounds, mRNA levels for *fdh1* were greatly increased over wild type (Fig. 7.4). However, mRNA levels for other genes important for methanogenesis differed significantly between mutants (Fig. 7.4). Based on the microarray profiles, and referring to the EGRIN model, there are a few possibilities for how deletion of *hmd* and Mmp 1381 leads to *fdh* expression in the presence of H_2. Hypotheses are harder to pose for Mmp 0267 because it is a hypothetical protein that does not appear in the EGRIN model as either contained within a gene cluster or as a putative regulator despite the fact that our results clearly indicate its involvement in Fdh regulation.

In the ∆*hmd* background grown under H_2-excess, two of the F_{420}-dependent steps of methanogenesis (specifically *fdh1* and *mer*) showed at least a two-fold increase in mRNA levels (Fig. 7.4) over wild type and a third, *fru*, had mRNA levels approximately 75% higher. Additionally, under H_2-limitation, this mutant displays an mRNA profile similar to cells grown under formate-limitation (26) since genes for *fdh2*, *fmd*, and molybdenum transport had elevated mRNA levels (Table 7.3). The H_2-excess expression profile is interesting. In the EGRIN model, the F_{420}-dependent steps of methanogenesis were found to respond to "H_2" as a signal, but how this signal is sensed remains a mystery (163).

Interestingly, in addition to *fdh*, there were a few genes with increased mRNA levels in the Mmp 1381 deletion background (Table 7.3). This may be consistent with the deletion of an mRNA

metabolizing enzyme. Among these genes is Mmp 0209. Mmp 0209 was a predicted transcription factor that regulates a gene cluster named bc_0044 (163). bc_0044 contains *fdhA*. These data suggest increased Fdh levels in ΔMmp 1381 may be a result of increased mRNA abundance for Mmp 0209. Deletion or overexpression of Mmp 0209 may verify the role this gene plays in *fdh* regulation. Assuming Mmp 1381 is indeed involved in RNA metabolism, another interesting future experiment would be to identify sequence or structural motifs of mRNAs that are impacted by Mmp 1381, and generate mutations in Mmp 0209 that result in the escape of Mmp 1381-dependent regulation for this gene.

How does deletion of *hmd* in a Δ*vhuAU* Δ*vhcA* background lead to growth on H_2 alone? Interestingly, ΔMmp 1381 in a Δ*vhuAU* Δ*vhcA* background also gains the ability to grow, albeit very slowly, on H_2 alone (Fig. 7.3). Analysis of the mRNA profiles of these two mutants reveals very few similarities that are not shared with ΔMmp 0267. However, it is worth noting that in both Δ*hmd* and ΔMmp 1381, genes for *fdh2* display increased mRNA abundance, with a higher mRNA level in Δ*hmd* than in ΔMmp 1381 (Fig. 7.4). Could Fdh2 be involved in the H_2 growth of these mutants in the Δ*vhuAU* Δ*vhcA* background? An easy way to address this hypothesis is to genetically eliminate *fdh2* in the Δ*vhuAU* Δ*vhuA* Δ*hmd* background and assay for growth on H_2. Fdh1 is found bound to Hdr (25), whereas, there is no evidence that Fdh2 is. If Fdh2 is reversible (capable of generating formate from $F_{420}H_2$), this may provide a basis for the ability of these mutants to grow with H_2 alone: Fru/Frc generates $F_{420}H_2$ from H_2, Fdh2 generates formate from $F_{420}H_2$, and Fdh1 uses formate to transfer electrons to Hdr. This scheme would also explain how Fru/Frc is involved in a cryptic pathway for heterodisulfide reduction (24). Chemical analysis of Δ*vhuAU* Δ*vhuA* Δ*hmd* cultures grown on H_2 could determine if formate is generated and consumed as an intermediate; presumably, large quantities of formate would need to be generated to provide sufficient substrate for growth and methanogenesis.

Tables and figures

Table 7.1. Strains, primers, and plasmids used in this study.

Strain	Description	Reference
MM901	*M. maripaludis* S2 Δ*upt*	(25, 154)
MM1272	MM901 Δ*vhuAU* Δ*vhcA*	(25)
MM1379	MM901 ΔMmp0267	This study
MM1380	MM901 ΔMmp1381	This study
MM1279	MM901 Δ*hmd*	(79)
MM1382	MM1272 ΔMmp0267	This study
MM1383	MM1272 ΔMmp1381	This study
MM1381	MM1272 Δ*hmd*	This study

Plasmid		Reference
pCRuptNeo	Vector for generating in-frame deletions in MM901	(25)
pCRuptNeoΔ*hmd*		(79)
pCRuptNeoΔMmp0267		This study
pCRuptNeoΔMmp1381		This study

Primer	Sequence
Mmp0267-us-F-Xba	AAAATCTAGACAGAAATTGAACACAGGCACTACCAGTATAC
Mmp0267-us-R-Asc	AAAAGGCGCGCCACACACTATCACTCTTTTCAGGTTTTCGATAAAACGG
Mmp0267-ds-F-Asc	AAAAGGCGCGCCTAAATGAAAAAAAGTTGAAAATATGGACGTAC
Mmp0267-ds-R-Not	AAAAGCGGCCGCTATAATTATACAAAGTGATATTGCAATTATCACGG
Mmp1381-us-F-Xba	AAAATCTAGAAATCTAAACATAAAACCAGATTTTCTTATCC
Mmp1381-us-R-Asc	AAAAGGCGCGCCTCATTATATCACATAAATTTAATATATTACAG
Mmp1381-ds-F-Asc	AAAAGGCGCGCCTAATTATCCCACATATTCTCTTTTTTAATATTTTAAATTTTG
Mmp1381-ds-R-Not	AAAAGCGGCCGCTTCCTAAACCTAATAATTCTCTTAATATCATACCG

Table 7.2. Putative mutations lacking Fdh regulation.

Strain	Mmp0034	Mmp0125	intergenic	Mmp0267	Mmp0466	Mmp1381	Mmp1719
sup3	-	-	-	-	-	-1 frameshift	-
sup4	-	-	-	-	-	P65H	-
sup8	-	-	-	-	-	-1 frameshift	-
sup11	-	-	-	-	-	+1 frameshift	-
sup13	-	-	-	-	-	-1 frameshift	T568M
sup14	-	-	-	-	-	-1 frameshift	-
sup18	-	-	*RBS of *hmd*	-	-	-	-
sup20	D85Y	-	-	-	-	-	-
sup23	-	-	-	-	-	+1 frameshift	-
sup26	-	H99P	-	-	-	-	-
sup33	-	-	-	-1 frameshift	+1 frameshift	-	-

Table 7.3. Annotated Genes with at least a four-fold difference in mRNA abundance in Δ*hmd*, ΔMmp 0267, or ΔMmp 1381 vs. MM901. Values are in log(2). Red highlighting indicates increased mRNA abundance and green indicates decreased mRNA abundance.

		MM901 H-excess	MM901 H-limited	Δhmd H-excess	Δhmd H-limited	ΔMmp0267 H-excess	ΔMmp0267 H-limited	ΔMmp1381 H-excess	ΔMmp1381 H-limited
Antisense_22		-0.9	0.6	1.8	3.4	0.1	3.5	0.3	4.0
MMP0127	H2-forming N5,N10-methylene-tetrahydromethanopterin dehydrogenease(EC:1.5.99.11)	-0.5	-3.4	-5.3	-5.2	-0.1	-0.9	0.0	-2.1
MMP0148	acetyl-CoA synthetase, AMP-forming(EC:6.2.1.1)	0.3	0.8	-1.0	-1.2	0.5	-0.9	-1.2	-1.1
MMP0192	hypothetical protein	3.7	0.6	0.8	0.1	2.0	0.4	2.0	0.8
MMP0209	Putative DNA binding protein or transcriptional regulator	-1.0	-0.7	-0.5	-0.4	-0.6	-0.3	1.2	2.3
MMP0210	Conserved hypothetical protein	-2.0	-1.3	-0.3	0.5	-0.1	0.8	0.4	1.7
MMP0249	Ribosomal L37ae protein	-1.1	-0.8	-0.7	-0.6	-0.5	-0.6	1.0	0.7
MMP0250	Putative RNA associated protein/ribosome maturation protein	-0.8	-0.6	-0.4	-0.3	-0.2	-0.3	1.3	1.0
MMP0251	proteasome, subunit alpha(EC:3.4.25.1)	-0.8	-0.7	-0.6	-0.3	-0.4	-0.2	0.9	1.3
MMP0348	Conserved hypothetical protein	0.1	1.1	-1.0	-1.0	0.0	-0.5	0.6	0.1
MMP0413	methyl-accepting chemotaxis sensory transducer	-1.8	-1.5	0.3	1.1	-0.3	1.2	0.3	1.4
MMP0479	hypothetical protein (only in select strains of M. maripaludis)	4.3	4.6	5.1	5.0	-1.1	-1.0	-0.4	-0.2
MMP0487	methyl-accepting chemotaxis sensory transducer	-1.0	-0.8	0.2	1.2	-0.4	1.0	0.0	1.2
MMP0502	hypothetical protein	3.2	0.7	1.0	-0.3	2.1	0.2	2.2	0.8
MMP0503	hypothetical protein (only in select strains of M. maripaludis)	2.2	2.7	0.1	-0.2	0.5	-0.1	1.1	0.1
MMP0508	molybdenum containing formylmethanofuran dehydrogenase, subunit E(EC:1.2.99.5)	0.4	0.6	0.3	3.5	-0.1	0.3	0.3	1.7
MMP0509	formylmethanofuran dehydrogenase, subunit A(EC:1.2.99.5)	0.1	0.3	0.1	3.1	-0.2	0.1	0.1	1.3
MMP0510	molybdenum containing formylmethanofuran dehydrogenase subunit C(EC:1.2.99.5,EC:1.2.99.5)	-0.1	0.3	0.1	3.1	-0.1	0.1	0.1	1.4
MMP0511	molybdenum containing formylmethanofuran dehydrogenase, subunit B(EC:1.2.99.5)	-0.1	0.3	0.0	2.6	-0.2	0.0	0.1	1.1
MMP0512	molybdenum containing formylmethanofuran dehydrogenase, subunit B(EC:1.2.99.5)	0.1	0.3	0.0	2.4	-0.2	0.0	0.3	1.0
MMP0514	Molybdenum ABC transporter, periplasmic molybdenum-binding protein	0.6	0.5	1.0	5.2	-0.1	2.2	0.1	2.9
MMP0646	hypothetical protein	-3.2	-2.2	0.3	0.3	0.8	0.9	-0.8	0.8
MMP0765	hypothetical	-0.1	0.7	0.0	1.3	-0.2	0.8	0.2	2.9
MMP0777	hypothetical protein	0.0	0.3	1.0	1.3	0.8	-2.0	0.4	1.2
MMP0851	conserved hypothetical protein, possibly metal binding	2.8	3.6	0.4	0.6	0.7	0.7	0.2	0.7
MMP0874	SAM (and some other nucleotide) binding motif	-2.8	-2.5	-0.9	0.0	-0.5	0.3	-1.9	0.5
MMP0875	S layer protein	-3.2	-3.1	-1.3	-0.6	-0.8	-0.4	-2.7	-0.9
MMP0888	putative cobalt transport protein	-1.4	-0.6	0.3	0.4	0.8	0.5	0.0	0.3
MMP0889	Cobalamin (vitamin B12) biosynthesis CbiM protein	-1.4	-0.6	0.4	0.6	0.9	0.7	0.1	0.5
MMP1176	putative iron transport system substrate-binding protein, N-term half	-3.8	-2.6	-0.5	0.0	-0.1	0.2	-1.0	-0.3
MMP1177	putative iron transport system substrate-binding protein, C-term half	-4.2	-2.8	-0.7	-0.1	-0.2	0.0	-1.2	-0.4
MMP1178	iron transport Periplasmic binding protein	-2.6	-0.4	-0.1	0.5	0.1	0.6	-0.5	0.3
MMP1179	SAM (and some other nucleotide) binding motif:Generic methyltransferase	0.4	0.2	0.1	2.2	-0.2	0.7	0.0	1.1
MMP1180	conserved hypothetical protein	0.2	0.2	0.3	2.4	-0.1	0.9	0.2	1.2
MMP1193	hypothetical protein	2.8	1.6	0.7	0.3	0.7	0.2	1.8	2.2
MMP1220	glycogen phosphorylase(EC:2.4.1.1)	0.1	-1.7	0.2	0.2	0.1	0.3	0.2	0.5
MMP1297	formate dehydrogenase beta subunit(EC:1.2.1.2)	-1.4	0.8	1.8	3.3	0.1	3.6	0.2	3.9
MMP1298	formate dehydrogenase alpha subunit(EC:1.2.1.2)	-1.8	0.3	1.5	2.9	-0.3	3.2	-0.2	3.6
MMP1299	carbonic anhydrase(EC:4.2.1.1)	-2.4	-0.8	0.8	2.3	-1.2	2.5	0.2	3.3
MMP1300	hypothetical protein	-3.0	-0.8	0.8	2.3	-1.4	2.4	-0.3	3.2
MMP1301	Formate transporter	-2.8	-0.5	1.2	2.3	-0.9	2.4	-0.1	2.8
MMP1302	hypothetical protein	-0.6	0.0	0.9	1.9	-0.5	2.3	-0.3	2.6
MMP1380	Chlorohydrolase	0.4	0.2	0.6	0.3	0.3	0.2	3.9	3.8
MMP1651	periplasmic molybdate-binding protein	-0.3	0.5	0.3	4.1	-0.8	0.9	-0.6	2.2
MMP1652	molybdate ABC transporter, substrate binding subunit	-0.5	1.3	1.0	3.7	-0.6	1.8	-1.0	2.5
MMP1666	flagellin B1 percursor	-3.6	-4.1	0.0	-1.0	-0.4	-0.5	-0.4	-0.8
MMP1667	flagellin B2	-3.7	-4.1	0.0	-0.9	-0.3	-0.4	-0.3	-0.6
MMP1668	flagellin B3	-3.6	-3.9	0.0	-0.8	-0.4	-0.4	-0.4	-0.6
MMP1669	flagella accessory protein C	-3.5	-3.7	0.0	-0.8	-0.6	-0.4	-0.5	-0.6
MMP1670	flagella accessory protein D	-3.4	-3.7	-0.2	-0.6	-0.7	-0.2	-0.5	-0.6
MMP1671	flagella accessory protein E	-3.1	-3.5	-0.2	-0.6	-0.7	-0.2	-0.5	-0.5
MMP1672	flagella accessory protein F	-3.2	-3.3	-0.2	-0.6	-0.8	-0.3	-0.5	-0.6
MMP1673	flagella accessory protein G	-1.8	-2.2	0.1	-0.1	-0.5	0.0	0.0	-0.2

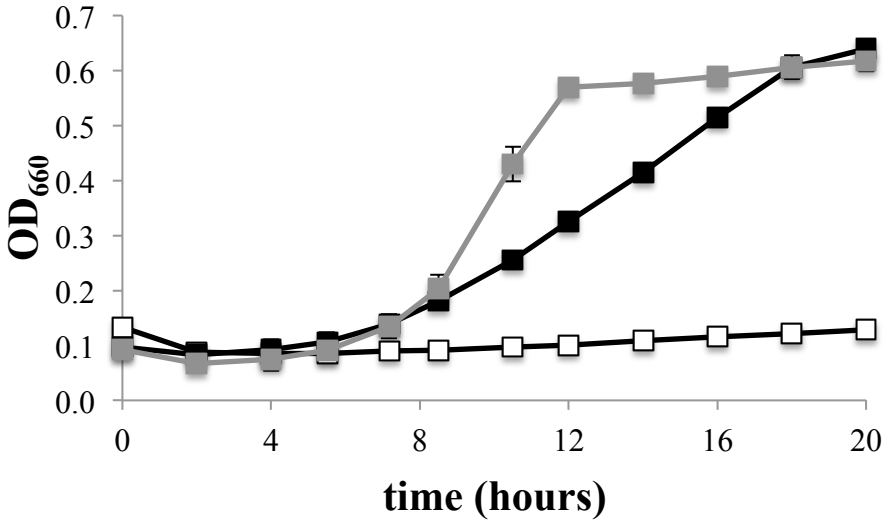

Figure 7.1. Growth of Δ*vhuAU* Δ*vhcA* with H_2 (white symbols), formate (grey symbols), or H_2 + formate (black symbols). A 4% inoculum was used. Curves are averages of three independent cultures. Error bars represent one standard deviation around the mean.

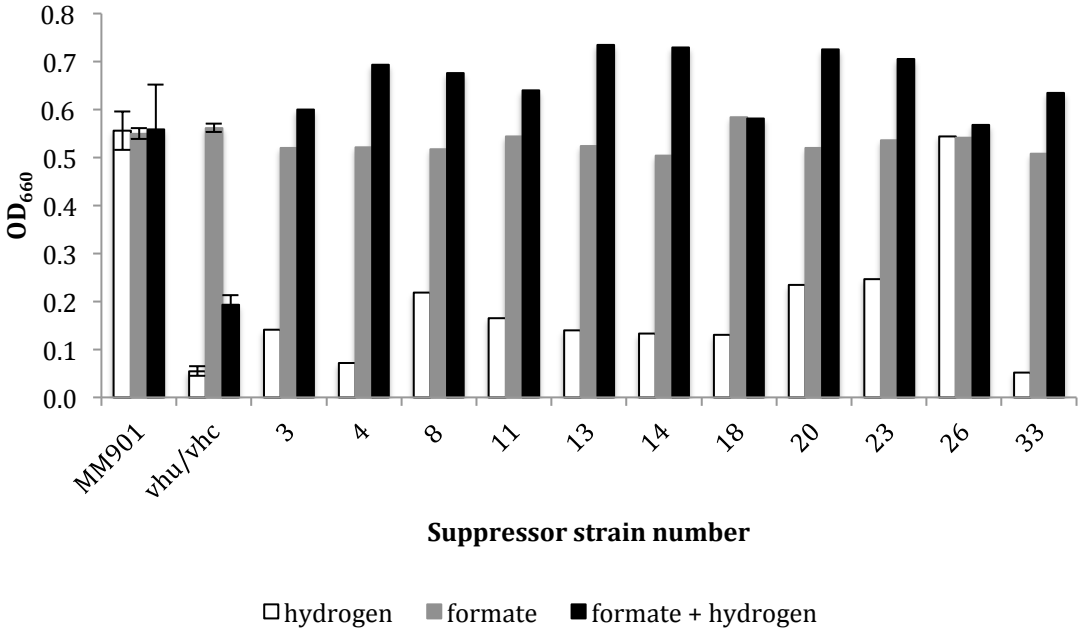

Figure 7.2. Phenotypes of 11 independently isolated Δ*vhuAU* Δ*vhcA* suppressor mutants that grow in the presence of H_2 + formate. Bars show growth after 14 hours of incubation. A 1% inoculum was used at the start of the experiment.

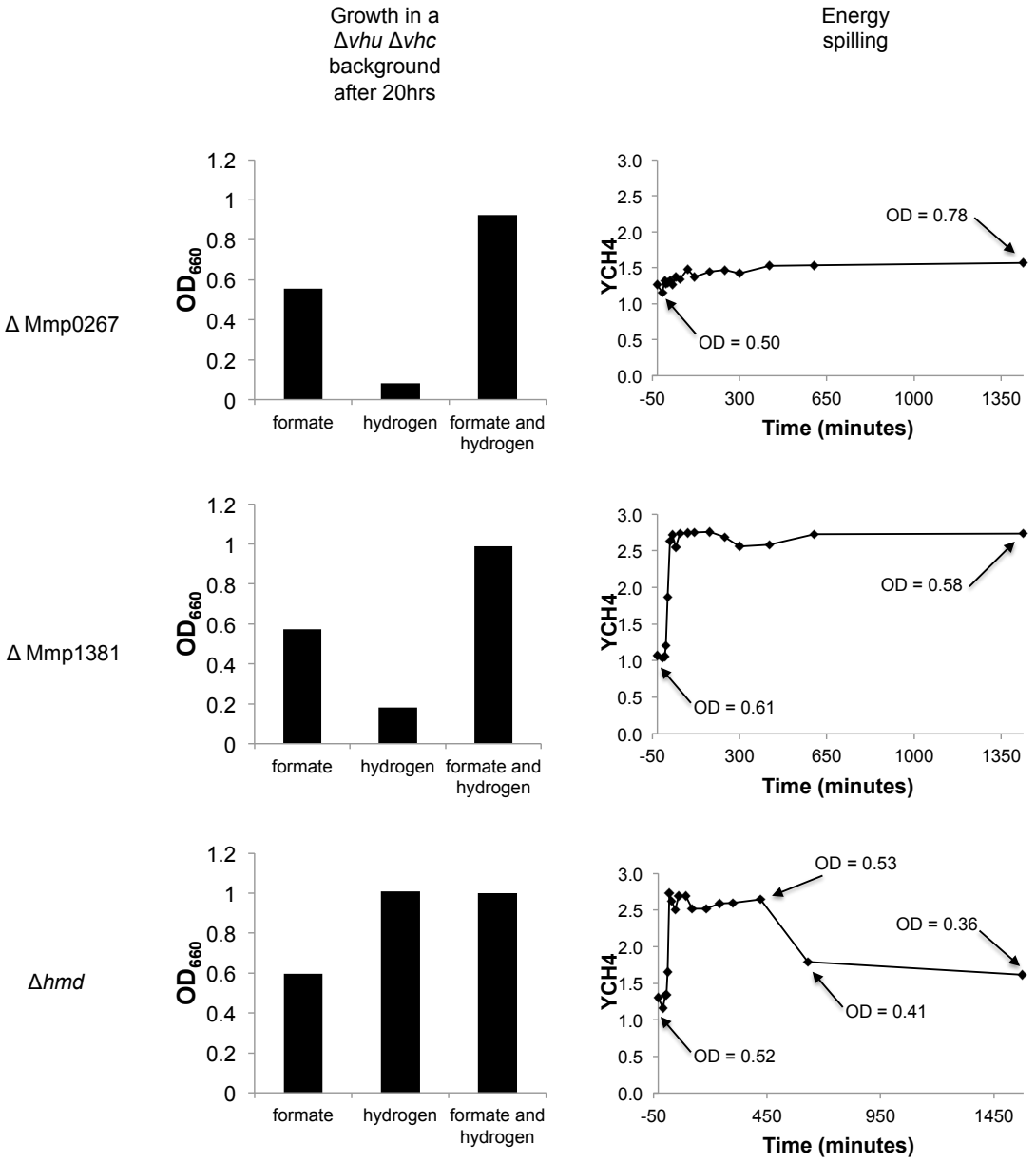

Figure 7.3. Batch (left) and continuous (right) culture phenotypes of Δ*hmd*, ΔMmp 0267, and ΔMmp 1381 strains. In the batch experiments the mutations were in a Δ*vhu* Δ*vhc* background. In the continuous culture experiments the mutations were in a wild type background. Arrows on continuous culture plots show time points that will be subjected to microarray analysis.

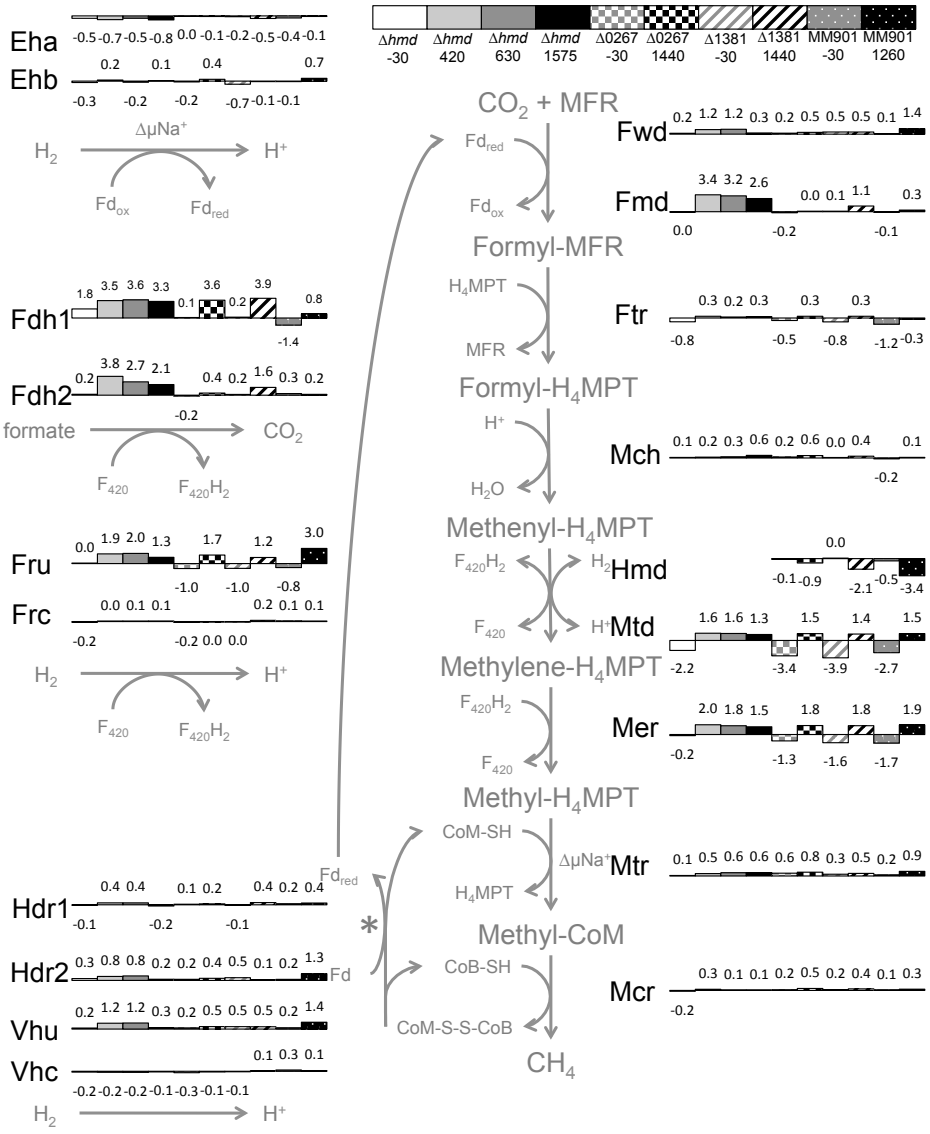

Figure 7.4. Expression of methanogenesis genes in Δ*hmd,* ΔMmp 0267, and ΔMmp 1381. Time (in minutes) either before or after transition from H_2-excess to H_2-limitation is indicated. Arrows in Fig. 7.3 indicate samples selected for array analysis. $\Delta\mu Na^+$, change in Na^+ across membrane; H_4MPT, tetrahydromethanopterin; MFR, methanofuran; CoM-SH, coenzyme M; CoB-SH, coenzyme B; CoM-S-S-CoB, heterodisulfide of CoM and CoB; $F_{420}/F_{420}H_2$, coenzyme F_{420}; Fd_{ox}/Fd_{red}, ferredoxin; Eha/Ehb, energy-converting hydrogenase A or B; Fdh, formate dehydrogenase; Ftr, formyltransferase; Fmd/Fwd, formylmethanofuran dehydrogenase; Fru/Frc, F_{420}-reducing hydrogenase; Hdr, heterodisulfide reductase; Hmd, H_2-dependent methylene-H_4MPT dehydrogenase; Mch, methenyl-H_4MPT cyclohydrolase; Mcr, methyl- CoM reductase; Mer, methylene-H_4MPT reductase; Mtd, F_{420}-dependent methylene-H_4MPT dehydrogenase; Mtr, methyl-H_4MPT:CoM methyltransferase; Vhu/Vhc, Hdr-associated hydrogenase. *Either H_2 or formate acts as the electron donor for these reactions.

CHAPTER 8

Perspectives and future directions

The Wolfe cycle and Eha

In the late 1970s Robert Gunsalus and Ralph Wolfe made an interesting observation with regards to the metabolism of hydrogenotrophic methanogenesis (48). Addition of the pathway intermediate methyl-CoM to cell extracts of *Methanothermobacter thermoautotrophicus* lead to the formation of methane, as expected, but the quantity of methane formed exceeded the methyl-CoM added by 12-fold. This phenomenon, termed the RPG effect in honor of Gunsalus, was later noted to occur with CoM-S-S-CoB as well (13). In 1988, because of these data, Rouvière and Wolfe speculated that methanogenesis might be a cyclic process with CoM-S-S-CoB reduction coupled to CO_2 reduction at the start of the pathway (Fig. 1.1) (116). Later work in members of the *Methanosarcinales* suggested that Hdr generated chemiosmotic potential and that this was consumed in the CO_2 reducing step; thus providing a basis for this observed coupling (55, 56). Therefore, the model of methanogenesis was revised as a linear pathway with the first and last steps separate.

There were several problems with the assumption that *Methanothermobacter* and *Methanosarcina* shared a common mechanism of heterodisulfide reduction (136). The most notable is that in *Methanosarcina* Hdr is membrane bound whereas in *Methanothermobacter* it is cytoplasmic. It is difficult to envision a model where a cytoplasmic enzyme generates membrane potential. It was not until 2008 that a reasonable explanation for this discrepancy was presented by Rudolf Thauer and colleagues (136). They speculated that Hdr from *Methanothermobacter* (and all other hydrogenotrophic methanogens) might be involved in flavin-based electron bifurcation (see below). This hypothesis was soon confirmed biochemically by Thauer's lab and by my isolation of an enzyme complex providing a structural basis for electron bifurcation (25, 70). The coupling of the first and last steps of methanogenesis renders the pathway a cycle. All metabolic cycles require a mechanism to replenish intermediates to guard against deteriorating flux. We finally showed in 2012 that the membrane bound hydrogenase Eha provides a basis to accomplish this (79). This final detail cemented the idea that methanogenesis in the hydrogenotrophs is a cyclic process, and Thauer renamed the pathway the Wolfe cycle to recognize Ralph Wolfe's contributions and his decades-old model of

a cyclic pathway of methanogenesis (134).

Eha in *Methanococcus maripaludis* is a large, 20 subunit, membrane bound hydrogenase which had no defined function until recently (79). The description of Eha as involved in the replenishing of methanogenesis provided an initial characterization of this hydrogenase. In order to show the function of Eha, a strain of *M. maripaludis* lacking all other hydrogenases encoded in the genome was constructed (79). Soon after, it was discovered Eha activity could be substituted by other pathways, making this hydrogenase dispensable (23). This provides an interesting avenue for the characterization of this large, multi-subunit enzyme. Future work can genetically eliminate individual subunits to characterize their importance to hydrogenase function. For example, it is known that Eha reduces ferredoxin, but it is unknown which, if any, of the ferredoxins encoded in the *eha* operon is important for activity (58). A similar genetic approach was successfully implemented to describe the roles of various subunits of the paralogous Ehb hydrogenase (90).

Electron bifurcation in methanogenesis

Flavin-based electron bifurcation was first described in 2008 as mechanism to generate low potential electrons from higher potential substrates; since then, numerous electron bifurcating protein complexes have been identified (11, 25, 64, 70, 78, 143-146). In hydrogenotrophic methanogens, electron bifurcation is likely essential for growth with H_2 making it difficult to study the importance of this phenomenon using a genetic approach. This is because there is only one reaction in these organisms that generates membrane potential: the methyl transfer from tetrahydromethanopterin (H_4MPT) to coenzyme M (CoM), which pumps 1.7 Na^+ out of the cell (84). Without electron bifurcation, the energy converting hydrogenase Eha would be needed to reduce ferredoxin for CO_2 reduction in the first step of methanogenesis (79). This reaction consumes membrane potential (136). There are other, inefficient mechanisms to reduce ferredoxin (23). In *M. maripaludis*, expression of the glycolytic enzyme glyceraldehyde-3-phosphate:ferredoxin oxidoreductase (GAPOR) presumably created a cycle capable of reducing ferredoxin from $F_{420}H_2$; however, this cycle consumes ATP (which costs 4 H^+ or Na^+ translocations to generate (136)) and does not alleviate the electron bifurcation requirement. An alternative pathway involves the oxidation of CO to CO_2 to generate reduced ferredoxin. This is interesting because CO is membrane diffusible, and this reaction does not consume either ATP or membrane potential. Therefore, it may be possible to construct mutants to disrupt electron

bifurcation in *M. mariplauids* grown with both formate and CO without compromising the bioenergetics of the cell: methyl transfer would still generate the membrane potential needed for growth.

Another approach to study electron bifurcation is through structural and biochemical studies. Unfortunately, there is very little crystallographic data regarding the many subunits of the heterodisulfide reductase protein complex (135). The flavin of Hdr is coordinated by the α subunit. It would be interesting to attempt crystallization of this subunit to visualize the structure of the electron bifurcating center. Additionally, it is currently unknown what the precise mechanism of electron transfer is. It was originally argued that electrons flow first in the direction of ferredoxin followed by flow to CoM-S-S-CoB (70). This is based on the observation that flavoproteins (FP) exhibit three redox potentials, the E_O' for FP/FPH_2, FP/FPH, and FPH/FPH_2, and that the E_O' of the FPH/FPH_2 is the most negative of the three. However, it was later argued that a one-electron transfer to ferredoxin followed by an electron transfer to CoM-S-S-CoB is not favorable (102). There is no reason to believe the first electron wouldn't flow directly to CoM-S-S-CoB (unless a conformational change is invoked). More likely, these two reductions occur more of less simultaneously with both CoM-S-S-CoB and the oxidized ferredoxin kept in close proximity to the flavin to capture the electrons; the reduction of CoM-S-S-CoB would generate a "red hot" intermediate state that immediately reduces ferredoxin (102). We are currently collaborating with Eduardus Duin at Auburn University to use electron paramagnetic resonance spectroscopy to try and differentiate between these two possible mechanisms. The first scheme should show two distinct electron transfer steps whereas the second would look like simultaneous transfer of both electrons.

Although there is strong evidence that formate acts as the electron donor for Hdr, there are still lingering questions as to how electrons go from formate to the active site of electron bifurcation. It is possible that $F_{420}H_2$ and not formate is the direct electron donor; however, this is unlikely. A mutant lacking functional *vhu* and *vhc* does not grow as robustly as wild type on H_2 (Fig. 2.3) despite the fact that both F_{420}-reducing hydrogenases and the Hmd-Mtd cycle are fully operational (25, 57). This strongly suggests $F_{420}H_2$ is not a physiologically important electron donor as suggested for *Methanococcus voltae* (19). The second possibility is that formate directly donates electrons to the Hdr complex without $F_{420}H_2$ acting as an intermediate. If this is the case, the FdhB subunit should be non-essential. Another interesting consideration is that a formate dehydrogenase from clostridia was recently observed to be electron bifurcating (144). It

would be very interesting if the *M. maripaludis* Fdh were also an electron bifurcating enzyme. Eight electrons from formate could enter the Hdr enzyme complex. If half of these are bifurcated towards F_{420} reduction at an FAD associated with FdhA and the other half enter HdrA to be further bifurcated to reduce ferredoxin and CoM-S-S-CoB this would provide the reducing equivalents for all four reductive steps of methanogenesis: 2 $F_{420}H_2$, formyl-methanofuran, and CoM and CoB. Biochemical assays using formate, $F_{420}H_2$, or both formate and F_{420}, along with CoM-S-S-CoB and oxidized ferredoxin, could determine which of these pathways functions in vivo.

Alternative electron donors to methanogenesis

Hydrogenotrophic methanogens have underappreciated metabolic versatility. For many years it was thought that H_2 was the primary electron donor for the pathway of methanogenesis. When alternate electron donors, such as formate, are used for growth, conventional wisdom stated that these were converted to H_2 via a formate:H_2 lyase activity and H_2 served as the electron donor. However, the work presented here challenges this assumption. Formate is as intimately linked into the methanogenic pathway as H_2. In fact, in *M. maripaludis*, a single formate dehydrogenase appears to fulfill the roles of at least five hydrogenases by replacing the functions of both F_{420}-reducing hydrogenases, both Hdr-associated hydrogenases, and the H_2-dependent methylene-tetrahydromethanopterin (H_4MPT) dehydrogenase (79). Some hydrogenotrophic methanogens are capable of using alcohols as electron donors for methanogenesis via F_{420}-reducing alcohol dehydrogenases (155); future work will determine if these enzymes are similarly integrated into the methanogenic pathway. Although formate dehydrogenase is closely integrated into methanogenesis, there are still anabolic and anaplerotic activities that rely on H_2 in wild type (79). However, even these can be bypassed with alternative, low redox potential electron donors like CO, or by hijacking a cycle involving reactions important to both glycolysis and gluconeogenesis (23).

Although GAPOR can generate reduced ferredoxin for methanogenesis (23), the prospects for engineering *M. maripaludis* to grow with glucose as the sole electron donor are not good. *M. maripaludis* lacks a transporter to bring glucose into the cell (58). Although a transporter could theoretically be introduced, most moderate to high affinity transporters consume membrane potential (66). Additionally, assuming glucose is oxidized to pyruvate, *M. maripaludis* is very inefficient at using pyruvate as an electron donor for methanogenesis (161), and incapable of

using the acetate generated: incorporation of the methyl group of acetate to methyl-H_4MPT causes a problem in that two electron pairs are needed for the downstream reactions centered on Hdr, but oxidation of the carboxyl of acetate only generates one pair. Therefore, we can effectively assume pyruvate would be the end product of glycolysis in *M. maripaludis* (141). Thus, the energy requirement for glucose transport, the activation/phosphorylation of glucose, and the inability to generate energy beyond oxidation to pyruvate or acetate means that more energy is expended to utilize glucose than what could be generated from the electrons derived. However, in the *Methanosarcinales*, acetate utilization is commonplace, and a strain of *Methanosarcina barkeri* was shown to grow with pyruvate as the sole energy source (14), suggesting the possibility of engineering these organisms to utilize glucose as a sole energy source. CH_4 generation from glucose is thermodynamically favorable ($\Delta G^{0'}$ = -16.8 kJ per mole electrons), but not as favorable as glucose fermentation to ethanol ($\Delta G^{0'}$ = -56.5 kJ per mole electrons), suggesting an explanation as to why this metabolism is not naturally occurring: methanogens would be outcompeted by fermenters (94, 165). Efforts to engineer alternative electron donors into *Methanosarcinales* have already shown some promise (76).

Regulators of methanogenesis

As outlined in chapter 7, we have recently identified a selection process to find genes involved in the regulation of formate dehydrogenase (*fdh*). This is most interesting because formate dehydrogenase exists in a regulatory cluster with several hydrogenases important to methanogenesis (163). Therefore, it is possible to not only elucidate details of *fdh* regulation, but conceivably the details of hydrogenase regulation as well. Our initial screen identified three putative proteins involved in the repression of *fdh* (*hmd*, Mmp 0267, and Mmp 1381). Microarray experiments to characterize the global effects of knockouts in these genes have verified that *fdh* mRNA is abundant in knockout mutants. It is also conceivable that isolation and characterization of a large number of suppressor strains may reveal more genes and proteins involved in *fdh* (or hydrogenase) regulation. Although this project is in its infancy, there are strong possibilities for many future research directions; every gene identified in this and subsequent screens unlocks new and interesting possibilities for characterizing the regulation of the methanogenic pathway.

References

1. **Abken, H. J., M. Tietze, J. Brodersen, S. Baumer, U. Beifuss, and U. Deppenmeier.** 1998. Isolation and characterization of methanophenazine and function of phenazines in membrane-bound electron transport of *Methanosarcina mazei* Go1. J Bacteriol **180:**2027-2032.

2. **Afting, C., A. Hochheimer, and R. K. Thauer.** 1998. Function of H_2-forming methylenetetrahydromethanopterin dehydrogenase from *Methanobacterium thermoautotrophicum* in coenzyme F_{420} reduction with H_2. Arch Microbiol **169:**206-210.

3. **Afting, C., E. Kremmer, C. Brucker, A. Hochheimer, and R. K. Thauer.** 2000. Regulation of the synthesis of H_2-forming methylenetetrahydromethanopterin dehydrogenase (Hmd) and of HmdII and HmdIII in *Methanothermobacter marburgensis*. Arch Microbiol **174:**225-232.

4. **Alber, B. E., and J. G. Ferry.** 1994. A carbonic anhydrase from the archaeon *Methanosarcina thermophila*. Proc Natl Acad Sci U S A **91:**6909-6913.

5. **Balch, W. E., and R. S. Wolfe.** 1979. Transport of coenzyme M (2-mercaptoethanesulfonic acid) in *Methanobacterium ruminantium*. J Bacteriol **137:**264-273.

6. **Barker, H.** 1940. Studies upon the methane fermentation. IV. The isolation and culture of *Methanobacterium omelianskii*. Antonie van Leeuwenhoek J. Microbiol. Serol. **6:**201-220.

7. **Baun, N. R., and W. W. Metcalf.** 2009. Methanogenesis by *Methanosarcina acetivorans* involves two structurally and functionally distinct classes of heterodisulfide reductase. Mol Microbiol **75:**843-853.

8. **Berg, I. A., D. Kockelkorn, W. H. Ramos-Vera, R. F. Say, J. Zarzycki, M. Hugler, B. E. Alber, and G. Fuchs.** 2010. Autotrophic carbon fixation in archaea. Nat Rev Microbiol **8:**447-460.

9. **Berghofer, Y., K. Agha-Amiri, and A. Klein.** 1994. Selenium is involved in the negative regulation of the expression of selenium-free [NiFe] hydrogenases in *Methanococcus voltae*. Mol Gen Genet **242:**369-373.

10. **Berk, H., and R. K. Thauer.** 1998. $F_{420}H_2$:NADP oxidoreductase from *Methanobacterium thermoautotrophicum*: identification of the encoding gene via functional overexpression in *Escherichia coli*. FEBS Lett **438:**124-126.

11. **Bertsch, J., A. Parthasarathy, W. Buckel, and V. Muller.** 2013. An electron-bifurcating caffeyl-CoA reductase. J Biol Chem **288:**11304-11311.

12. **Bobik, T. A., and R. S. Wolfe.** 1989. Activation of formylmethanofuran synthesis in cell extracts of *Methanobacterium thermoautotrophicum*. J Bacteriol **171:**1423-1427.

13. **Bobik, T. A., and R. S. Wolfe.** 1988. Physiological importance of the heterodisulfide of coenzyme M and 7-mercaptoheptanoylthreonine phosphate in the reduction of carbon dioxide to methane in *Methanobacterium*. Proc Natl Acad Sci U S A **85:**60-63.

14. **Bock, A. K., and P. Schonheit.** 1995. Growth of *Methanosarcina barkeri* (Fusaro) under nonmethanogenic conditions by the fermentation of pyruvate to acetate: ATP synthesis via the mechanism of substrate level phosphorylation. J Bacteriol **177:**2002-2007.

15. **Börner, G., M. Karrasch, and R. Thauer.** 1989. Formylmethanofuran dehydrogenase activity in cell extracts of *Methanobacterium thermoautotrophicum* and of *Methanosarcina barkeri*. FEBS Lett **244:**21-25.

16. **Bose, A., M. A. Pritchett, and W. W. Metcalf.** 2008. Genetic analysis of the methanol- and methylamine-specific methyltransferase 2 genes of *Methanosarcina acetivorans* C2A. J Bacteriol **190:**4017-4026.

17. **Bott, M., and R. K. Thauer.** 1987. Proton-motive-force-driven formation of CO from CO_2 and H_2 in methanogenic bacteria. Eur J Biochem **168:**407-412.

18. **Bradford, M. M.** 1976. A rapid and sensitive method for the quantitation of microgram quantities of protein utilizing the principle of protein-dye binding. Anal Biochem **72:**248-254.

19. **Brodersen, J., G. Gottschalk, and U. Deppenmeier.** 1999. Membrane-bound $F_{420}H_2$-dependent heterodisulfide reduction in *Methanococcus voltae*. Arch Microbiol **171:**115-121.

20. **Burke, S. A., and J. A. Krzycki.** 1997. Reconstitution of Monomethylamine:Coenzyme M methyl transfer with a corrinoid protein and two methyltransferases purified from *Methanosarcina barkeri*. J Biol Chem **272:**16570-16577.

21. **Buurman, E. T., M. J. Teixeira de Mattos, and O. M. Neijssel.** 1991. Futile cycling of ammonium ions via the high affinity potassium uptake system (Kdp) of *Escherichia coli*. Arch Microbiol **155:**391-395.

22. **Cedervall, P. E., M. Dey, A. R. Pearson, S. W. Ragsdale, and C. M. Wilmot.** 2010. Structural insight into methyl-coenzyme M reductase chemistry using coenzyme B analogues. Biochemistry **49:**7683-7693.

23. **Costa, K. C., T. J. Lie, M. A. Jacobs, and J. A. Leigh.** 2013. H_2-independent growth of the hydrogenotrophic methanogen *Methanococcus maripaludis*. MBio **4** :e00062-13.

24. **Costa, K. C., T. J. Lie, Q. Xia, and J. A. Leigh.** 2013. VhuD facilitates electron flow from H_2 or formate to heterodisulfide reductase in *Methanococcus maripaludis*. J Bacteriol. **195:**5160-5165.

25. **Costa, K. C., P. M. Wong, T. Wang, T. J. Lie, J. A. Dodsworth, I. Swanson, J. A. Burn, M. Hackett, and J. A. Leigh.** 2010. Protein complexing in a methanogen suggests electron bifurcation and electron delivery from formate to heterodisulfide reductase. Proc Natl Acad Sci U S A **107:**11050-11055.

26. **Costa, K. C., S. H. Yoon, M. Pan, J. A. Burn, N. S. Baliga, and J. A. Leigh.** 2013. Effects of H_2 and formate on growth yield and regulation of methanogenesis in *Methanococcus maripaludis*. J Bacteriol **195:**1456-1462.

27. **Daniels, L., G. Fuchs, R. K. Thauer, and J. G. Zeikus.** 1977. Carbon monoxide oxidation by methanogenic bacteria. J Bacteriol **132:**118-126.

28. **de Poorter, L. M., W. J. Geerts, and J. T. Keltjens.** 2007. Coupling of *Methanothermobacter thermautotrophicus* methane formation and growth in fed-batch and continuous cultures under different H_2 gassing regimens. Appl Environ Microbiol **73:**740-749.

29. **de Poorter, L. M., W. J. Geerts, and J. T. Keltjens.** 2005. Hydrogen concentrations in methane-forming cells probed by the ratios of reduced and oxidized coenzyme F_{420}. Microbiology **151:**1697-1705.

30. **DiMarco, A. A., M. I. Donnelly, and R. S. Wolfe.** 1986. Purification and properties of the 5,10-methenyltetrahydromethanopterin cyclohydrolase from *Methanobacterium thermoautotrophicum*. J Bacteriol **168:**1372-1377.

31. **Dodsworth, J. A., N. C. Cady, and J. A. Leigh.** 2005. 2-Oxoglutarate and the PII homologues NifI1 and NifI2 regulate nitrogenase activity in cell extracts of *Methanococcus maripaludis*. Mol Microbiol **56:**1527-1538.

32. **Dodsworth, J. A., and J. A. Leigh.** 2006. Regulation of nitrogenase by 2-oxoglutarate-reversible, direct binding of a PII-like nitrogen sensor protein to dinitrogenase. Proc Natl Acad Sci U S A **103:**9779-9784.

33. **Dolfing, J., B. Jiang, A. M. Henstra, A. J. Stams, and C. M. Plugge.** 2008. Syntrophic growth on formate: a new microbial niche in anoxic environments. Appl Environ Microbiol **74:**6126-6131.

34. **Dominski, Z.** 2007. Nucleases of the metallo-beta-lactamase family and their role in DNA and RNA metabolism. Crit Rev Biochem Mol Biol **42:**67-93.

35. **Donnelly, M. I., and R. S. Wolfe.** 1986. The role of formylmethanofuran: tetrahydromethanopterin formyltransferase in methanogenesis from carbon dioxide. J Biol Chem **261:**16653-16659.

36. **Duin, E. C., and M. L. McKee.** 2008. A new mechanism for methane production from methyl-coenzyme M reductase as derived from density functional calculations. J Phys Chem B **112:**2466-2482.

37. **Dybas, M., and J. Konisky.** 1989. Transport of coenzyme M (2-mercaptoethanesulfonic acid) and methylcoenzyme M [(2-methylthio)ethanesulfonic acid] in *Methanococcus voltae*: identification of specific and general uptake systems. J Bacteriol **171:**5866-5871.

38. **Eikmanns, B., G. Fuchs, and R. K. Thauer.** 1985. Formation of carbon monoxide from CO_2 and H_2 by *Methanobacterium thermoautotrophicum*. Eur J Biochem **146:**149-154.

39. **Eng, J. K., A. L. McCormack, and J. R. Yates.** 1994. An approach to correlate tandem mass spectra of peptides with amino acid sequences in a protein database. J amer Soc Mass Spectrom **5:**976-989.

40. **Ermler, U., W. Grabarse, S. Shima, M. Goubeaud, and R. K. Thauer.** 1997. Crystal structure of methyl-coenzyme M reductase: the key enzyme of biological methane formation. Science **278:**1457-1462.

41. **Evguenieva-Hackenberg, E., and U. Blasi.** 2013. Attack from both ends: mRNA degradation in the crenarchaeon *Sulfolobus solfataricus*. Biochem Soc Trans **41:**379-383.

42. **Fardeau, M. L., J. P. Peillex, and J. P. Belaich.** 1987. Energetics of the growth of *Methanobacterium thermoautotrophicum* and *Methanococcus thermolithotrophicus* on ammonium chloride and dinitrogen. Arch Microbiol **144:**128-131.

43. **Fournier, G. P., and J. P. Gogarten.** 2008. Evolution of aceticlastic methanogenesis in *Methanosarcina* via horizontal gene transfer from cellulolytic Clostridia. J Bacteriol **190:**1124-1127.

44. **Galagan, J. E., C. Nusbaum, A. Roy, M. G. Endrizzi, P. Macdonald, W. FitzHugh, S. Calvo, R. Engels, S. Smirnov, D. Atnoor, A. Brown, N. Allen, J. Naylor, N. Stange-Thomann, K. DeArellano, R. Johnson, L. Linton, P. McEwan, K. McKernan, J. Talamas, A. Tirrell, W. Ye, A. Zimmer, R. D. Barber, I. Cann, D. E. Graham, D. A. Grahame, A. M. Guss, R. Hedderich, C. Ingram-Smith, H. C. Kuettner, J. A. Krzycki, J. A. Leigh, W. Li, J. Liu, B. Mukhopadhyay, J. N. Reeve, K. Smith, T. A. Springer, L. A. Umayam, O. White, R. H. White, E. Conway de Macario, J. G. Ferry, K. F. Jarrell, H. Jing, A. J. Macario, I. Paulsen, M. Pritchett, K. R. Sowers, R. V. Swanson, S. H. Zinder, E. Lander, W. W. Metcalf, and B. Birren.** 2002. The genome of *M. acetivorans* reveals extensive metabolic and physiological diversity. Genome Res **12:**532-542.

45. **Gao, J., G. J. Opiteck, M. S. Friedrichs, A. R. Dongre, and S. A. Hefta.** 2003. Changes in the protein expression of yeast as a function of carbon source. J Proteome Res **2:**643-649.

46. **Gong, W., B. Hao, Z. Wei, D. J. Ferguson, Jr., T. Tallant, J. A. Krzycki, and M. K. Chan.** 2008. Structure of the alpha2epsilon2 Ni-dependent CO dehydrogenase component of the *Methanosarcina barkeri* acetyl-CoA decarbonylase/synthase complex. Proc Natl Acad Sci U S A **105:**9558-9563.

47. **Gottschalk, G., and R. K. Thauer.** 2001. The Na(+)-translocating methyltransferase complex from methanogenic archaea. Biochim Biophys Acta **1505:**28-36.

48. **Gunsalus, R. P., and R. S. Wolfe.** 1977. Stimulation of CO_2 reduction to methane by methylcoenzyme M in extracts *Methanobacterium*. Biochem Biophys Res Commun **76:**790-795.

49. **Hamann, N., G. J. Mander, J. E. Shokes, R. A. Scott, M. Bennati, and R. Hedderich.** 2007. A cysteine-rich CCG domain contains a novel [4Fe-4S] cluster binding motif as deduced from studies with subunit B of heterodisulfide reductase from *Methanothermobacter marburgensis*. Biochemistry **46:**12875-12885.

50. **Harms, U., and R. K. Thauer.** 1996. The corrinoid-containing 23-kDa subunit MtrA of the energy-conserving N5-methyltetrahydromethanopterin:coenzyme M methyltransferase complex from *Methanobacterium thermoautotrophicum*. EPR spectroscopic evidence for a histidine residue as a cobalt ligand of the cobamide. Eur J Biochem **241:**149-154.

51. **Hayden, H. S., R. Lim, M. J. Brittnacher, E. H. Sims, E. R. Ramage, C. Fong, Z. Wu, E. Crist, J. Chang, Y. Zhou, M. Radey, L. Rohmer, E. Haugen, W. Gillett, V. Wuthiekanun, S. J. Peacock, R. Kaul, S. I. Miller, C. Manoil, and M. A. Jacobs.** 2012. Evolution of *Burkholderia pseudomallei* in recurrent melioidosis. PLoS One **7:**e36507.

52. **Haydock, A. K., I. Porat, W. B. Whitman, and J. A. Leigh.** 2004. Continuous culture of *Methanococcus maripaludis* under defined nutrient conditions. FEMS Microbiol Lett **238:**85-91.

53. **Hedderich, R.** 2004. Energy-converting [NiFe] hydrogenases from archaea and extremophiles: ancestors of complex I. J Bioenerg Biomembr **36:**65-75.

54. **Hedderich, R., A. Berkessel, and R. K. Thauer.** 1990. Purification and properties of heterodisulfide reductase from *Methanobacterium thermoautotrophicum* (strain Marburg). Eur J Biochem **193:**255-261.

55. **Heiden, S., R. Hedderich, E. Setzke, and R. Thauer.** 1994. Purification of a two-subunit cytochrome-b-containing heterodisulfide reductase from methanol-grown *Methanosarcina barkeri*. Eur J Biochem **221:**855 - 861.

56. **Heiden, S., R. Hedderich, E. Setzke, and R. K. Thauer.** 1993. Purification of a cytochrome b containing H_2:heterodisulfide oxidoreductase complex from membranes of *Methanosarcina barkeri*. Eur J Biochem **213:**529-535.

57. **Hendrickson, E. L., A. K. Haydock, B. C. Moore, W. B. Whitman, and J. A. Leigh.** 2007. Functionally distinct genes regulated by hydrogen limitation and growth rate in methanogenic archaea. Proc Natl Acad Sci U S A **104:**8930-8934.

58. **Hendrickson, E. L., R. Kaul, Y. Zhou, D. Bovee, P. Chapman, J. Chung, E. Conway de Macario, J. A. Dodsworth, W. Gillett, D. E. Graham, M. Hackett, A. K. Haydock, A. Kang, M. L. Land, R. Levy, T. J. Lie, T. A. Major, B. C. Moore, I. Porat, A. Palmeiri, G. Rouse, C. Saenphimmachak, D. Soll, S. Van Dien, T. Wang, W. B. Whitman, Q. Xia, Y. Zhang, F. W. Larimer, M. V. Olson, and J. A. Leigh.** 2004. Complete genome sequence of the genetically tractable hydrogenotrophic methanogen *Methanococcus maripaludis*. J Bacteriol **186:**6956-6969.

59. **Hendrickson, E. L., and J. A. Leigh.** 2008. Roles of coenzyme F_{420}-reducing hydrogenases and hydrogen- and F_{420}-dependent methylenetetrahydromethanopterin dehydrogenases in reduction of F_{420} and production of hydrogen during methanogenesis. J Bacteriol **190:**4818-4821.

60. **Hendrickson, E. L., Y. Liu, G. Rosas-Sandoval, I. Porat, D. Soll, W. B. Whitman, and J. A. Leigh.** 2008. Global responses of *Methanococcus maripaludis* to specific nutrient limitations and growth rate. J Bacteriol **190:**2198-2205.

61. **Hippler, B., and R. K. Thauer.** 1999. The energy conserving methyltetrahydromethanopterin:coenzyme M methyltransferase complex from methanogenic archaea: function of the subunit MtrH. FEBS Lett **449:**165-168.

62. **Hochheimer, A., R. Hedderich, and R. K. Thauer.** 1998. The formylmethanofuran dehydrogenase isoenzymes in *Methanobacterium wolfei* and *Methanobacterium thermoautotrophicum*: induction of the molybdenum isoenzyme by molybdate and constitutive synthesis of the tungsten isoenzyme. Arch Microbiol **170:**389-393.

63. **Hochheimer, A., R. A. Schmitz, R. K. Thauer, and R. Hedderich.** 1995. The tungsten formylmethanofuran dehydrogenase from *Methanobacterium thermoautotrophicum* contains sequence motifs characteristic for enzymes containing molybdopterin dinucleotide. Eur J Biochem **234:**910-920.

64. **Huang, H., S. Wang, J. Moll, and R. K. Thauer.** 2012. Electron bifurcation involved in the energy metabolism of the acetogenic bacterium *Moorella thermoacetica* growing on glucose or H_2 plus CO_2. J Bacteriol **194:**3689-3699.

65. **Hunte, C., H. Palsdottir, and B. L. Trumpower.** 2003. Protonmotive pathways and mechanisms in the cytochrome bc1 complex. FEBS Lett **545:**39-46.

66. **Jahreis, K., E. F. Pimentel-Schmitt, R. Bruckner, and F. Titgemeyer.** 2008. Ins and outs of glucose transport systems in eubacteria. FEMS Microbiol Rev **32:**891-907.

67. **Kaberdin, V. R., D. Singh, and S. Lin-Chao.** 2011. Composition and conservation of the mRNA-degrading machinery in bacteria. J Biomed Sci **18:**23.

68. **Kaesler, B., and P. Schonheit.** 1989. The role of sodium ions in methanogenesis. Formaldehyde oxidation to CO_2 and $2H_2$ in methanogenic bacteria is coupled with primary electrogenic Na^+ translocation at a stoichiometry of 2-3 Na^+/CO_2. Eur J Biochem **184:**223-232.

69. **Kaster, A. K., M. Goenrich, H. Seedorf, H. Liesegang, A. Wollherr, G. Gottschalk, and R. K. Thauer.** 2011. More than 200 genes required for methane formation from H(2) and CO(2) and energy conservation are present in *Methanothermobacter marburgensis* and *Methanothermobacter thermautotrophicus*. Archaea **2011:**973848.

70. **Kaster, A. K., J. Moll, K. Parey, and R. K. Thauer.** 2011. Coupling of ferredoxin and heterodisulfide reduction via electron bifurcation in hydrogenotrophic methanogenic archaea. Proc Natl Acad Sci U S A **108:**2981-2986.

71. **Kato, S., T. Kosaka, and K. Watanabe.** 2008. Comparative transcriptome analysis of responses of *Methanothermobacter thermautotrophicus* to different environmental stimuli. Environ Microbiol **10:**893-905.

72. **Ladapo, J., and W. B. Whitman.** 1990. Method for isolation of auxotrophs in the methanogenic archaebacteria: role of the acetyl-CoA pathway of autotrophic CO_2 fixation in *Methanococcus maripaludis*. Proc Natl Acad Sci U S A **87:**5598-5602.

73. **Lawrence, S. H., and J. G. Ferry.** 2006. Steady-state kinetic analysis of phosphotransacetylase from *Methanosarcina thermophila*. J Bacteriol **188:**1155-1158.

74. **Leigh, J. A.** 2011. Growth of methanogens under defined hydrogen conditions. Methods Enzymol **494:**111-118.

75. **Leigh, J. A., S. V. Albers, H. Atomi, and T. Allers.** 2011. Model organisms for genetics in the domain Archaea: methanogens, halophiles, *Thermococcales* and *Sulfolobales*. FEMS Microbiol Rev **35:**577-608.

76. **Lessner, D. J., L. Lhu, C. S. Wahal, and J. G. Ferry.** 2010. An engineered methanogenic pathway derived from the domains Bacteria and Archaea. MBio **1**:e00243-10.

77. **Lessner, D. J., L. Li, Q. Li, T. Rejtar, V. P. Andreev, M. Reichlen, K. Hill, J. J. Moran, B. L. Karger, and J. G. Ferry.** 2006. An unconventional pathway for reduction of CO_2 to methane in CO-grown *Methanosarcina acetivorans* revealed by proteomics. Proc Natl Acad Sci U S A **103:**17921-17926.

78. **Li, F., J. Hinderberger, H. Seedorf, J. Zhang, W. Buckel, and R. K. Thauer.** 2008. Coupled ferredoxin and crotonyl coenzyme A (CoA) reduction with NADH catalyzed by the butyryl-CoA dehydrogenase/Etf complex from *Clostridium kluyveri*. J Bacteriol **190:**843-850.

79. **Lie, T. J., K. C. Costa, B. Lupa, S. Korpole, W. B. Whitman, and J. A. Leigh.** 2012. Essential anaplerotic role for the energy-converting hydrogenase Eha in hydrogenotrophic methanogenesis. Proc Natl Acad Sci U S A **109:**15473-15478.

80. **Lie, T. J., K. C. Costa, D. Pak, V. Sakesan, and J. A. Leigh.** 2013. Phenotypic evidence that the function of the [Fe]-hydrogenase Hmd in *Methanococcus maripaludis* requires seven hcg (hmd co-occurring genes) but not hmdII. FEMS Microbiol Lett **343:**156-160.

81. **Lie, T. J., J. A. Dodsworth, D. C. Nickle, and J. A. Leigh.** 2007. Diverse homologues of the archaeal repressor NrpR function similarly in nitrogen regulation. FEMS Microbiol Lett **271:**281-288.

82. **Lie, T. J., and J. A. Leigh.** 2002. Regulatory response of *Methanococcus maripaludis* to alanine, an intermediate nitrogen source. J Bacteriol **184:**5301-5306.

83. **Lie, T. J., G. E. Wood, and J. A. Leigh.** 2005. Regulation of *nif* expression in *Methanococcus maripaludis*: roles of the euryarchaeal repressor NrpR, 2-oxoglutarate, and two operators. J Biol Chem **280:**5236-5241.

84. **Lienard, T., B. Becher, M. Marschall, S. Bowien, and G. Gottschalk.** 1996. Sodium ion translocation by N5-methyltetrahydromethanopterin: coenzyme M methyltransferase from *Methanosarcina mazei* Go1 reconstituted in ether lipid liposomes. Eur J Biochem **239:**857-864.

85. **Liu, H., R. G. Sadygov, and J. R. Yates, 3rd.** 2004. A model for random sampling and estimation of relative protein abundance in shotgun proteomics. Anal Chem **76:**4193-4201.

86. **Liu, Y., M. Sieprawska-Lupa, W. B. Whitman, and R. H. White.** 2010. Cysteine is not the sulfur source for iron-sulfur cluster and methionine biosynthesis in the methanogenic archaeon *Methanococcus maripaludis*. J Biol Chem **285:**31923-31929.

87. **Lockerby, D. L., H. R. Rabin, L. E. Bryan, and E. J. Laishley.** 1984. Ferredoxin-linked reduction of metronidazole in *Clostridium pasteurianum*. Antimicrob Agents Chemother **26:**665-669.

88. **Lupa, B., E. L. Hendrickson, J. A. Leigh, and W. B. Whitman.** 2008. Formate-dependent H_2 production by the mesophilic methanogen *Methanococcus maripaludis*. Appl Environ Microbiol **74:**6584-6590.

89. **Ma, K., D. Linder, K. O. Stetter, and R. K. Thauer.** 1991. Purification and properties of N5,N10-methylenetetrahydromethanopterin reductase (coenzyme F_{420}-dependent) from the extreme thermophile *Methanopyrus kandleri*. Arch Microbiol **155:**593-600.

90. **Major, T. A., Y. Liu, and W. B. Whitman.** 2010. Characterization of energy-conserving hydrogenase B in *Methanococcus maripaludis*. J Bacteriol **192:**4022-4030.

91. **Matthews, R. G., and C. W. Goulding.** 1997. Enzyme-catalyzed methyl transfers to thiols: the role of zinc. Curr Opin Chem Biol **1:**332-339.

92. **May, H. D., P. S. Patel, and J. G. Ferry.** 1988. Effect of molybdenum and tungsten on synthesis and composition of formate dehydrogenase in *Methanobacterium formicicum*. J Bacteriol **170:**3384-3389.

93. **May, H. D., N. L. Schauer, and J. G. Ferry.** 1986. Molybdopterin cofactor from *Methanobacterium formicicum* formate dehydrogenase. J Bacteriol **166:**500-504.

94. **McInerney, M. J., and P. S. Beaty.** 1988. Anaerobic community structure from a nonequilibrium thermodynamic perspective. Can J Microbiol **34:**487-493.

95. **Metcalf, W. W., J. K. Zhang, E. Apolinario, K. R. Sowers, and R. S. Wolfe.** 1997. A genetic system for archaea of the genus *Methanosarcina*: liposome-mediated transformation and construction of shuttle vectors. Proc Natl Acad Sci U S A **94:**2626-2631.

96. **Meuer, J., S. Bartoschek, J. Koch, A. Kunkel, and R. Hedderich.** 1999. Purification and catalytic properties of Ech hydrogenase from *Methanosarcina barkeri*. Eur J Biochem **265:**325-335.

97. **Meuer, J., H. C. Kuettner, J. K. Zhang, R. Hedderich, and W. W. Metcalf.** 2002. Genetic analysis of the archaeon *Methanosarcina barkeri* Fusaro reveals a central role for Ech hydrogenase and ferredoxin in methanogenesis and carbon fixation. Proc Natl Acad Sci U S A **99:**5632-5637.

98. **Moore, B. C., and J. A. Leigh.** 2005. Markerless mutagenesis in *Methanococcus maripaludis* demonstrates roles for alanine dehydrogenase, alanine racemase, and alanine permease. J Bacteriol **187:**972-979.

99. **Morgan, R. M., T. D. Pihl, J. Nolling, and J. N. Reeve.** 1997. Hydrogen regulation of growth, growth yields, and methane gene transcription in *Methanobacterium thermoautotrophicum* deltaH. J Bacteriol **179:**889-898.

100. **Mukhopadhyay, B., E. F. Johnson, and R. S. Wolfe.** 2000. A novel pH_2 control on the expression of flagella in the hyperthermophilic strictly hydrogenotrophic methanarchaeaon *Methanococcus jannaschii*. Proc Natl Acad Sci U S A **97:**11522-11527.

101. **Mukund, S., and M. W. Adams.** 1995. Glyceraldehyde-3-phosphate ferredoxin oxidoreductase, a novel tungsten-containing enzyme with a potential glycolytic role in the hyperthermophilic archaeon *Pyrococcus furiosus*. J Biol Chem **270:**8389-8392.

102. **Nitschke, W., and M. J. Russell.** 2012. Redox bifurcations: mechanisms and importance to life now, and at its origin: a widespread means of energy conversion in biology unfolds. Bioessays **34:**106-109.

103. **Noll, I., S. Muller, and A. Klein.** 1999. Transcriptional regulation of genes encoding the selenium-free [NiFe]-hydrogenases in the archaeon *Methanococcus voltae* involves positive and negative control elements. Genetics **152:**1335-1341.

104. **Oza, J. P., K. R. Sowers, and J. J. Perona.** 2012. Linking energy production and protein synthesis in hydrogenotrophic methanogens. Biochemistry **51:**2378-2389.

105. **Pandelia, M. E., H. Ogata, L. J. Currell, M. Flores, and W. Lubitz.** 2010. Inhibition of the [NiFe] hydrogenase from *Desulfovibrio vulgaris* Miyazaki F by carbon monoxide: an FTIR and EPR spectroscopic study. Biochim Biophys Acta **1797:**304-313.

106. **Park, M. O., T. Mizutani, and P. R. Jones.** 2007. Glyceraldehyde-3-phosphate ferredoxin oxidoreductase from *Methanococcus maripaludis*. J Bacteriol **189:**7281-7289.

107. **Pelmenschikov, V., M. R. Blomberg, P. E. Siegbahn, and R. H. Crabtree.** 2002. A mechanism from quantum chemical studies for methane formation in methanogenesis. J Am Chem Soc **124:**4039-4049.

108. **Pfeiffer, M., H. Bestgen, A. Burger, and A. Klein.** 1998. The vhuU gene encoding a small subunit of a selenium-containing [NiFe]-hydrogenase in *Methanococcus voltae* appears to be essential for the cell. Arch Microbiol **170:**418-426.

109. **Pfeiffer, M., R. Bingemann, and A. Klein.** 1998. Fusion of two subunits does not impair the function of a [NiFeSe]-hydrogenase in the archaeon *Methanococcus voltae*. Eur J Biochem **256:**447-452.

110. **Porat, I., W. Kim, E. L. Hendrickson, Q. Xia, Y. Zhang, T. Wang, F. Taub, B. C. Moore, I. J. Anderson, M. Hackett, J. A. Leigh, and W. B. Whitman.** 2006. Disruption of the operon encoding Ehb hydrogenase limits anabolic CO_2 assimilation in the archaeon *Methanococcus maripaludis*. J Bacteriol **188:**1373-1380.

111. **Porat, I., and W. B. Whitman.** 2009. Tryptophan auxotrophs were obtained by random transposon insertions in the *Methanococcus maripaludis* tryptophan operon. FEMS Microbiol Lett **297:**250-254.

112. **Purec, L., A. I. Krasna, and D. Rittenberg.** 1962. The inhibition of hydrogenase by carbon monoxide and the reversal of this inhibition by light. Biochemistry **1:**270-275.

113. **Rasband, W. S.**, ImageJ, U. S. National Institutes of Health., Bethesda, Maryland, USA, http://imagej.nih.gov/ij/, 1997-2012.

114. **Reeve, J. N.** 1993. Structure and organization of genes. *In* J. G. Ferry (ed.), Methanogenesis: ecology, physiology, biochemistry and genetics. Chapman and Hall, New York, N.Y.

115. **Rother, M., and W. W. Metcalf.** 2004. Anaerobic growth of *Methanosarcina acetivorans* C2A on carbon monoxide: an unusual way of life for a methanogenic archaeon. Proc Natl Acad Sci U S A **101:**16929-16934.

116. **Rouviere, P. E., and R. S. Wolfe.** 1988. Novel biochemistry of methanogenesis. J Biol Chem **263:**7913-7916.

117. **Rudnick, H., S. Hendrich, U. Pilatus, and K. Blotevogel.** 1990. Phosphate accumulation and the occurance of polyphosphates and cyclic 2,3-diphosphoglycerate in *Methanosarcina frisia*. Arch Microbiol **154:**584-588.

118. **Russell, J. B.** 2007. The energy spilling reactions of bacteria and other organisms. J Mol Microbiol Biotechnol **13:**1-11.

119. **Sarmiento, F. B., J. A. Leigh, and W. B. Whitman.** 2011. Genetic systems for hydrogenotrophic methanogens. Methods Enzymol **494:**43-73.

120. **Sattler, C., S. Wolf, J. Fersch, S. Goetz, and M. Rother.** 2013. Random mutagenesis identifies factors involved in formate-dependent growth of the methanogenic archaeon *Methanococcus maripaludis*. Mol Genet Genomics.

121. **Schauer, N. L., J. G. Ferry, J. F. Honek, W. H. Orme-Johnson, and C. Walsh.** 1986. Mechanistic studies of the coenzyme F_{420} reducing formate dehydrogenase from *Methanobacterium formicicum*. Biochemistry **25:**7163-7168.

122. **Schneider, C. A., W. S. Rasband, and K. W. Eliceiri.** 2012. NIH Image to ImageJ: 25 years of image analysis. Nat Methods **9:**671-675.

123. **Schoenberg, D. R., and L. E. Maquat.** 2012. Regulation of cytoplasmic mRNA decay. Nat Rev Genet **13:**246-259.

124. **Selig, M., K. B. Xavier, H. Santos, and P. Schonheit.** 1997. Comparative analysis of Embden-Meyerhof and Entner-Doudoroff glycolytic pathways in hyperthermophilic archaea and the bacterium *Thermotoga*. Arch Microbiol **167:**217-232.

125. **Setzke, E., R. Hedderich, S. Heiden, and R. K. Thauer.** 1994. H_2: heterodisulfide oxidoreductase complex from *Methanobacterium thermoautotrophicum*. Composition and properties. Eur J Biochem **220:**139-148.

126. **Shima, S., E. Warkentin, W. Grabarse, M. Sordel, M. Wicke, R. K. Thauer, and U. Ermler.** 2000. Structure of coenzyme F(420) dependent methylenetetrahydromethanopterin reductase from two methanogenic archaea. J Mol Biol **300:**935-950.

127. **Shimoyama, T., S. Kato, S. Ishii, and K. Watanabe.** 2009. Flagellum mediates symbiosis. Science **323:**1574.

128. **Simianu, M., E. Murakami, J. M. Brewer, and S. W. Ragsdale.** 1998. Purification and properties of the heme- and iron-sulfur-containing heterodisulfide reductase from *Methanosarcina thermophila*. Biochemistry **37:**10027-10039.

129. **Stams, A. J., and C. M. Plugge.** 2009. Electron transfer in syntrophic communities of anaerobic bacteria and archaea. Nat Rev Microbiol **7:**568-577.

130. **Stojanowic, A., G. J. Mander, E. C. Duin, and R. Hedderich.** 2003. Physiological role of the F_{420}-non-reducing hydrogenase (Mvh) from *Methanothermobacter marburgensis*. Arch Microbiol **180:**194-203.

131. **Tabb, D. L., W. H. McDonald, and J. R. Yates, 3rd.** 2002. DTASelect and Contrast: tools for assembling and comparing protein identifications from shotgun proteomics. J Proteome Res **1:**21-26.

132. **te Brommelstroet, B. W., C. M. Hensgens, J. T. Keltjens, C. van der Drift, and G. D. Vogels.** 1990. Purification and properties of 5,10-methylenetetrahydromethanopterin reductase, a coenzyme F420-dependent enzyme, from *Methanobacterium thermoautotrophicum* strain delta H. J Biol Chem **265:**1852-1857.

133. **Tersteegen, A., and R. Hedderich.** 1999. *Methanobacterium thermoautotrophicum* encodes two multisubunit membrane-bound [NiFe] hydrogenases. Transcription of the operons and sequence analysis of the deduced proteins. EurJ Biochem **264:**930-943.

134. **Thauer, R. K.** 2012. The Wolfe cycle comes full circle. Proc Natl Acad Sci U S A **109:**15084-15085.

135. **Thauer, R. K., A. K. Kaster, M. Goenrich, M. Schick, T. Hiromoto, and S. Shima.** 2010. Hydrogenases from methanogenic archaea, nickel, a novel cofactor, and H_2 storage. Annu Rev Biochem **79:**507-536.

136. **Thauer, R. K., A. K. Kaster, H. Seedorf, W. Buckel, and R. Hedderich.** 2008. Methanogenic archaea: ecologically relevant differences in energy conservation. Nat Rev Microbiol **6:**579-591.

137. **Thauer, R. K., A. R. Klein, and G. C. Hartmann.** 1996. Reactions with Molecular Hydrogen in Microorganisms: Evidence for a Purely Organic Hydrogenation Catalyst. Chem Rev **96:**3031-3042.

138. **Tsao, J. H., S. M. Kaneshiro, S. S. Yu, and D. S. Clark.** 1994. Continuous culture of *Methanococcus jannaschii*, an extremely thermophilic methanogen. Biotechnol Bioeng **43:**258-261.

139. **Tumbula, D. L., and W. B. Whitman.** 1999. Genetics of *Methanococcus*: possibilities for functional genomics in Archaea. Mol Microbiol **33:**1-7.

140. **van der Oost, J., G. Schut, S. W. Kengen, W. R. Hagen, M. Thomm, and W. M. de Vos.** 1998. The ferredoxin-dependent conversion of glyceraldehyde-3-phosphate in the hyperthermophilic archaeon *Pyrococcus furiosus* represents a novel site of glycolytic regulation. J Biol Chem **273:**28149-28154.

141. **Verhees, C. H., S. W. Kengen, J. E. Tuininga, G. J. Schut, M. W. Adams, W. M. De Vos, and J. Van Der Oost.** 2003. The unique features of glycolytic pathways in Archaea. Biochem J **375:**231-246.

142. **Vorholt, J. A., M. Vaupel, and R. K. Thauer.** 1996. A polyferredoxin with eight [4Fe-4S] clusters as a subunit of molybdenum formylmethanofuran dehydrogenase from *Methanosarcina barkeri*. Eur J Biochem **236:**309-317.

143. **Wang, S., H. Huang, J. Kahnt, A. P. Mueller, M. Kopke, and R. K. Thauer.** 2013. An NADP-specific electron-bifurcating [FeFe]-hydrogenase in a functional complex with formate dehydrogenase in *Clostridium autoethanogenum* grown on CO. J Bacteriol. Published ahead of print 26 July 2013, doi: 10.1128/JB.00678-1

144. **Wang, S., H. Huang, J. Kahnt, and R. K. Thauer.** 2013. An electron-bifurcating formate dehydrogenase in *Clostridium acidurici*. Appl Environ Microbiol. Published ahead of print 19 July 2013, doi: 10.1128/AEM.02015-13

145. **Wang, S., H. Huang, J. Kahnt, and R. K. Thauer.** 2013. A reversible electron-bifurcating ferredoxin- and NAD-dependent [FeFe]-hydrogenase (HydABC) in *Moorella thermoacetica*. J Bacteriol **195:**1267-1275.

146. **Wang, S., H. Huang, J. Moll, and R. K. Thauer.** 2010. NADP+ reduction with reduced ferredoxin and NADP+ reduction with NADH are coupled via an electron-bifurcating enzyme complex in *Clostridium kluyveri*. J Bacteriol **192:**5115-5123.

147. **Wasserfallen, A.** 1994. Formylmethanofuran synthesis by formylmethanofuran dehydrogenase from *Methanobacterium thermoautotrophicum* Marburg. Biochem Biophys Res Commun **199:**1256-1261.

148. **Wasserfallen, A., J. Nolling, P. Pfister, J. Reeve, and E. Conway de Macario.** 2000. Phylogenetic analysis of 18 thermophilic *Methanobacterium* isolates supports the proposals to create a new genus, *Methanothermobacter* gen. nov., and to reclassify several isolates in three species, *Methanothermobacter thermautotrophicus* comb. nov.,

Methanothermobacter wolfeii comb. nov., and *Methanothermobacter marburgensis* sp. nov. Int J Syst Evol Microbiol **50 Pt 1:**43-53.

149. **Weiss, D. S., P. Gartner, and R. K. Thauer.** 1994. The energetics and sodium-ion dependence of N5-methyltetrahydromethanopterin:coenzyme M methyltransferase studied with cob(I)alamin as methyl acceptor and methylcob(III)alamin as methyl donor. Eur J Biochem **226:**799-809.

150. **Welander, P. V., and W. W. Metcalf.** 2005. Loss of the mtr operon in *Methanosarcina* blocks growth on methanol, but not methanogenesis, and reveals an unknown methanogenic pathway. Proc Natl Acad Sci U S A **102:**10664-10669.

151. **Welander, P. V., and W. W. Metcalf.** 2008. Mutagenesis of the C1 oxidation pathway in *Methanosarcina barkeri*: new insights into the Mtr/Mer bypass pathway. J Bacteriol **190:**1928-1936.

152. **Welte, C., and U. Deppenmeier.** 2011. Re-evaluation of the function of the F_{420} dehydrogenase in electron transport of *Methanosarcina mazei*. FEBS J **278:**1277-1287.

153. **Welte, C., C. Kratzer, and U. Deppenmeier.** 2010. Involvement of Ech hydrogenase in energy conservation of *Methanosarcina mazei*. FEBS J **277:**3396-3403.

154. **Whitman, W. B., J. Shieh, S. Sohn, D. S. Caras, and U. Premachandran.** 1986. Isolation and characterization of 22 mesophilic methanococci. Syst Appl Microbiol **7:**235-240.

155. **Widdel, F., and R. Wolfe.** 1989. Expression of secondary alcohol dehydrogenase in methanogenic bacteria and purifcation of the F_{420}-specific enzyme from *Methanogenium thermophilum* strain TC1. Arch Microbiol **152:**322-328.

156. **Wood, G. E., A. K. Haydock, and J. A. Leigh.** 2003. Function and regulation of the formate dehydrogenase genes of the methanogenic archaeon *Methanococcus maripaludis*. J Bacteriol **185:**2548-2554.

157. **Worm, P., A. J. Stams, X. Cheng, and C. M. Plugge.** 2011. Growth- and substrate-dependent transcription of formate dehydrogenase and hydrogenase coding genes in *Syntrophobacter fumaroxidans* and *Methanospirillum hungatei*. Microbiology **157:**280-289.

158. **Xia, Q., E. L. Hendrickson, Y. Zhang, T. Wang, F. Taub, B. C. Moore, I. Porat, W. B. Whitman, M. Hackett, and J. A. Leigh.** 2006. Quantitative proteomics of the archaeon *Methanococcus maripaludis* validated by microarray analysis and real time PCR. Mol Cell Proteomics **5:**868-881.

159. **Xia, Q., T. Wang, E. L. Hendrickson, T. J. Lie, M. Hackett, and J. A. Leigh.** 2009. Quantitative proteomics of nutrient limitation in the hydrogenotrophic methanogen *Methanococcus maripaludis*. BMC Microbiol **9:**149.

160. **Yang, Y. L., J. N. Glushka, and W. B. Whitman.** 2002. Intracellular pyruvate flux in the methane-producing archaeon *Methanococcus maripaludis*. Arch Microbiol **178:**493-498.

161. **Yang, Y. L., J. Ladapo, and W. B. Whitman.** 1992. Pyruvate oxidation by *Methanococcus* spp. Arch Microbiol **158:**271-275.

162. **Yoon, S. H., D. J. Reiss, J. C. Bare, D. Tenenbaum, M. Pan, J. Slagel, R. L. Moritz, S. Lim, M. Hackett, A. L. Menon, M. W. Adams, A. Barnebey, S. M. Yannone, J. A. Leigh, and N. S. Baliga.** 2011. Parallel evolution of transcriptome architecture during genome reorganization. Genome Res **21:**1892-1904.

163. **Yoon, S. H., S. Turkarslan, D. J. Reiss, M. Pan, J. A. Burn, K. C. Costa, T. J. Lie, J. Slagel, R. L. Moritz, M. Hackett, J. A. Leigh, and N. S. Baliga.** in press. A systems level predictive model for global gene regulation of methanogenesis in a hydrogenotrophic methanogen. Genome Res.

164. **Yu, J. P., J. Ladapo, and W. B. Whitman.** 1994. Pathway of glycogen metabolism in *Methanococcus maripaludis*. J Bacteriol **176:**325-332.

165. **Zinder, S. H.** 1993. Physiological Ecology of Methanogens, p. 128 - 206. *In* J. G. Ferry (ed.), Methanogenesis: Ecology, Physiology, Biochemistry & Genetics. Chapman & Hall, New York.

166. **Zirngibl, C., W. Van Dongen, B. Schworer, R. Von Bunau, M. Richter, A. Klein, and R. K. Thauer.** 1992. H_2-forming methylenetetrahydromethanopterin dehydrogenase, a novel type of hydrogenase without iron-sulfur clusters in methanogenic archaea. Eur J Biochem **208:**511-520.

167. **Zybailov, B., M. K. Coleman, L. Florens, and M. P. Washburn.** 2005. Correlation of relative abundance ratios derived from peptide ion chromatograms and spectrum counting for quantitative proteomic analysis using stable isotope labeling. Anal Chem **77:**6218-6224.

VITA

Kyle C. Costa

Education

2007 **B.S. Biology**, minor in chemistry
University of Nevada, Las Vegas

2013 **Ph.D. Microbiology**
University of Washington, Seattle

Research papers

1. **Costa KC**, Hallmark J, Moser DP, Soukup DA, Labahn S and Hedlund BP. 2008. Erratum: "Geomicrobiological changes in two ephemeral desert playa lakes in the western United States" (*Geomicrobiol J*. vol. 25 (5)). *Geomicrobiol J*. 25(7-8):456.

2. **Costa KC**, Navarro JB, Shock EL, Zhang C, Soukup D and Hedlund BP. 2009. Microbiology and geochemistry of Great Boiling and Mud Hot Springs in the United States Great Basin. *Extremophiles*. 13:447-459.

3. Vick TJ, Dodsworth JA, **Costa KC**, Shock EL and Hedlund BP. 2010. Microbiology and geochemistry of Little Hot Creek, a hyperthermophilic hot spring environment in the Long Valley Caldera. *Geobiology*. 8:140-154.

4. **Costa KC**, Wong PM, Wang T, Lie TA, Dodsworth JA, Swanson I, Burn JA, Hackett M and Leigh JA. 2010. Protein complexing in a methanogen suggests electron bifurcation and electron delivery from formate to heterodisulfide reductase. *Proc Natl Acad Sci USA*. 107:11050-11055.

5. Lie TJ*, **Costa KC***, Lupa B, Korpole S, Whitman WB and Leigh JA. 2012. Essential anaplerotic role for the energy converting hydrogenase Eha in hydrogenotrophic methanogenesis. *Proc Natl Acad Sci USA*. 109:15473-15478.
*These authors contributed equally to this work

6. **Costa KC**, Lie TJ, Jacobs M and Leigh JA. 2013. H_2-independent growth of the hydrogenotrophic methanogen *Methanococcus maripaludis*. *mBio.* 4:e00062-13.

7. **Costa KC**, Yoon SH, Pan M, Burn JA, Baliga N and Leigh JA. 2013. Effects of H_2 and formate on growth yeild and regulation of methanogenesis in *Methanococcus maripaludis*. *J Bacteriol.* 195:1456-1462.

8. Lie TJ, **Costa KC**, Pak D, Sakesan V and Leigh JA. 2013. Phenotypic evidence that the function of the [Fe]-hydrogenase Hmd in *Methanococcus maripaludis* requires seven hcg (hmd-cooccuring genes) but not hmdII. *FEMS Microbiol Lett.* 343:156-160.

9. Yoon SH, Reiss DJ, Pan M, Burn J, **Costa KC**, Lie TJ, Slagel J, Moritz RL, Hackett M, Leigh JA and Baliga NS. A systems level predictive model for global gene regulation of methanogenesis in a hydrogenotrophic methanogen *Genome Res.* 23:1839–1851.

10. **Costa KC**, Lie TJ, Xia Q and Leigh JA. VhuD facilitates electron flow from H_2 or formate to heterodisulfide reductase in *Methanococcus maripaludis*. *J Bacteriol.* 195: 1456-1462.

Book Chapters

11. Hedlund BP and Costa KC. 2010. Genus *Neptunomonas*. *In* Kenneth N. Timmis (ed.) *Handbook of Hydrocarbon and Lipid Microbiology*, Springer Verlag, Heidelberg, Germany.

12. Cho J, Janssen PH, Costa KC and Hedlund BP. 2011. Class II. Opitutae. *In* N.R. Krieg, J.T. Staley, B.P. Hedlund, B.J. Paster, N. Ward, W. Ludwig, and W.B. Whitman (eds.) *Bergey's Manual of Systematic Bacteriology*, 2nd Edition, Volume 4: 817-819, Springer Verlag, New York, USA.

13. Janssen PH, Costa KC and Hedlund, BP. 2011. Class III. Spartobacteria class. nov. *In* N.R. Krieg, J.T. Staley, B.P. Hedlund, B.J. Paster, N. Ward, W. Ludwig, and W.B. Whitman (eds.) *Bergey's Manual of Systematic Bacteriology*, 2nd Edition, Volume 4: 834-836, Springer Verlag, New York, USA.

14. Hedlund BP, Cho J, Derien M and Costa KC. (2011) Phylum XXII. Lentisphaerae. *In* N.R. Krieg, J.T. Staley, B.P. Hedlund, B.J. Paster, N. Ward, W. Ludwig, and W.B. Whitman (eds.) *Bergey's Manual of Systematic Bacteriology*, 2nd Edition, Volume 4: 785-793, Springer Verlag, New York, USA.

National and International Presentations

2007 **Costa, K.C.**, E.L. Shock, J.B. Navarro, C. Zhang, D. Soukup, B.P. Hedlund. Thermodynamic Modeling as a predictive tool for determining energy availability in Great Basin hot springs. American Society for Microbiology Annual Meeting.

2010 **Costa, K.C.**, P.M. Wong, T. Wang, M. Hackett, J.A. Leigh. Purification of heterodisulfide reductase from *Methanococcus maripaludis*: protein interactions and energy conservation in methanogenesis. American Society for Microbiology annual meeting.

2011 **Costa, K.C.**, Lie, T.J., Leigh, J.A. Formate acts directly as an electron donor for all four reductive steps of methanogenesis. GRC (Archaea: Ecology, Metabolism, and Molecular Biology).

2011 **Costa, K.C.**, Lie, T.J., Leigh, J.A. H_2 is not an Essential Intermediate for Hydrogenotrophic Methanogens. West Coast Bacterial Physiologists Annual Asilomar conference.

2012 **Costa, K.C.**, Lie, T.J., Jacobs, M., Leigh, J.A. Ferredoxin reduction and H_2 production by a hydrogenotrophic methanogen capable of H_2-independent growth. GRC (Molecular Basis of Microbial One-Carbon Metabolism)

Teaching Experience

Teaching assistant

University of Nevada, Las Vegas School of Life Sciences
Courses taught: BIOL 351L – spring 2006 (microbiology lab for majors)
Co-taught as an undergraduate TA

University of Washington Department of Microbiology
Courses taught: MICROM 302 – spring 2009 (microbiology lab for non-majors)
MICROM 411 – winter 2010 (microbial genetics lab)

Undergraduate and graduate course lectures

University of Washington Department of Microbiology
Lectures taught: MICROM 431 – winter 2011: a 1 hour lecture on the use of molecular techniques in the design and execution of a research project
MICROM 412 – spring 2011: a 1 hour lecture on early metabolic evolution and diversity of the *Archaea*
CONJ 557 – spring 2011, spring 2012, spring 2013: a 75 minute lecture on the origin of life and early evolution